



UNIVERSITAT POLITÈCNICA DE CATALUNYA
BARCELONATECH

GRUP DE COMUNICACIONS ÒPTIQUES

MASTER THESIS

ALL-FIBER MACH-ZEHNDER INTERFEROMETER FOR DWDM-PON BIDIRECTIONAL MULTIPLEXING

AUTOR: ANNA KURYSHEVA

TUTOR: JOSEP PRAT GOMA

JULY 2015

*A person who never made a mistake
never tried anything new.
Albert Einstein.*

ACKNOWLEDGMENTS

There are many people I would like to thank for all their support and help during the development of this Master Thesis. First of all, I would like to thank my supervisor of this Master Thesis, Josep Prat, who gave me the opportunity to develop it within the optical communications group (GCO) as well as for all his help, offered during this time.

This project would not have been possible without the help and patience of Victor Polo undertaken in the laboratory and for teaching me his practical experience. I also want to thank to all the fellow GCO their advice, suggestions and good humor to resolve the difficulties of everyday during the developing my Master Thesis.

On the personal level, I would like to thank to my family. The last years have been a great experience for me. I had the pleasure to meet and talk with many admirable persons from around the world. I learnt to complete and defend my work.

Finally, I cannot forget my friends who were always helping me, encouraging me and showing me the way that has made it possible to get here.

To all thank you very much.

ABSTRACT

Optical transmission is getting more popular in the access network due to the increasing demand for bandwidth. New services like IP television (IPTV) transmission, video on demand (VoD) etc. over Internet together along high speed Internet access are confronting the demand of higher bandwidth at the customer end in today's Ethernet network backbone. Even though today's well deployed XDSL (i.e., VDSL/VDSL2+, SHDSL) solutions can satisfy bandwidth demand but are limited to the restriction regarding distance. Hereby, the suitable solution for high bandwidth demand with a long reach can be met by reaching optical cable to customer end directly. One of the possible ways would be to install passive optical network (PON).

Fiber-to-the Home technology is one of the main research objectives of the last years in optical fiber communication. The increasing development of data communications and the emerging of applications demand a redesign of the access network in order to accomplish new bandwidth and latency requirements. Wireless communications are a good alternative for quick deployment and low implementation, but this technology can not compete against optical communications in terms of available bandwidth, latency and robustness.

Access optical networks are capable of solving those requirements for present and future applications. Broadband access network based on FTTH will dramatically accelerate from now due to further progress in services.

In order to achieve cost effective solutions for FTTH, present investigations are centered in access networks which mainly use passive optical components to avoid the use of power sources and costly control equipment between the central office (Optical Line Termination-OLT) and the user premises (ONU).

Bidirectional single-fiber strategy seems to be the most interesting architecture; ONU becomes a key element in access networks and an interesting area of investigation. For a total successful FTTH deployment the network unit model should be simple, robust flexible and cost-available for the final customer.

According to the cost the best solution for having cost-effective and performance system will be performance in the access part. The cost-effective solution could be to build cascade system of MZI optical devices for increasing users in our measurement system. This project will evaluate the new optical fiber access to the home (FTTH) network that uses DWDM technology, the key of implantation cost-effective solution in access part is to use bidirectional optical devices like all fiber MZI and Commercial Interleaver in order to test and compare these devices in laboratory.

TABLE OF CONTENTS

LIST OF FIGURES	10
LIST OF TABLES	14
1. INTRODUCTION	16
1.1. Principle of working of access networks	16
1.2. Architectures	18
1.2.1. TDM-PON architecure.	18
1.2.2. xWDM - PON architectures.	20
1.3. Architecture elements.	21
2. MZI AND INTERLEAVER THEORY AND COMPARISON	25
2.1. Mach-Zehnder Interferometer (MZI) description	25
2.1.1 Ideal MZI	25
2.1.2. Non-Ideal MZI	30
2.1.3. Influence of Polarization	33
2.1.4. Instability of the MZI	33
2.2. Passive Interleaver description	34
2.2.1. Principle of working	35
2.2.2. 50 GHz Passive Interleaver	37
2.3. Comparison of commercial Interleaver and MZI-based Interleaver.	38
2.4. Summary	39
3. DESIGN OF DOUBLE-STAGE MZI. MATLAB SIMULATION	41
3.1. Introduction	41
3.2. Objectives	41

TABLE OF CONTENTS

3.3.	Schema and Concept	42
3.4.	Matlab simulation	45
3.4.1.	Ideal simulation	45
3.4.2.	Non-Ideal simulation	49
3.5.	Simulation Results	50
3.5.1.	Ideal Simulation Results	50
3.5.2.	Non-Ideal Simulation Results	54
3.6.	Summary	59
4.	THE MAIN PARAMETERS. IN-LAB EXPERIMENTATION	61
4.1.	Theoretical Review	61
4.1.1.	Review of the parameters for MZI and commercial Interleaver	61
4.2.	Experimental Affairs.	64
4.2.1.	Preparing the acquisition system.	65
4.2.2.	Equipment Used.	65
4.2.3.	MZI Measurements.	68
4.2.4.	Interleaver Parameters Measurements.	76
4.2.5.	Downstream system: behavior of MZI and Interleaver	80
4.2.6.	Upstream systems: behavior of three devices (MZI, Interleaver and coupler)	88
4.2.7.	Behavior of both devices in Downstream with data	91
4.2.8.	Behavior of three devices in Upstream with data signals	97
4.2.9.	OLT and Access WDM Network. Test and Measurement	100
4.3.	Summary.	108
5.	GENERAL CONCLUSION	110
	APPENDIX 1: MATLAB IDEAL MZI SIMULATION.	113

TABLE OF CONTENTS

APPENDIX 2: MATLAB NON-IDEAL MZI SIMULATION.	119
APPENDIX 3: INTERLEAVER DATASHEET.	125
APPENDIX 4: BER TABLES.	127
REFERENCES	133

LIST OF FIGURES

CHAPTER 1 FIGURES

Figure 1.1.	General structure of a telecommunication network	17
Figure 1.2.	A typical TDM-PON architecture	19
Figure 1.3.	A typical WDM - PON network architecture	20
Figure 1.4.	Elements of an optical network	22

CHAPTER 2 FIGURES

Figure 2.1.	Block diagram of ideal Mach-Zehnder Interferometer as Passive Optical Device	25
Figure 2.2.	Illustration of an MZI with two inputs and two outputs	26
Figure 2.3.	Power transmission of ideal MZI1 response	29
Figure 2.4.	Power transmission of ideal MZI2 response	30
Figure 2.5.	Power spectrum of a non-ideal MZI1: the coupling ratios are 51%:49% and 55%:45%	32
Figure 2.6.	Power spectrum of a non-ideal MZI2: the coupling ratios are 51%:49% and 55%:45%	32
Figure 2.7.	Original interleaver: even and odd channels are separated onto two different ports	36
Figure 2.8.	Interleaver functional types. All filter functions are periodic in frequency and are reciprocal. a) Original interleaver: even and odd channels are separated onto two different ports. b) Separation of channels out to 1:4 or higher. c) Banded interleaver, separates even and odd bands of channels. More difficult than 1:2 interleaver because of higher filter roll-off. d) Asymmetric interleaver separates one channel in N	36

CHAPTER 3 FIGURES

Figure 3.1.	Double-Stage MZI schema with 4 users input and split output signals . . .	42
Figure 3.2.	Complete System modeled as a Black Box	44

Figure 3.3.	4 Users in time domain with different frequencies.	46
Figure 3.4.	Input signal (4 users) in frequency domain	47
Figure 3.5.	Input signal and first Transfer Function of MZI1	50
Figure 3.6.	Output1 of the MZI1: Users 1 and 3	51
Figure 3.7.	Input signal and second Transfer Function of MZI1	51
Figure 3.8.	Output2 of the MZI1: Users 2 and 4	52
Figure 3.9.	Output11 and first Transfer Function of MZI2	52
Figure 3.10.	Output1 of the MZI2: User 1	53
Figure 3.11.	Output11 and second Transfer Function of MZI2	53
Figure 3.12.	Output2 of the MZI2: User 3	54
Figure 3.13.	Complete System	55
Figure 3.14.	Input signal and first Transfer Function (T1) of MZI1	55
Figure 3.15.	Input signal and second Transfer Function (T2) of MZI1	56
Figure 3.16.	Output1 of the MZI1: Odd users	56
Figure 3.17.	Output2 of the MZI1: Even users	57
Figure 3.18.	Output11 and first Transfer Function of MZI2	57
Figure 3.19.	Output11 and second Transfer Function of MZI2	58
Figure 3.20.	Output1 of the MZI2: User 1	58
Figure 3.21.	Output2 of the MZI2: User 3	59

CHAPTER 4 FIGURES

Figure 4.1.	Some examples of real GCO-UPC Laboratory configurations	65
Figure 4.2.	50GHz Oplink Interleaver	66
Figure 4.3.	Symbol gallery	68
Figure 4.4.	Schema of the response obtainment from input a_1 to output b_2	69
Figure 4.5.	Frequency response of MZI shown in OSA screen	69
Figure 4.6.	ER obtainment. Left: input a_2 to output b_1 . Right: input a_2 to output b_2 . . .	70

Figure 4.7.	Frequency response of MZI captured with MATLAB	70
Figure 4.8.	FSR obtainment. Left: input a2 to output b1. Right: input a2 to output b2. .	71
Figure 4.9.	Return Loss measurement schema	73
Figure 4.10.	Polarization Dependent Loss measurement schema	74
Figure 4.11.	Polarization Dependent Loss measurement In-Lab configuration	74
Figure 4.12.	PDL of MZI from input a1 to output b1	75
Figure 4.13.	PDL of MZI from input a1 to output b2	75
Figure 4.14.	Schema of the Interleaver odd response obtainment	76
Figure 4.15.	Frequency response of Interleaver shown in OSA screen	76
Figure 4.16.	ER obtainment in Interleaver response	77
Figure 4.17.	Frequency response of Interleaver captured with MATLAB	77
Figure 4.18.	FSR obtainment of the Interleaver captured with MATLAB	78
Figure 4.19.	RL measurement of the Interleaver schema	78
Figure 4.20.	Polarization Dependent Loss measurement schema for Interleaver . . .	79
Figure 4.21.	PDL of MZI from input a1 to output b1	79
Figure 4.22.	Set up with MZI in the GCO Laboratory	81
Figure 4.23.	Schema of the MZI Set up	81
Figure 4.24.	Schema of the simulated situation	82
Figure 4.25.	Signal generated with two lasers and coupler	82
Figure 4.26.	Output b1 of the MZI	83
Figure 4.27.	Output b2 of the MZI	84
Figure 4.28.	Interleaver set up in GCO Laboratory	85
Figure 4.29.	Schema of the Interleaver Set up	85
Figure 4.30.	Signal generated with two lasers and coupler	86
Figure 4.31.	Odd output of the Interleaver	87
Figure 4.32.	Even output of the Interleaver	87
Figure 4.33.	Set up with coupler in GCO Laboratory	89
Figure 4.34.	Laser 1 signal	89

Figure 4.35.	Laser 2 signal	90
Figure 4.36.	Coupler output signal	90
Figure 4.37.	Schema of the MZI Set up modulating the lasers	92
Figure 4.38.	Signal generated with two lasers modulated and coupler	92
Figure 4.39.	Output b1 of the MZI	93
Figure 4.40.	Output b2 of the MZI	93
Figure 4.41.	Schema of the Interleaver Set up modulating the lasers	94
Figure 4.42.	Signal generated with two lasers modulated and coupler	95
Figure 4.43.	Even Output of the Interleaver	95
Figure 4.44.	Odd Output of the Interleaver	96
Figure 4.45.	Set up with coupler and modulated signal in GCO Laboratory	97
Figure 4.46.	Modulated Laser 1 signal	98
Figure 4.47.	Modulated Laser 2 signal	98
Figure 4.48.	Output modulated signal of the Coupler	99
Figure 4.49.	Access Network + OLT Detector schematic under Interleaver use	100
Figure 4.50.	In-Lab configuration with Interleaver	101
Figure 4.51.	In-Lab configuration with Interleaver	102
Figure 4.52.	In-Lab configuration with Interleaver	102
Figure 4.53.	IL vs Wavelength in 3 real BER cases and in the ideal case for Interleaver device	103
Figure 4.54.	Access Network + OLT Detector schematic under Interleaver use	104
Figure 4.55.	In-Lab configuration with MZI	105
Figure 4.56.	In-Lab configuration with MZI	105
Figure 4.57.	In-Lab configuration with MZI	106
Figure 4.58.	IL vs Wavelength in 3 real BER cases and in the ideal case for MZI device	106
Figure 4.59.	Frequency response movements of the MZI along the time	107

LIST OF TABLES

CHAPTER 1 TABLES

Table 1.1.	Characteristics of GPON and EPON	19
------------	--------------------------------------------	----

CHAPTER 2 TABLES

Table 2.1.	Parameter of the commercial 50GHz Passive Interleaver	38
Table 2.2.	Comparison between Commercial Interleaver and Interleaver based on MZI	38

CHAPTER 3 TABLES

Table 3.1.	ER and IL of each port	44
------------	----------------------------------	----

CHAPTER 4 TABLES

Table 4.1.	Equivalence between FSR and ΔL	62
Table 4.2.	Summary of experimental IL Results	72
Table 4.3.	Final results of MZI	84
Table 4.4.	Final results of Interleaver	88
Table 4.5.	Comparison between MZI and Interleaver in Downstream set up	88
Table 4.6.	Coupler measurements	91
Table 4.7.	IL Comparison between MZI, Interleaver and Coupler	91
Table 4.8.	Final results of MZI	94
Table 4.9.	Final results of Interleaver with data	96
Table 4.10.	Comparison between MZI and Interleaver in Downstream set up	97
Table 4.11.	Coupler measurements with data signal	99
Table 4.12.	IL Comparison between MZI, Interleaver and Coupler	99

The recent report reveals that the total number of Optic Fiber users all over the globe is about 654.6 Million (Q1-2013) with a huge increase in the last quarter. This makes us to consider the Optical Networks as the solution for the future. However there is need to improve the current systems and for that reason WDM-Passive Optical Networks are the best bet for the next generation broadband networks. This thesis tries to improve this WDM-PON and some of its components.

Passive Optical Networks are currently being deployed worldwide to provide broadband multimedia services. As the users demands keep increasing PON system upgrade is inevitable in the near future. Also it is mandatory for service providers to provide new services without disturbing existing users while keeping the optical distribution network (ODN) untouched [1]. When upgrading PON system and services, it is preferable for service providers to add additional equipment at OLT side or make a replacement of optical devices in the access part, including both ODNs and ONUs, untouched. PON optical devices are coming into the market offering higher bandwidth year by year. High bandwidth will be needed for the optical access system which will provide a high bandwidth, more passive reach and more amounts of ONTs per feeder line [1].

The first chapter provides a brief background of optical communication system developments. It focuses on bidirectional transmission techniques for Passive Optical Network and a review of possible multiplication optical architectures has been performed: TDM-PON, WDM-PON, DWDM-PON, UDWDM-PON. Following, aspects with reference to the standardization as well as differences between the two main trends Ethernet and Gigabit – PON are exposed. This chapter introduces the basic concepts of PON network thus it is the kind of technology that may be deployed in the near future and we illustrate with a brief explanation about FTTH(x) deployment around the world, also we describe more in details optical elements and working principle of fiber. And at the last section we expose the state of the art on Mach-Zehnder Interferometer and Interleaver technologies applied to the access network model which has been given as a straight point of this thesis.

1.1. Principle of working of access networks

In this section access network is defined and evaluated according to its architecture. The functions of each part of the network are studied. There is deep study about PON (Passive Optical Network), thus it is the kind of technology that may be deployed in the near future. Its elements are studied and architecture solution is met.

The general structure of a telecommunication network consists of three main portions as shows in Figure 1.1: Backbone (or Core) Network, metro/regional network, and access network. Backbone networks are used for long-distance transport and metro/regional networks for grooming and multiplexing functions managing higher aggregated traffic.

An optical access network also called Fiber to the “x” (FTTx) networks. Compared with metro and backbone networks, access networks managed links with lower speeds rates and bandwidth capacities. An Access network is defined as the set of equipment and infrastructure needed to

perform the connection between the user's equipment and the carrier premise. The carrier premise is the point at which service providers interconnect with the access network. The local access network is also known as "the last mile" and "the local loop". Several types of access networks can be deployed, but this Master thesis is focused on optical ones, since they are considered the best way to build a flexible, future proof and full-service network platform with potentially unlimited capacity [2].

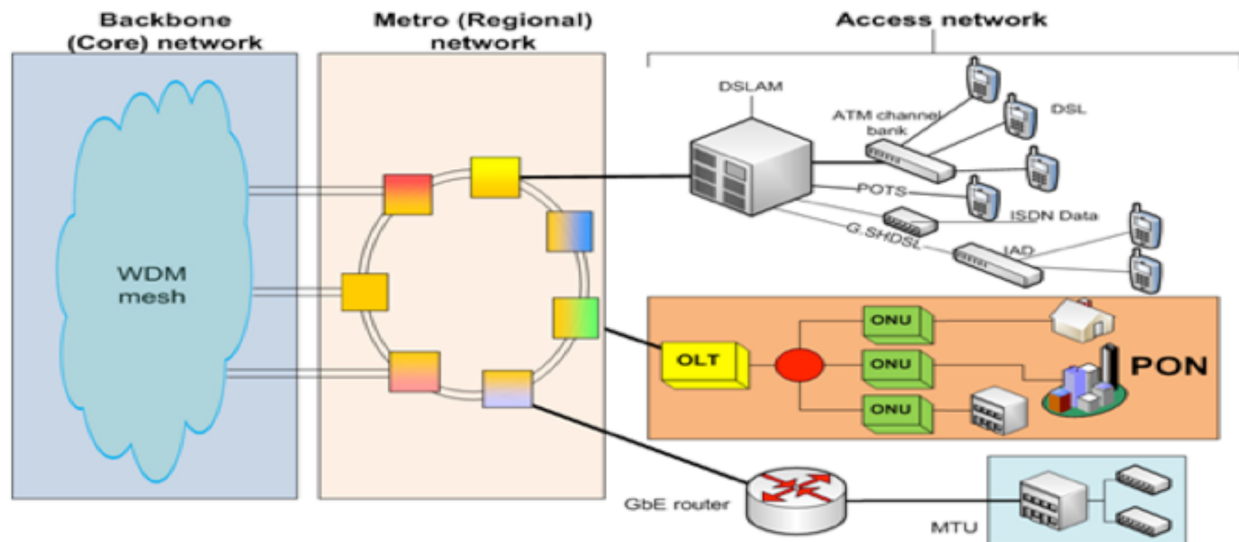


Figure 1.1. General structure of a telecommunication network

A passive optical network (PON) is a particular type of FTTx networks that uses P2MP (point-to-multipoint fiber premises) in which unpowered optical splitters are used to share part of the infrastructure enable a single optical fiber to serve multiple premises. Each splitter typically splits a fiber into 16, 32, or 64 fibers, depending on the manufacturer, and several splitters can be aggregated in a single cabinet. A beam splitter cannot provide any switching or buffering capabilities; the resulting connection is called a point-to-multipoint link. For such a connection, the optical network terminals on the customer's end must perform some special functions which would not otherwise be required. For example, due to the absence of switching capabilities, each signal leaving the central office must be broadcast to all users served by that splitter (including to those for whom the signal is not intended). It is therefore up to the optical network terminal to filter out any signals intended for other customers. In addition, since beam splitters cannot perform buffering, each individual optical network terminal must be coordinated in a multiplexing scheme to prevent signals leaving the customer from colliding at the intersection. Two types of multiplexing are possible for achieving this: wavelength-division multiplexing and time-division multiplexing. With wavelength-division multiplexing, each customer transmits their signal using a unique wavelength. With time-division multiplexing, the customers "take turns" transmitting information.

Over the past years, a series of network architectures have been shown up, mainly inspired by wavelength and time division multiplexing (WDM, TDM) [3].

Fiber-to-the-X (FTTX) technology has been extensively studied worldwide, aiming at the delivery of high bandwidth to users and for converging wireless and wire line communication.

1.2. Architectures

1.2.1. TDM-PON architecture

A TDM-PON uses a passive power splitter as the remote terminal that divide the incoming signal power to the different ONU's connected. Here all the users shared the same wavelength to transmit the information. In downstream, the signal from the OLT is multiplexed in different time slots and broadcasted to several ONU's (Weak security), where each ONU's recognize the data through the address labels embedded in the signal. The upstream traffic is transmitting by each ONU in burst mode and a mechanism to avoid collisions must be implemented. Two approaches could be used one or two fibers and one or two wavelength to provide bidirectional transmission. This in turns requires a TDM scheme to avoid crosstalk between the data stream sent by the users, which have to be also allocated with the help of MAC intelligence due to different drop span lengths. Each user obtains a time slot in this way, which is dedicated solely to its own data transmission. The allocation of time slot can vary over time to incorporate a dynamic bandwidth allocation mechanism between the users.

Typically in a standard commercial TDM-PON structure the OLT is connected to the ONUs via a 1:32 splitter and the maximum distance covered is usually 20 km. However in the scientific literature much higher split values up to 1:4000 have been reported [4]. Some advantages of TDM compared with WDM are that it not requires a complex wavelength management control and that the OLT power requirements are lower. However the main drawbacks are the lower bandwidth and granularity performances. PON standards like APON, BPON, EPON and G-PON uses this architecture.

GPON, EPON, XG-PON and 10G-EPON bandwidth is allocated by TDM (time division multiplexing) based schemes. Downstream, all data is transmitted to all ONUs; incoming data is than filtered based on port ID. In the upstream direction, the OLT controls the upstream channel by assigning a different time slot to each ONU. The OLT provides dynamic bandwidth allocation and prioritization between services using a MAC (Media Access Control) protocol [5].

TDM-PON networks splitters are used that: downstream, split the optical signal that reaches the OLT sending it to each ONT and upstream, combine each optical signal with the same wavelength emitted by each ONT into a single beam (see Figure 1.2). This reduces the cost of aggregation outside the exchange, since the cost of the optical splitter is low and it requires no power supply and no maintenance.

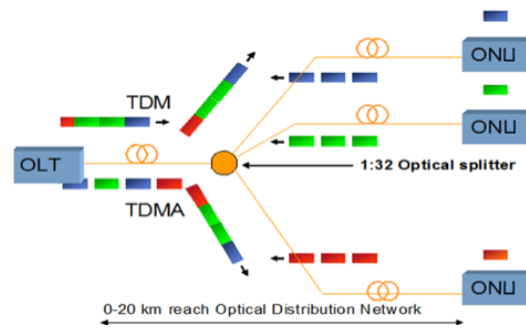


Figure 1.2. A typical TDM-PON architecture

It can be consistently combined with active Ethernet P2P and P2M configurations under one homogenous management system [6].

GPON and EPON have different characteristics in relation to the aggregated line rate and efficiency of the TDMA protocol that is the portion of total speed that can be used for payload. These two technologies also differ in terms of the power budget allowed between the OLT and the ONU, the ratios on the splitters and finally, GPON has a number of advantages due to greater protocol efficiency. Table 1.1 exemplifies the characteristics of these two architectures.

GPON vs. EPON	GPON (ITU-T G984)	EPON(IEEE 802.3ah)
Standard	ITU G.984	IEEE802ah
Data Packet Cell Size	53 to 1518 bytes	1518 bytes
Downstream line speed	2448 Mb/s	1250 Mb/s
Upstream line speed	1244 Mb/s	1250 Mb/s
Maximum derivation	1:64, 1:32 (typical)	1:32, 1:16 (typical)
Reach	20 km	10-20km
ODN Power Budgets	20-30 dB	21-26 –dB
Traffic supported	Ethernet, ATM,TDM	Ethernet
Voice	ATM, VoIP or TDM	VoIP

Table 1.1. Characteristics of GPON and EPON

At the technological level the most obvious difference between these two network types is the architectural approach at Layer 2 level. GPON with sub-layers in Layer 2 offers different types of traffic, such as: IP on Fast, Gigabit, or 10 Gbit Ethernet; TDM over SDH interfaces; and ATM between 155-622 Mbps. EPON, meanwhile, employs a single level 2 Layer that only uses Ethernet for transporting data, voice and video [6].

1.2.2. xWDM-PON architecture

TDMA PONs cannot fight with the requirements of future network evolution with respect to aggregated bandwidth (despite trends to increase the total bit rate to 10 Gb/s, e.g., for the so-called 10GE-PON) and the allowable power budget. The power budget limits both the PON splitting ratio and the reach/distance between OLT and ONU. The use of passive 1:N power splitters leads to severe losses (for example, a 1:32 splitter imposes an insertion/splitting loss >17 dB) and limits the attainable link lengths). These problems can be mitigated with wavelength division multiplexing (WDM) PONs. Here, ONUs are assigned individual wavelengths. This provides higher bandwidth to each ONU. In addition, each ONU operates on the individual bit rate rather than the aggregate (WDM) bit rate. Since ONUs are separated via physical wavelengths, aspects of privacy/security and network integrity are intrinsically accounted for [3]. These almost exclusively assume dense WDM-PONs, or ultra-dense WDM-PONs (DWDM-, UDWDM-PONs). While many of the proposals are technically interesting, it is clear that cost and performance, i.e., bandwidth per user, splitting ratio and maximum reach, are the dominant criteria for commercial success [6].

WDM-PON

Another approach to increase the share of common infrastructure can be the multiplexing in the optical frequency domain. The optical power splitter of TDM-PONs is thereby replaced by a WDM multiplexer as shown in Figure 1.3. A WDM-PON uses a passive WDM coupler as the remote terminal. A WDM-PON uses a passive WDM coupler as the RT. Signals for different ONUs are carried on independent wavelengths and multiplexed on a shared fiber infrastructure. Each ONU only receives its own wavelength creating a logical point-to-point connection where each ONU can transmit at its own bit rate without losses by power splitting and dedicated bandwidth with QoS. WDM has better security than TDM permitting simple fault localization. Also WDM presents better scalability resulting in higher bandwidth capacities without modifying the TDM infrastructure and long reaches are achieved. WDM-PON increases the spectral efficiency of the access networks by taking advantage of the high optical bandwidth of optical fibers. However WDM devices are significantly more expensive and a limitation in the number of wavelengths available is present and powerful OLTs are needed. Also each ONU needs a laser tuned in the specific wavelength so the implementation presents a high cost. Next Generation Fiber to the home technologies aim to use WDM-PON like the most viable solution in order to fully fit with the requirements specified [7].

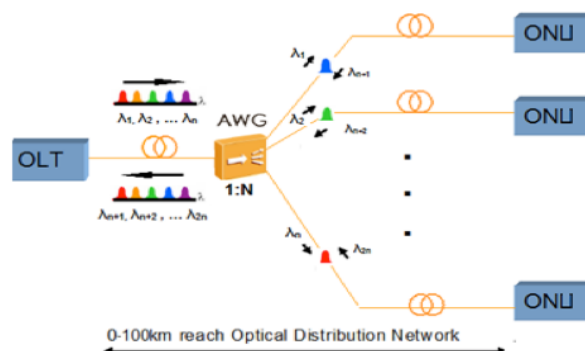


Figure 1.3. A typical WDM - PON network architecture

DWDM-PON

Dense Wavelength Division Multi/Demultiplexing (DWDM) – a class of WDM devices having a channel spacing less than or equal to 100 GHz (about 0.8 nm at 1550 nm), 200GHz as well. Devices within this class can cover one or more spectral bands. The key components of DWDM: single-mode LASER with stabilized wavelength (C Band and, L Band) by temperature, optical multiplexer-demultiplexer, optical amplifier (EDFA). Technical requirement of this method is that, it is going to work just with lasers which having very specific wavelengths. Therefore wavelengths are stable and then DWDM multiplexers/demultiplexers capable to distinguish each wavelength without crosstalk. Significant savings are possible with so called bi-directional transmission using DWDM, bidirectional systems are implemented in the same fiber [7].

Dense Wavelength Division Multi/Demultiplexing (DWDM) system can accommodate increases in demand for information traffic capacity by increasing the number of wavelength channels. Since it is more economical than installing new optical fiber cables, it is becoming more and more popular as every product is required to be more cost-effective. Until now, to cope with the increasing demand for information traffic capacity, further increasing the number of channels of DWDM system has been advanced by increasing the number of channels of Optical Multi/Demultiplexers itself, such as Arrayed Waveguide Grating (AWG). However, because it is necessary to get/make wavelength channel spacing narrower in such methods, it is very difficult to manufacture Optical Multi/Demultiplexers that separate adjacent channel signals precisely and satisfy required characteristics across all channels [7].

1.3. Architecture elements

In this section we will describe the elements of optical network, see Figure 1.4.

Access refers to a local network connecting the end user to the first Central Office (CO). Fiber Access Network shows a generic FTTH network based on DWDM deployments.

A PON consists of an optical line terminal (OLT) at the service provider's central office (CO) and a number of optical network units (ONUs) near end users. A PON configuration reduces the amount of fiber and CO equipment required compared with point to point architectures. The network equipment in the CO, or OLT, is connected via an optical splitter to the ONT installed at the customer's premises. Because multiple customers share the optical fiber and OLT, PONs substantially reduces the investment required to serve a given number of customers. PON systems use 1310 nm wavelength for the upstream and 1490 nm wavelength for the downstream. Sometimes a 1550 nm wavelength broadcast video overlay is added.

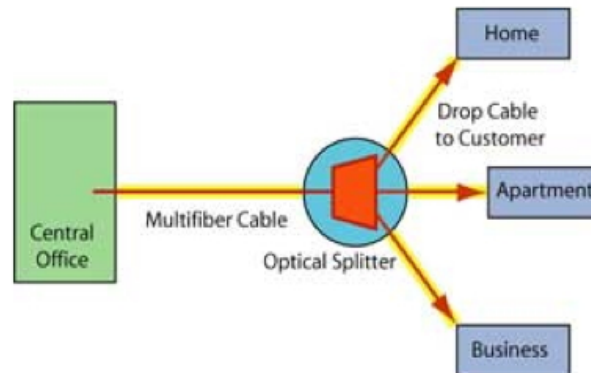


Figure 1.4. Elements of an optical network

CO Equipment

The CO centralizes the light generation for the whole network and its control. The optics at the CO includes OLT boards, WDM multiplexers, optical amplifiers, equalizers, protection switches and monitors. Protection is centrally actively controlled from the OLT.

OLT: basic device in PON deployments. It includes the OLT optical transmitter and the OLT optical receiver and aggregates the traffic from the customers to the core network or drops the data from the core network to the final user.

OLT's include the following features:

- A downstream frame processing for receiving an asynchronous transfer mode cell to generate a downstream frame, and converting a parallel data of the downstream frame into a serial data thereof.
- A wavelength division multiplexing for performing an electro/optical conversion of the serial data of the downstream frame and performing a wavelength division multiplexing thereof.
- An upstream frame processing for extracting data from the wavelength division multiplexing means, searching an overhead field, delineating a slot boundary, and processing a physical layer operations administration and maintenance (PLOAM) cell and a divided slot separately.
- A control signal generation for performing a media access control (MAC) protocol and generating variables and timing signals used for the downstream frame processing means and the upstream frame processing means.
- A control for controlling the downstream frame processing and the upstream frame processing by using the variables and the timing signals from the control signal generation.

ODF: this frame serves as an interface between the fibers that arrive to the central office and the equipment installed in it.

Tunable Laser at the OLT can be used.

ODN Equipment

The connection between the optical network terminal at the customer's premises and the equipment at the provider's Central Office is called Optical Distribution Network (ODN).

Optical fiber, MZI, Interleaver, Couplers can be used in ODN.

A passive optical network (PON) is a particular type of FTTH networks that uses P2MP (point-to-multipoint fiber premises) in which optical MZI or Commercial Interleaver are used to share part of the infrastructure enable a single optical fiber to serve multiple premises.

MZI and Interleaver are components of future access networks. MZI and Interleaver are used to combine different wavelengths from different fibers into a single fiber and they separate incoming wavelengths from the input fiber to different fibers. To implement Access part with these devices can use different techniques. We will focus on MZI it is one of the optical devices in the Access part which is combine carriers with coupler, channels are transmitted through the fibers and then separate each channel with another coupler and it is the technology which offers more benefits and can be integrated thus its potential cost is low. The design of MZI allows them to perform as Interleaver, with low price cost but with poor quality. In order to improve such a situation, Interleaving filter, which separates the incoming spectrum into two complementary sets of periodic spectra, has been studied in-depth. For example, in the laboratory it is possible to construct easily a DWDM system with 50-100 GHz.

Customer Equipment

At each customer's premises is a special type of Network Interface Device (NID). This device is called either an optical network terminal (ONT) or an optical network unit (ONU).

ONU: as we understood terminal equipment installed in customer's premise. It converts the optical signal into some format understandable to the customer's devices. Optical Network Unit use thin film filter technology to convert between optical and electrical signals.

The ONU terminates the PON and presents the native service interfaces to the user. These services can include voice (plain old telephone service (POTS) or voice over IP-VoIP), data (typically Ethernet), video.

In this architecture, each fiber leaving the Central Office (CO) goes to exactly one customer. Such networks can provide excellent bandwidth since each customer gets their own dedicated fiber extending all the way to the Central Office. However, this approach is extremely costly due to the amount of fiber and central office machinery required. It is usually used only in instances where the service are is very small and close to the CO. More commonly each fiber leaving the CO is actually shared by many customers. It is not until such a fiber gets relatively close to the customers that it is split into individual customer-specific fibers. Likewise OLTs, ONTs parameters and prices vary depending on the solution adopted.

CHAPTER 2

MZI AND INTERLEAVER THEORY AND COMPARISON

This master thesis is based on the use of Mach-Zehnder Interferometer (MZI) working as an Interleaver to reach the Next-Generation Access Networks goals. Nowadays, the implemented technology used in those Access Networks are Optical Interleavers which are responsible to split the Dense Wavelength-Division Multiplexing (DWDM) users. However, other techniques are being developed and this project tries to describe and compare this new techniques.

One of those new methods is to use a double-stage of stabilized MZIs instead of Interleavers to provide more strength (less losses) and cheaper devices to the Access Networks.

In this chapter is described the theoretical part of the MZI Device and Interleaver along with the comparison between them and few conclusions.

2.1. Mach-Zehnder Interferometer (MZI) description

The Mach-Zehnder Interferometer (MZI) is analyzed in this project as the most important device being considered in our measurement system.

It was concluded that the technique has a better quality in the reconstructed signal, as well as a better understanding of the problem, which uses a MZI (Mach-Zehnder Interferometer). While, for the results being satisfactory, the interferometer must meet minimum requirements in terms of FSR. The fact that the FSR imposed is four times the bandwidth of the laser device imposes physical limitations, which in turn must be optimized so that the device behaves satisfactory.

2.1.1. Ideal MZI

To fully characterize the MZI, as well as its limitations and further associated problems, it is advisable to use a more general terminology describing its functionality and its relevant parameters. Without taking into account any polarization effects, a possible approach to describe the transfer function of the device is to use the transfer matrix theory. In this theory, 2x2 matrices are used to represent transformation of field [8]:

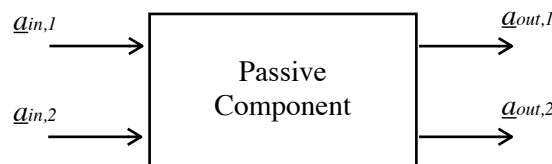


Figure 2.1. Block diagram of ideal Mach-Zehnder Interferometer as Passive Optical Device

The relation between in and out ports of the passive device are written as

$$\begin{pmatrix} \underline{a}_{out1} \\ \underline{a}_{out2} \end{pmatrix} = \begin{pmatrix} m_{11} & m_{12} \\ m_{21} & m_{22} \end{pmatrix} \cdot \begin{pmatrix} \underline{a}_{in1} \\ \underline{a}_{in2} \end{pmatrix} \quad (2.1)$$

The input and output vectors \underline{a}_1 and \underline{a}_2 correspond to the electric field of input signals and output phases, respectively, while the elements of the transfer matrix model the properties of the passive component, m_{ij} .

The schematic description of the MZI is shown below (Fig 2.2.)

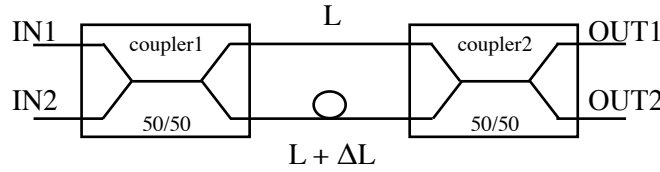


Figure 2.2. Illustration of an MZI with two inputs and two outputs

For our application we have to consider just one input. The input two will be left without signal.

In this case, the basic principle of this device is the Interferometer effect: at the first coupler the power of the input signal is divided equally along both outputs but the output 2 will get a $\pi/2$ phase shift relative to the output 1. After that the signal goes by the two arms with different lengths (L and $L + \Delta L$), what produces a delay in one of the arms (T_b) and therefore another phase shift between them. Before to get the last coupler the signal coming from the bottom-arm has a $\pi/2 + \beta\Delta L$ shift phase relative to the top-arm signal.

Finally when combined the two signals at the last coupler the signals which come from the input i and go to the input j (when $i \neq j$) get a $\pi/2$ shift phase again leaving a total relative phase difference between the two signals of $\pi/2 + \beta\Delta L - \pi/2 = \beta\Delta L$. For the proper operation of the MZI we will chose $\beta\Delta L = k\pi$ with odd k to have the signals in phase.

To summarize, the complete transfer matrix is follows:

$$M_{MZI} = \frac{1}{2} \begin{bmatrix} 1 & j \\ j & 1 \end{bmatrix} \cdot \begin{bmatrix} e^{j\Delta\varphi_1} & 0 \\ 0 & e^{j\Delta\varphi_2} \end{bmatrix} \cdot \begin{bmatrix} 1 & j \\ j & 1 \end{bmatrix} \quad (2.2)$$

In this moment we are going to detail the behavior of each component of the MZI as long as describe their mathematical expressions to understand the final effect that the MZI produces to the signal.

Beginning with an ideal 3dB optical coupler with power division 50%:50%, its transfer matrix is M_{3dB} :

$$M_{3dB} = \frac{1}{\sqrt{2}} \cdot \begin{bmatrix} 1 & j \\ j & 1 \end{bmatrix} \quad (2.3)$$

Where j is the imaginary unit ($j^2 = -1$) and it shows the $\pi/2$ phase change. In this coupler, as mentioned above, 50% of the power in each input port is coupled in the output ports and each input port is transferred to both of the output ports.

For a device that causes a delay between their outputs, as the bloc for the two fiber sections of fiber MZI, the transfer matrix is:

$$M_{\Delta\varphi} = \begin{pmatrix} e^{j\Delta\varphi_1} & 0 \\ 0 & e^{j\Delta\varphi_2} \end{pmatrix} = e^{j\Delta\varphi_2} \cdot \begin{pmatrix} e^{j\Delta\varphi} & 0 \\ 0 & 1 \end{pmatrix} \quad (2.4)$$

$$\Delta\varphi = \Delta\varphi_1 - \Delta\varphi_2$$

Note that $\Delta\phi$ represents the phase imbalance between the two arms of the MZI, and $\Delta\phi_1$ and $\Delta\phi_2$ stand for the supplementary optical phases when electric field travelled along the upper arm or in the other, respectively. Then $\Delta\phi_1$ and $\Delta\phi_2$ are defined by:

$$\Delta\varphi_1 = \frac{2\pi}{\lambda_0} \cdot n \cdot (L + \Delta L)$$

$$\Delta\varphi_2 = \frac{2\pi}{\lambda_0} \cdot n \cdot (L)$$
(2.5)

The supplementary length of fiber ΔL in the upper arm has to delay electrical field by the electrical field by the bit duration T_b , so we can write:

$$\Delta\varphi \equiv \Delta\varphi_1 - \Delta\varphi_2 = \frac{2\pi}{\lambda} \cdot n \cdot \Delta L = \omega_0 \cdot T \quad (2.6)$$

defining the optical frequency as ω_0 .

Once established partial matrices, with Eq. 2.3 and Eq. 2.4 the total transfer matrix of the MZI device is:

$$M_{MZI} = M_{3dB} \cdot M_{\Delta\varphi} \cdot M_{3dB}$$

$$M_{MZI} = \frac{e^{j\Delta\varphi_2}}{2} \cdot \begin{pmatrix} e^{j\Delta\varphi} - 1 & j(e^{j\Delta\varphi} + 1) \\ j(e^{j\Delta\varphi} + 1) & 1 - e^{j\Delta\varphi} \end{pmatrix} \quad (2.7)$$

For the proper operation of the system we want to test we must insert the optical field in input port 1 and leave the second input disconnected. In this case the output fields amplitudes can be written as:

$$\begin{pmatrix} \underline{a}_{out1} \\ \underline{a}_{out2} \end{pmatrix} = \begin{pmatrix} m_{11} & m_{12} \\ m_{21} & m_{22} \end{pmatrix} \cdot \begin{pmatrix} \underline{a}_{in1} \\ 0 \end{pmatrix} \quad (2.8)$$

For evaluation of power transmission in the two output ports, the optical powers of the device can be expressed as:

$$\begin{aligned}
P_{out1} &= \frac{1}{4} \cdot (e^{j\omega_0 T} - 1) \cdot (e^{-j\omega_0 T} - 1) \cdot P_{in1} \\
P_{out2} &= \frac{1}{4} \cdot (e^{j\omega_0 T} - 1) \cdot (e^{-j\omega_0 T} - 1) \cdot P_{in2}
\end{aligned} \tag{2.9}$$

These equations give as the final transfer function of the MZI:

$$\begin{aligned}
T_1 &= \frac{P_{out1}}{P_{in1}} = \frac{1}{4} \cdot (e^{j\omega_0 T} - 1) \cdot (e^{-j\omega_0 T} - 1) = \sin^2(\omega_0 T) \\
T_2 &= \frac{P_{out2}}{P_{in2}} = \frac{1}{4} \cdot (e^{j\omega_0 T} - 1) \cdot (e^{-j\omega_0 T} - 1) = \cos^2(\omega_0 T)
\end{aligned} \tag{2.10}$$

where $\omega_0 = 2\pi f$, and f is the optical frequency.

These two last expressions bring definition of four parameters for the MZI. First, the FSR (Free Spectrum Range) is defined as the spectral period of transmission spectrum. The differential delay T_b is then equal to $1/\text{FSR}$. Three, the Insertion loss (IL) of MZI will be the absolute max value of transmission in dB scale, in each port. For an ideal MZI, the IL is 0 dB in two ports. Last, the isolation of MZI will be the gap between maximal and minimal transmission values of the spectrum, also in each port [8]. Here, the minimal transmission is 0 ($-\infty$ dB) and the maximum is 1 (0 dB). The ideally isolation for the two ports is ∞ . The power transmission in dB scale of the two output ports are represented in Figure 2.3. and in Figure 2.4.

1. First, we define commonly called FSR (Free Spectral Range) and the period of the transmission spectrum, so that the differential delay, T , is equal to $1/\text{FSR}$.

The simulated case has a FSR, which will work with lasers with modulation bandwidths. The gap between the two branches needs to obtain the desired FSR and can be designed using the following expression:

$$FSR = \frac{c}{\Delta L \cdot n_{eff}} \tag{2.11}$$

Where ΔL is the length difference between the two branches and n_{eff} is effective refractive index (1.4682 for this study).

As you can see, the calculation is independent of the FSR loss factors; this will ensure that always meets one of the fundamental requirements, independently of the non-idealities of the components that comprise the MZI.

2. Second, the *insertion losses* of the MZI take the maximum value of the coefficient transmission in dB at each port. In the ideal case these losses are null; in the case of taking them into account as L_{MZI} :

$$L_{MZI1} \equiv \max(T_1) \tag{2.12}$$

$$L_{MZI2} \equiv \max(T_2)$$

3. Finally, we define *an extinction ratio* of output ports (ER) as the ratio between the maximum and minimum value of the transmission coefficient, respectively:

$$ER_1 \equiv \frac{\max(T_1)}{\min(T_1)} \quad (2.13)$$

$$ER_2 \equiv \frac{\max(T_2)}{\min(T_2)}$$

Obviously, the maximum possible value of the transmission coefficient at any port is 1 (0 dB Insertion loss is always null), while the minimum is 0 ($-\infty$ dB). Thus, the ideal value of the extinction ratio is $+\infty$.

In Figure 2.3. and Figure 2.4. we can see the graphic representation of each transmission coefficients port, in dB, depending on frequency. We can also see the FSR and indicated ER, assuming insertion losses null.

Likewise, the transfer function of the MZI is periodic, of the form:

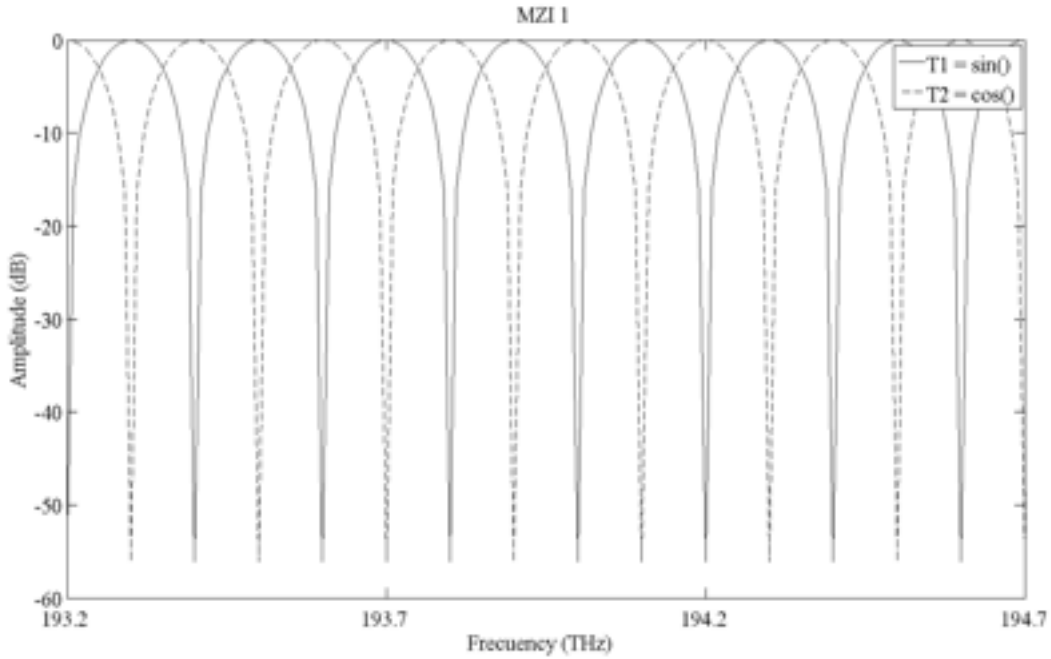


Figure 2.3. Power transmission of ideal MZI1 response

As it may be seen in the figure above, idealities are not considered in the ER MZI (Extinction Ratio), tends to be infinite. Figure 2.3 and Figure 2.4 are representing frequency response of ideal case. It means in this case we don't have loss, shift deviation, losses in fiber, temperature shift. Difference between two graphs is in FSR. In this case in Figure 2.3 is FSR1, which has double FSR, but in Figure 2.4 is FSR2. In Figure 2.3 we have double FSR ($2 \times \text{FSR}$) to correct behavior of complex system to separate users in the correct way.

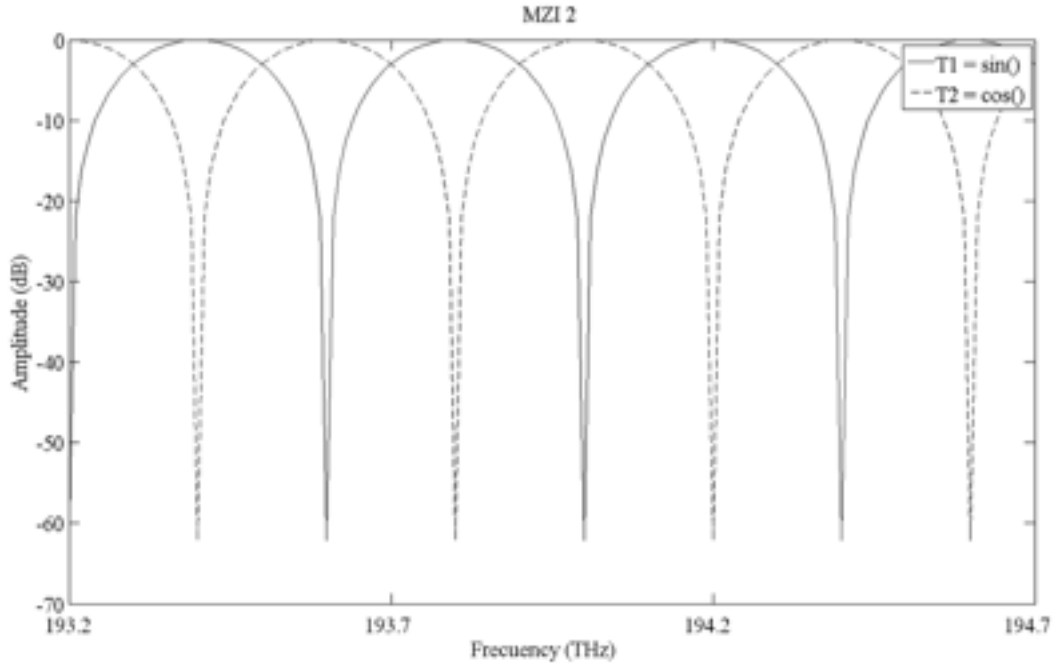


Figure 2.4. Power transmission of ideal MZI2 response

2.1.2. Non-Ideal MZI

Limitations and problems

MZI behavior described above occurs only in ideal conditions. In practice there are many factors, both intrinsically related to their own MZI (losses unequal arms of the interferometer, couplers imperfect) and external causes ('offset' frequency, temperature, polarization), which directly affect their performance. Then we will detail these limitations and their impact on the performance of the MZI (FSR and ER, mainly).

Intrinsic degradation of MZI

Some of the factors that influence the performance degradation are due to MZI exclusively on the characteristics of its constituent elements. Then will evaluate its impact on the MZI transfer function depending on the frequency.

As seen in Figure 2.2, a MZI is formed by a low number of elements. One of these elements is the coupler, which is why we are going to detail how the non-idealities affect the behavior of the interferometer

Transmission spectra of non-ideal MZIs

The transmissions T_1 and T_2 for the two outputs take a different form Eq. 2.10. For an optical coupler with a_1^2/b_1^2 coupling ratios, the transfer matrix can be written as Eq. 2.14. Adding a loss in one of the two arms, the phase shifter's matrix became Eq. 2.15 [8]:

The following transfer matrix of a coupler has the form:

$$M_{ACOP} = \begin{bmatrix} a & jb \\ jb & a \end{bmatrix} \quad (2.14)$$

With $a^2 + b^2 = 1$:

$$M'_{\Delta\varphi} = \begin{pmatrix} e^{j\Delta\varphi_1} & 0 \\ 0 & \alpha \cdot e^{j\Delta\varphi_2} \end{pmatrix} = e^{j\Delta\varphi_2} \cdot \begin{pmatrix} e^{j\Delta\varphi} & 0 \\ 0 & \alpha \end{pmatrix} \quad (2.15)$$

where α takes places for the optical loss in the under arm. The total transfer matrix is calculated as previous, leading to:

$$M'_{MZI} = e^{j\Delta\varphi_2} \cdot \begin{pmatrix} a_2 & jb_2 \\ jb_2 & a_2 \end{pmatrix} \cdot \begin{pmatrix} e^{j\Delta\varphi} & 0 \\ 0 & \alpha \end{pmatrix} \cdot \begin{pmatrix} a_1 & jb_1 \\ jb_1 & a_1 \end{pmatrix} \quad (2.16)$$

The transfer function remains equivalent as follows:

$$M_{MZI} = \begin{bmatrix} a_1 \cdot a_2 \cdot e^{j\varphi_1} - b_1 \cdot b_2 \cdot e^{j\varphi_2} & a_1 \cdot b_2 \cdot j \cdot e^{j\varphi_1} + b_1 \cdot a_2 \cdot j \cdot e^{j\varphi_2} \\ b_1 \cdot a_2 \cdot j \cdot e^{j\varphi_1} + a_1 \cdot b_2 \cdot j \cdot e^{j\varphi_2} & a_1 \cdot a_2 \cdot e^{j\varphi_2} - b_1 \cdot b_2 \cdot e^{j\varphi_1} \end{bmatrix} \quad (2.17)$$

where the index i in a_i and b_i denotes the i^{th} coupler of MZI device. For an ideal MZI, we take a_1 , a_2 , b_1 and b_2 equal to 1, and $\alpha = 1$.

Operating, we have that transfer functions of the two ports T_1 and T_2 of the MZI response to the expression:

$$\begin{cases} T'_1 = a_1^2 \cdot a_2^2 + b_1^2 \cdot b_2^2 \cdot \alpha^2 - 2 \cdot a_1 a_2 b_1 b_2 \cdot \alpha \cdot \cos(2\pi\nu T_b) \\ T'_1 = a_1^2 \cdot b_2^2 + b_1^2 \cdot a_2^2 \cdot \alpha^2 + 2 \cdot a_1 a_2 b_1 b_2 \cdot \alpha \cdot \cos(2\pi\nu T_b) \end{cases} \quad (2.18)$$

Operating leads to expressions for calculating the Insertion Loss (IL) and Extinction Ratio (ER).

With Eq. 2.16 we can write the isolation ER value in each port:

$$ER_1(dB) = 10 \cdot \log \left[\left(\frac{a_1 \cdot a_2 + b_1 \cdot b_2}{a_1 \cdot a_2 - b_1 \cdot b_2} \right)^2 \right] \quad (2.19)$$

$$ER_2(dB) = 10 \cdot \log \left[\left(\frac{a_1 \cdot b_2 + b_1 \cdot a_2}{a_1 \cdot b_2 - b_1 \cdot a_2} \right)^2 \right] \quad (2.20)$$

Thus we see that the ratio of extinction that was infinite in the ideal case, you can see really limited in the case of not having a 50%:50% ratio in the couplers.

Interestingly, the ratio of extinction at port 2 is not affected by the use of imperfect couplers, unless they are identical. In the case are slightly different from the two ports will be affected by a worsening extinction ratio. Another parameter of the MZI is affected by the imperfection of couplers are insertion losses.

The insertion loss of a non-ideal MZI is not equal to 0 dB, and will be different for the two output ports:

$$IL_1(dB) = \left| 10 \cdot \log \left[(a_1 \cdot a_2 + b_1 \cdot b_2)^2 \right] \right| \quad (2.21)$$

$$IL_2(dB) = \left| 10 \cdot \log \left[(a_1 \cdot b_2 + b_1 \cdot a_2)^2 \right] \right| \quad (2.22)$$

In Figure 2.5, Figure 2.6 you can see the graphic representation of each transmission coefficients port, in dB, depending on frequency. We can also see the FSR and indicated ER.

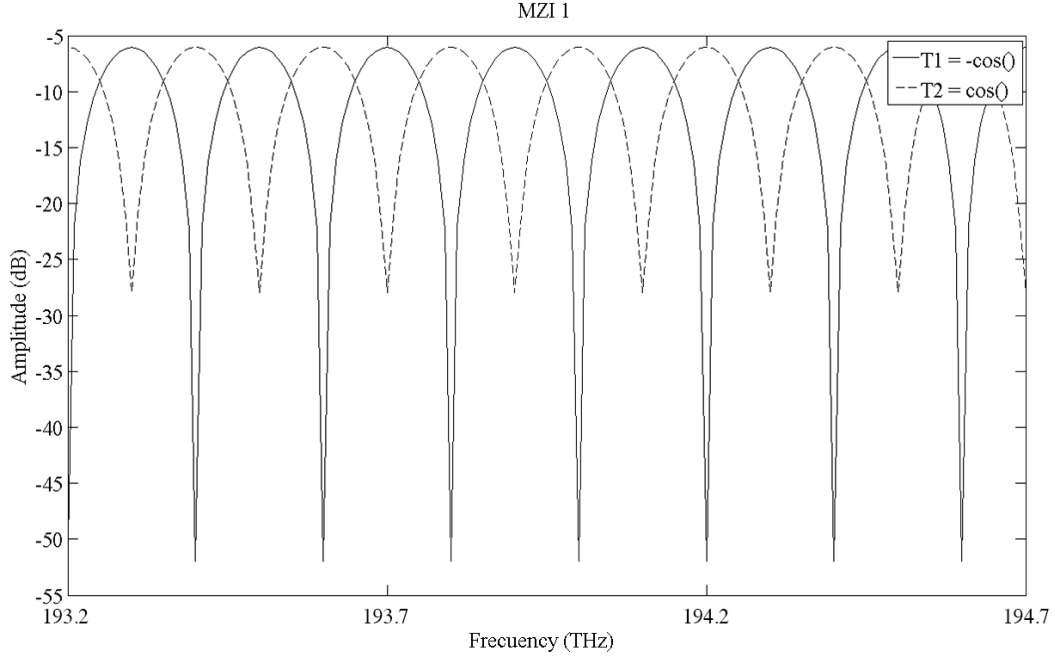


Figure 2.5. Power spectrum of a non-ideal MZI1: the coupling ratios are 51 %:49% and 55 %;45%

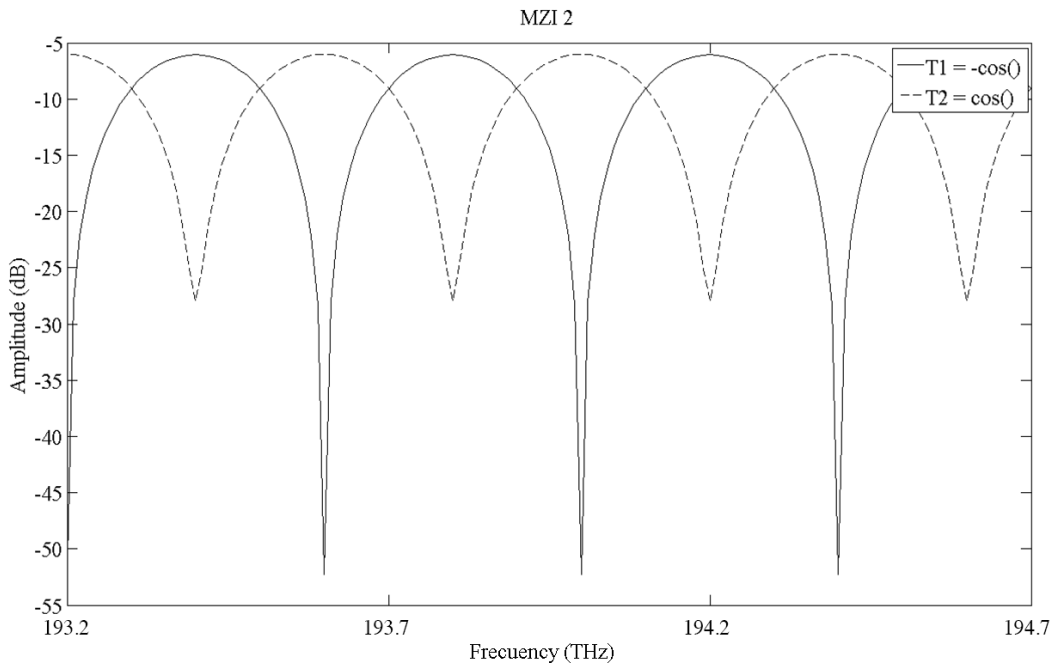


Figure 2.6. Power spectrum of a non-ideal MZI2: the coupling ratios are 51 %:49% and 55 %;45%

2.1.3. Influence of Polarization

We said that the MZI was polarization sensitive: when light travels in two arms, polarization is randomly fluctuating. At the second optical coupler, it is highly probable that polarizations of fields in two arms will be different, and the interference will not be completely destructive. A few part of optical power will be transmitted and the isolation value will be degraded by this way. In order to reduce these isolations degradations, the lengths of the two arms has to be as small as possible and the implementation of this system must be without mechanical constraints to ensure a low sensitivity of the whole MZI device to polarization effects.

There is source MZI dependence to polarization which can cause losses in the interferometer. In order to achieve the best performance, the state of polarization of waves each of the paths must be the closest one to the other wave. Bias differences may be caused by the birefringence of the optical fiber.

Birefringence has its origin in the phenomenon caused when an optical signal is propagated through a waveguide, the refractive index of which is higher than the surroundings. Also birefringence of the fiber could be because of the difference in propagation speed due to no idealities in the geometry. The physical cause of the differences in propagation velocities is that each component has a different refractive index. The difference between refractive indexes allow numerically quantify the birefringence of the fiber.

2.1.4. Instability of the MZI

The main problem of system is stabilized and adjusts fluctuates frequency response of MZI.

MZI thermal drift

Thermal drift caused by internal heating of equipment during normal operation or by changes in external ambient temperature.

If the interferometer is in a variable temperature (written as T in the following equations) environment, two effects will induce a frequency shift on the interferometer transmission spectra [8]:

1. The thermo-optic effect which modifies the value of the core index, resulting in a variation of the effective index δn_{eff} , thus inducing a variation of the propagation constant $\delta\beta$ [8].
2. Thermal expansion effect where phase variation induced by the differential length variation $\delta(\Delta L)$. The variation of the differential phase between the two arms obtained by these two effects is finally given by 2.24 [8].

$$\Delta\varphi = \beta \cdot \Delta L \Rightarrow \delta(\Delta\varphi) = \delta\beta \cdot \Delta L + \beta \cdot \delta(\Delta L) \quad (2.23)$$

$$\delta\Delta\varphi = \frac{2\pi}{\lambda} \delta n_{eff} \cdot \Delta L + \beta \cdot a_t \cdot \Delta L \cdot \delta T \quad (2.24)$$

With these two formulas we can obtain $\delta\Delta L$ – differential length variation to see difference of insertion loss in two arms [8].

$$\beta \cdot \delta(\Delta L) = \frac{2\pi}{\lambda} \delta n_{eff} \cdot \Delta L + \beta \cdot a_t \cdot \Delta L \cdot \delta T - \delta\beta \cdot \Delta L \quad (2.25)$$

This frequency shift shows that MZI filters have to be temperature-stabilized when used as passive structure. We needed it to maintain the transmission peaks on channels.

The implementations of this system have to be without mechanical constraints to provide a low sensitivity of the whole MZI device.

A temperature stabilized MZI must be used. For this application an accurate temperature stabilization process has to be developed which will consist of a general regulation circuit which stabilizes the temperature for the whole MZI device and if not it will bring losses to every channels because of unbalanced system.

Initially, we have to isolate system from environment changes temperature to provide a low sensitivity of the whole MZI device. We can perform this by packaging the MZI device in an aluminum box stabilized with Peltier elements. With this solution according to the theoretical part the general MZI insulation reduces exterior temperature fluctuation on the MZI; the peaks present no more frequency shift, but the peak frequencies still do not correspond to the ITU frequencies.

To adjust the center of frequency of both arms we will insert Peltier₁ for one arm and Peltier₂ for another arm for appropriately tuning by using different heating of the arm.

In this paper, we present interleaving filter with a tandem configuration based on Mach-Zehnder Interferometers (MZIs). MZI needs to have two fundamental criteria to be like Interleaver: high Extinction Ratio and stability in frequency. When a MZI device is working like a filter it has the same behavior than an Interleaver but the difference is in the quality. If we can control the stability of MZI device and reduce insertion losses we can achieve that performance of MZI like a good quality Interleaver which we are going to describe in the next section.

2.2. Passive Interleaver description

Optical Interleaving filters are attractive components in Wavelength Division Multi/Demultiplexing (WDM) systems especially narrower than 100GHz channel spacing system. An innovative technique for expanding the number of channels per fiber involves an optical device, called an optical Interleaver. For example, in most DWDM equipment, the standard channel spacing is 100 GHz. But spacing the signal-carrying frequencies every 50 or even 25 GHz can double or even quadruple the number of channels per fiber. This job is accomplished by an optical Interleaver. Such a device takes two multiplexed signals with 100-GHz spacing and interleaves them, creating a DWDM signal with channels spaced 50 GHz apart. The process can be repeated, creating even denser composite signals with 25-GHz or 12.5-GHz spacing. The signals at the receiving end are recovered with the same devices used as splitters or optical de-interleavers. Thus, devices and/or networks can be upgraded without requiring that all devices be upgraded, or network bandwidth can.

Optical Interleaver products used as a DEMUX (or MUX) device. When used in the MUX configuration, the Interleaver combines two stream of periodic optical signals (one stream carries even channels and the other carries odd channels) into one stream of signals of half the channel spacing. When used in the demux configuration, the signal is separated into two complementary streams (even and odd channels) of twice the channel spacing. Each optical Interleaver device is optimized to cover either C- or L-band wavelengths, with the option of covering C+L band. The current standard optical Interleaver product family supports 100-200, 50-100, 25-50, and 12.5-25 GHz channel spacing, covering up to 90, 180, 360, and 720 channels, respectively, as well as other custom spacings in that range, such as 33.33-66.66 GHz. Dual-stage optical Interleavers are also available.

2.2.1. Principle of working

A workshop on interleaver technologies was maintained as part of the Optical Fiber Communication Workshop Series [9]. In order to improve such a situation, Interleaving filter, which separates the incoming spectrum into two complementary sets of periodic spectra, has been studied in-depth. For example, it is possible to construct easily a DWDM system with 50-GHz or narrower-channel spacing by combining an interleaving filter and two WDM filters [10].

There are several types of interleaving filters, such as Birefringent Gires-Tournois (BGT) interferometer-type, Bulk Birefringent Crystal-type, fiber-type and Planar Lightwave Circuit (PLC)-type. Each type has merits and demerits. The composition of BGT interferometer-type

is similar to Michelson interferometer. It consists of a Polarization Beam Splitters, Waveplate and a Gires-Tournois (GT) cavity [10]. Although a GT cavity has similar structure to a Fabry-Perot cavity, the reflectivities of two facets in each mirror are very different. One is 100 % reflective and the other has a low reflectivity of 11 %. As almost all of the optical paths of a BGT interferometer are in air, temperature dependent refractive index change is very small. Therefore, it does not need a temperature controller to keep the device temperature constant. Bulk birefringent crystal-type consists of several parts such as a Polarization Beam Splitter, a Multiple-Waveplate and a Polarization Rotator that are all made of birefringent materials. The principle and design concept of periodical box-like response is similar to that of a cascaded Mach-Zehnder Interferometers (MZIs) circuit based on a PLC. By using two kinds of Birefringent materials that have opposite temperature coefficient to each other, a thermalization (formation of temperature-independent) succeeded. Fiber-type is based on a cascaded-MZIs configuration that consists of several couplers and two different lengths of optical fiber connecting between couplers. The principle is the same as that of a PLC. Fiber-type has a low insertion loss because it is made of optical fiber. Because the refractive index of optical fiber has large temperature dependence, it is necessary to keep the temperature constant when using it. Therefore, it is necessary to provide a temperature controller and electrical power supply to drive it, which is a weak point of this type of Interleaving filter in comparison with the other two types mentioned above [10].

In this project we present Fiber Type 1x2 (such as 50/100-GHz) interleaving filters with configuration based on Mach-Zehnder Interferometers (MZIs). The circuit using Planar Lightwave Circuit (PLC) technique. An interleaver is a periodic optical filter that combines or separates a comb of dense wavelength-division multiplexed (DWDM) signals. The periodic nature of the interleaver filter reduces the number of Fourier components required for a flat passband and high-isolation rejection band. This is in contrast to single-channel add/drop filters that synthesize a single narrow-band filter over a wide rejection band. Because the interleaver requires fewer Fourier components, the same flat top, sharp edge response of a higher-order narrow-band filter can be realized with only a few sections.

An interleaver, also known as a slicer, is an optical filter having at least one input and two complementary outputs, with an optical transfer function that is periodic in frequency. The original design separates (or combines) even channels from odd channels across a DWDM comb. This is denoted a 1:2 interleaver. The logical extension is the periodic separation of one in every $2n$ channels, such as the 1:4 function illustrated in Fig. 2.8(b). A different variation is the banded interleaver, Fig. 2.8(c), where bands of channels are periodically separated. This is a more difficult

filter to make because the filter roll-off must be steeper in relation to the filter period. Finally, in contrast with the previous three filters, the asymmetric filter periodically separates one channel in N , Fig. 2.8(d) [9].

This way, for example, even-numbered optical channels can be routed to one output port while the odd-numbered channels will emerge from the other output port, as illustrated in Fig.2.7. Such an interleaver can also be used the other way round, i. e. for combining two “combs” of optical channels, one shifted by half a channel spacing with respect to the other, into a single comb with half the channel spacing.

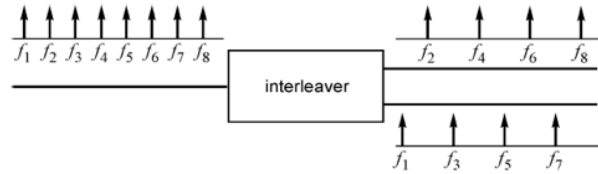


Figure 2.7. Original interleaver: even and odd channels are separated onto two different ports

Besides the basic 1:2 interleaver function illustrated in Fig.2.7, more complicated configurations may be used, as shown in Fig.2.8. In principle, any optical (de)multiplexer having a periodic response with frequency may be used as an interleaver, for example arrayed waveguide gratings (AWG), Fabry–Perot resonators or ring resonators. Interleavers that are applied in optical telecommunications should have a frequency-periodic response, because the ITU grid specifying the optical channels defines a set of equidistant optical frequencies. Despite this, these devices are sometimes referred to as wavelength slicers or wavelength interleavers. (If an interleaver is periodic in frequency it will not be strictly periodic in wavelength since $\lambda = c/f$, with c the vacuum speed of light.) If needed, however, strictly wavelength periodic interleavers can be designed [9].

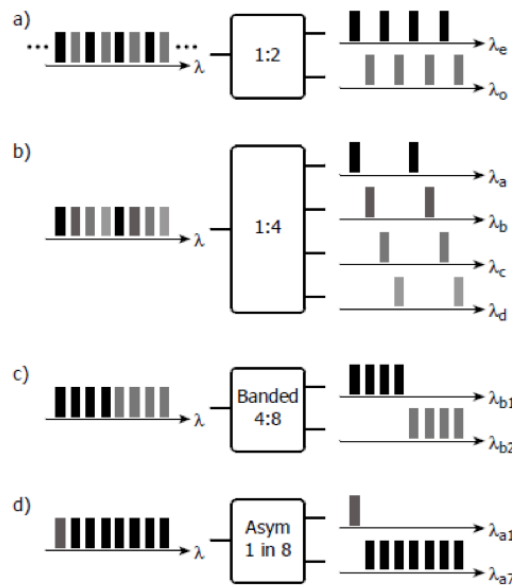


Fig. 2.8. Interleaver functional types. All filter functions are periodic in frequency and are reciprocal. a) Original interleaver: even and odd channels are separated onto two different

ports. b) Separation of channels out to 1:4 or higher. c) Banded interleaver, separates even and odd bands of channels. More difficult than 1:2 interleaver because of higher filter roll-off. d) Asymmetric interleaver separates one channel in N [9].

The filter function of an interleaver and its period are separable. Interleavers have been demonstrated that resolve a comb of DWDM frequencies on 100 GHz, 50 GHz, 25 GHz, and 12.5 GHz centers. The period is governed by the free spectral range of the core elements, where narrower channel spacing is achieved by a longer optical path. There are many specifications and design goals that are common to interleavers regardless of the particular technology used for implementation [9].

The study of interleaver technologies is interesting because of the variety of successful architectures. In terms of the variety of interleaver solutions, there is no clear technology; each technology has its unique features and its own economics. Application will determine which technology is most suitable, and different applications may require different technologies. Moreover, with the technological and theoretical foundations laid thus far, more sophisticated applications and denser function integration will continue to improve the economics and application breadth for interleaving filters, cementing their existence in the optical network [9].

2.2.2. 50 GHz Passive Interleaver

Optical Interleaver is an elegant solution that lets operators flexibly implement scalable DWDM networks. Low-dispersion Interleavers greatly expand wavelength channel counts in DWDM systems. It is the best solution to upgrade existing 100 GHz spacing transport system. DWDM Interleavers feature excellent wide, flat passband and high isolation. Both MUX and DEMUX functions are supported. These Interleavers are a-thermal and therefore require no temperature control. Its stable center wavelength accuracy over C or L band 80 channels is suitable for higher bit rate application [9].

The Interleaver can be deployed with the initial DWDM installation to make the DWDM system compatible with future versions and to avoid downtime when the additional capacity is required. The use of 50-GHz channel spacing is a good option for increasing capacity. To accomplish this upgrade, a 50/100-GHz Interleaver/de-Interleaver is required for multiplexing and demultiplexing the additional channels [9].

A summary of its features could be :

- Compact size
- Low dispersion
- Completely Passive
- Ultra-low Insertion Loss
- Highly stable and reliable
- Epoxy-free optical path
- Environmental green plan Compliance
- High channel isolation
- Wide clear bandwidth
- Full C- or L- band coverage
- A-thermal design

Performance Specification

In the Table 2.1 below we can see parameters of 50 GHz Passive Interleaver.

Parameter	Min	Max	Units
Frequency	192000	196000	GHz
Insertion loss		1.35 dB	dB
Ripple		0.04	dB
Insertion loss Uniformity		0.20	dB
Adjacent Channel Isolation	22.8		dB
PDL		0.09	dB
PMD		<0.30	ps
Chromatic Dispersion (absolute value)		20.0	ps/nm
Return Loss	54		dB
Directivity	64		dB

Table 2.1. Parameter of the commercial 50GHz Passive Interleaver

2.3. Comparison of commercial Interleaver and MZI based Interleaver

In this table 2.2 we are going to compare Commercial Optical Interleaver with Interleaver based on MZI filters which we are going to design in the laboratory. One of the main problem of MZI device that it does not has stability and that's why it is necessary to provide a temperature controller and electrical power supply to drive it, which is a weak point of this type of Interleaving filter in comparison with Commercial Passive Interleaver , but also MZI offers advantages: it is propose a simple and cost-effective design.

Commercial Interleaver	Interleaver based on MZI
High cost: about 900€	Low cost: less than 50€ counting all components inside
Low insertion loss: about 2 dB	Low insertion loss: about 2.4 dB
Easy to scale	Easy to scale
Small size: 15x10x4 cm	Bigger size: 80x80x5 cm
Only possible to built it in special laboratories	Can be built in all optics laboratories
Stable	Not stable without external control or feedback circuit.

Table 2.2. Comparison between Commercial Interleaver and Interleaver based on MZI

2.4. Summary

We determined two optical device: commercial Optical Interleaver 50 GHz and Interleaver based on Mach-Zehnder Interferometer .MZI device are commonly used to form Interleaver. It is the Interleaver with simple structure, low cost and compact size, can be easily implemented with inexpensive material and mature preparation technology, but MZI device is also going to have disadvantages in terms of non-stability and insertion loss. We have to analyze environmental temperature sensitivity and fabrication tolerance which making MZI device unbalanced.

CHAPTER 3

DESIGN OF DOUBLE-STAGE MZI MATLAB SIMULATION

The previous step before to build any system is to design and simulate it according the theory studied in advance. In this 3rd chapter we will describe the process of that simulation and it is organized as follows: in first section we introduce the idea of implementation of double-stage Mach-Zehnder Interferometer, after that in the second section we describe the main objectives of the project. Moving forward to the third section we will see the system implementation of all-fiber MZI and finally in the fourth and fifth section we present the purpose of simulation of the designed double-stage MZI with Matlab and its results. The last section, number 6, is reserved for the summary to close the chapter 3.

3.1. Introduction

In order to improve transmission efficiency of optical-fiber communication system presently and system in the future, an optical interleaver proposed and investigated which is based on structure of MZI and offers the advantages of compactness, ruggedness, and better compatibility with other integrated optical circuits. Simple method of designing optical interleaver is proposed for all fiber unbalanced Mach-Zehnder interferometer (MZI) with fiber coupled structure. The results of designing example with double-stage MZIs structure are presented.

The best solution could be to build cascade system of MZI optical devices for increasing users.

According to the cost the best solution for having cost- effective and performance system will be performance in the access part. MZI is the most important optical device being considered in our measurement system. We propose MZI a cost effective way for smooth evolution of PON system with less loss and maximum number of users by cascade building of MZI. With this current system which we are going presented and tested in the lab is going to provide high value of services to large part of population information society.

3.2. Objectives

- i. Study and evaluate through both theoretic analysis and simulations with the software Matlab the performance of Ideal and Non-Ideal MZI as an Optical filter.
- ii. Study theoretically the Mach-Zehnder Interferometer Optical Filter.
- iii. Plot and analyze results of MZI with Matlab.

3.3. Schema and Concept

Assuming that we understood the principle structure and behavior of a single MZI, we will proceed describing the final system desired and how it will work without focusing on each MZI since their behavior is already discussed in the chapter 2.

The final goal of our system is to split the DWDM users in the access network avoiding the use of interleavers but using cascaded-MZIs. The number of stages and MZIs will depend on the number of users following the next simple equation:

$$N_{STAGES} = \log_2(N_{USERS}) \quad (3.1)$$

$$N_{MZIs} = N_{USERS} - 1 \quad (3.2)$$

In this project, although in normal conditions of DWDM we have about 16 or 32 users, we have chosen 4 users to proof that our system works as expected. That means we will simulate a double-stage MZI.

The configuration of the double-stage MZI is shown in Figure 3.1, which consists of three Mach-Zehnder Interferometer (MZI1, MZI2 and MZI3).

In that figure are represented the MZIs as a black box with only one input due we don't use the second input in any MZI.

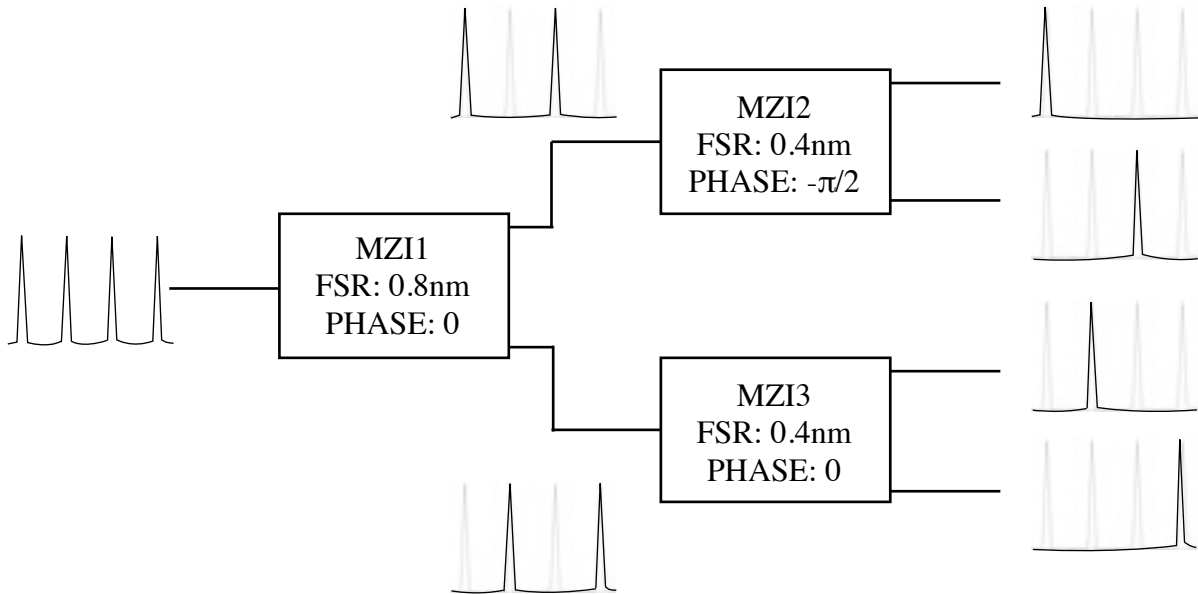


Figure 3.1. Double-Stage MZI schema with 4 users input and split output signals

This figure shows that it is necessary to halve the FSR in each stage. We can obtain the desired FSR₁ and FSR₂ using the following expression:

$$FSR_1 = \frac{c}{2 \cdot n_{eff} \cdot \Delta L_1} \quad (3.3)$$

$$FSR_2 = \frac{c}{2 \cdot n_{eff} \cdot \Delta L_2} \quad (3.4)$$

Where ΔL_1 and ΔL_2 are the length difference between the two arms of the first stage (MZI1) and the second stage (MZI2 and MZI3) severally and where n_{eff} is the effective refractive index (1.4682 for this simulation).

As mentioned above we will not describe each MZI because although each stage has different FSR the description would be exactly the same than in chapter 2 but changing the length of the fiber (ΔL) between both couplers of each MZI.

Note that in this point we are able to define our system as a black box with one input and four outputs (see Figure 3.2) but in this case we should re-define the Insertion Loss and the Extinction Ratio for our total system.

Assuming that every MZI has the same technology parameters and therefore the same Matrix function, the Equations 2.19 to 2.22 are re-defined for our total system as follows:

$$ER_1(dB) = 20 \cdot \log \left[\left(\frac{a_1 \cdot a_2 + b_1 \cdot b_2}{a_1 \cdot a_2 - b_1 \cdot b_2} \right)^2 \right] \quad (3.5)$$

$$ER_2(dB) = 10 \cdot \log \left[\left(\frac{a_1 \cdot a_2 + b_1 \cdot b_2}{a_1 \cdot a_2 - b_1 \cdot b_2} \right)^2 \right] + 10 \cdot \log \left[\left(\frac{a_1 \cdot b_2 + b_1 \cdot a_2}{a_1 \cdot b_2 - b_1 \cdot a_2} \right)^2 \right] \quad (3.6)$$

$$ER_3(dB) = 10 \cdot \log \left[\left(\frac{a_1 \cdot b_2 + b_1 \cdot a_2}{a_1 \cdot b_2 - b_1 \cdot a_2} \right)^2 \right] + 10 \cdot \log \left[\left(\frac{a_1 \cdot a_2 + b_1 \cdot b_2}{a_1 \cdot a_2 - b_1 \cdot b_2} \right)^2 \right] \quad (3.7)$$

$$ER_4(dB) = 20 \cdot \log \left[\left(\frac{a_1 \cdot b_2 + b_1 \cdot a_2}{a_1 \cdot b_2 - b_1 \cdot a_2} \right)^2 \right] \quad (3.8)$$

$$IL_1(dB) = \left| 20 \cdot \log \left[\left(a_1 \cdot a_2 + b_1 \cdot b_2 \right)^2 \right] \right| \quad (3.9)$$

$$IL_2(dB) = \left| 10 \cdot \log \left[\left(a_1 \cdot a_2 + b_1 \cdot b_2 \right)^2 \right] \right| + \left| 10 \cdot \log \left[\left(a_1 \cdot b_2 + b_1 \cdot a_2 \right)^2 \right] \right| \quad (3.10)$$

$$IL_3(dB) = \left| 10 \cdot \log \left[\left(a_1 \cdot b_2 + b_1 \cdot a_2 \right)^2 \right] \right| + \left| 10 \cdot \log \left[\left(a_1 \cdot a_2 + b_1 \cdot b_2 \right)^2 \right] \right| \quad (3.11)$$

$$IL_4(dB) = \left| 20 \cdot \log \left[\left(a_1 \cdot b_2 + b_1 \cdot a_2 \right)^2 \right] \right| \quad (3.12)$$

Where the sub-indexes means the outputs in the Figure 3.2. Finally we will define the total ER and IL as follows:

$$ER_{TOTAL} = \sum_{i=1}^4 10 \cdot \log(ER_i) \quad (3.13)$$

$$IL_{TOTAL} = \sum_{i=1}^4 IL_i \quad (3.14)$$

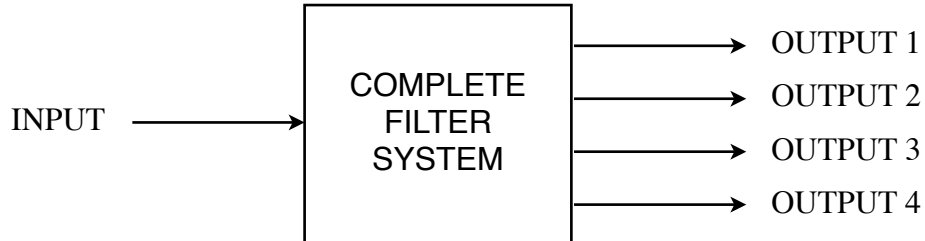


Figure 3.2. Complete System modeled as a Black Box

For the above simulation, it was considered that the couplers have the following deviations:

$$a_1 = 51\%$$

$$b_1 = 49\%$$

$$a_2 = 55\%$$

$$b_2 = 45\%$$

Then being maximum values ER and IL such that:

ER ₁	36.87 dB
ER ₂	40.36 dB
ER ₃	40.36 dB
ER ₄	43.84 dB
IL ₁	12.01 dB
IL ₂	12.04 dB
IL ₃	12.04 dB
IL ₄	12.08 dB

Table 3.1. ER and IL of each port

Using these values we are going to have high deviation and high IL, that is why we have to choose a balance design of coupler to get less loss. If we are not going to have balanced system it will bring losses in every channel. For this reason it is important to work in all balanced system. We can view this non-equality effect differently to everywhere in terms of ER.

3.4. Matlab Simulation

At this point we are already able to start the simulation performed with Matlab tool and then we will evaluate and compare our simulation with the theoretical description of our system.

3.4.1. Ideal Simulation

To start with the ideal simulation of the complete system we should take a look again to the ideal transfer functions of the MZIs (Equations 2.10):

$$\begin{aligned} T_1 &= \frac{P_{out1}}{P_{in1}} = \frac{1}{4} \cdot (e^{j\omega_0 T} - 1) \cdot (e^{-j\omega_0 T} - 1) = \sin^2(\omega_0 T) \\ T_2 &= \frac{P_{out2}}{P_{in2}} = \frac{1}{4} \cdot (e^{j\omega_0 T} - 1) \cdot (e^{-j\omega_0 T} - 1) = \cos^2(\omega_0 T) \end{aligned} \quad (3.15)$$

In order to simulate that and keeping in mind we will need two different FSR for the both stages we will start defining a function with two parameters (FSR1 and FSR2).

After that, we should consider that we have 4 users and we will set the frequency of each user also as a parameter to be able to change them whenever we want.

Moving forward our first function in Matlab looks like the following:

```
function[] = sim_mzi(FSR1,FSR2,f1,f2,f3,f4)
```

```
end
```

Inside of that function we will have to build the input signal (4 users with f1, f2, f3, f4 frequencies) but before that we will define the needed constants. For now our function have the following:

```
function[] = sim_mzi(FSR1,FSR2,f1,f2,f3,f4)
```

```
%Constants
```

```
c = 3e8;
```

```
neff = 1.4682;
```

```
n = 2.387;
```

```
%
```

```
%Setting the 4 users
```

```
fmuest4 = (1/(25*f4));
```

```
t = 0:fmuest4:10;
```

```
u1 = sin(2*pi*f1*t);
```

```
u2 = sin(2*pi*f2*t);
```

```
u3 = sin(2*pi*f3*t);
```

```
u4 = sin(2*pi*f4*t);
```

```
%
```

```
end
```

At this point, and using the *plot* function in Matlab we can see the four users.

```
%Plotting user1
plot(t,u1,'k');
xlabel('Time (s)');
ylabel('Amplitude');
title('User1');
```

```
%
```

We can see the result of this function in the Figure 3.3. Note that this figure shows the users in time domain which is not useful for our simulation since we are considering the system with its frequency behavior. We have to convert this signals from the users in time domain to the frequency domain before to apply the transfer function of the MZIs.

In order to do that the Matlab *fft* and *fftshift* functions simplify the process and we can define the frequency input signal as follows:

```
%Creating the frequency signal of U1+U2+U3+U4
```

```
S = u1+u2+u3+u4;
```

```
N = length(S);
```

```
X = abs(fft(S,N));
```

```
X = fftshift(X);
```

```
F = [-N/2:N/2-1]/N;
```

```
%
```

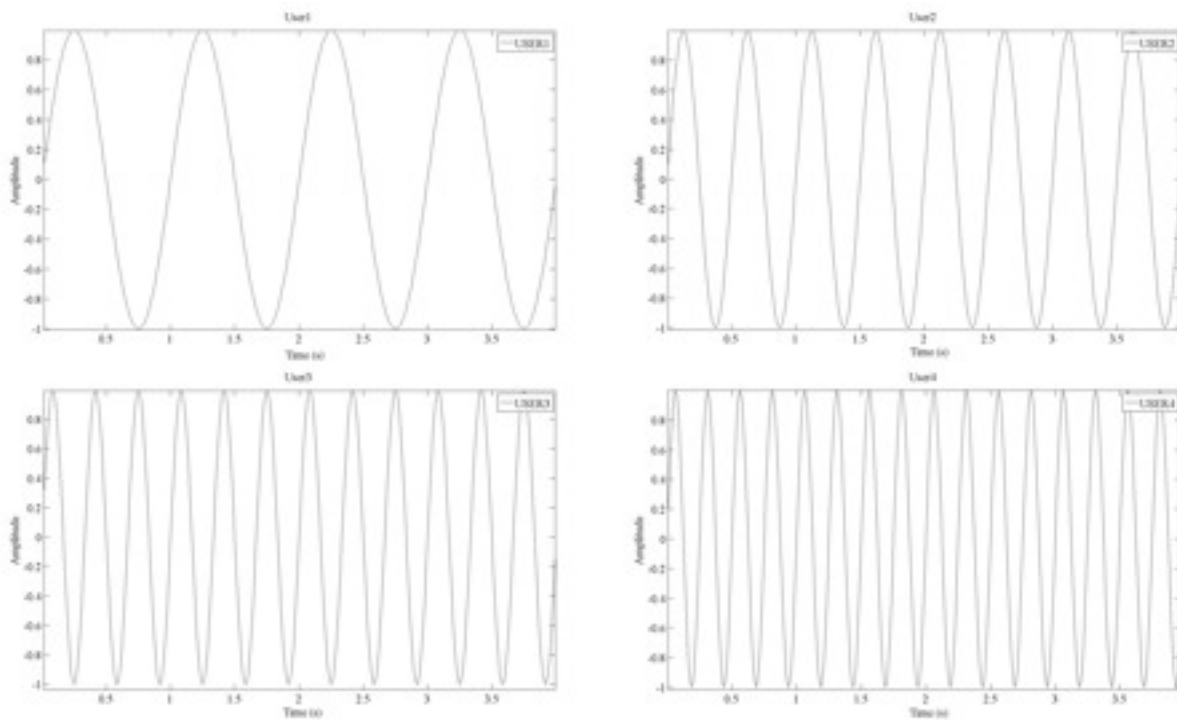


Figure 3.3. 4 Users in time domain with different frequencies

To see the results of this input signal we will use to simulate our systems we should plot it and we get the Figure 3.4.

```
%Plotting input signal (f)
plot(F.*1e11,X,'k');
xlim([0 5e9]);
xlabel('Frequency (THz)');
ylabel('Amplitude');
%
```

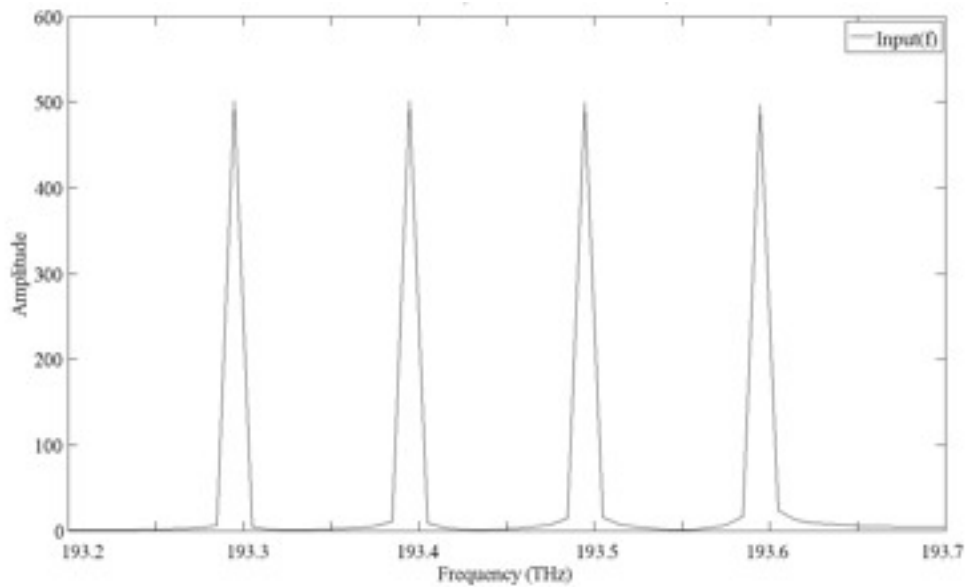


Figure 3.4. Input signal (4 users) in frequency domain

Once we already have the input signal prepared we have to define the transfer functions of each arm of the first MZI following the equations 2.10:

```
%FIRST MZI

%Setting f, length_dif and w
f = (1:(1/(0.0025*f4)):50e3);
length_dif = c/(neff*FSR1);
w1 = (2.*pi.*neff.*f.*length_dif)/(c*2);

%

%MZI 1 T1
T11 = sin(w1).^2;

%

%MZI 1 T2
T12 = cos(w1).^2;

%
```

Note we have defined ΔL as *length_dif*.

The last step to be able to simulate the system is to multiply the input signal and the transfer function of the MZI. In order to do that we prepare an auxiliary signal and after that we proceed multiplying:

```

%Auxiliary signal
    auxSignal=X((length(X)+2)/2:length(S));
%
%Getting output11 and output12
    out11= T11.*auxSignal;
    out12= T12.*auxSignal;
%

```

At this point we could already plot the outputs *out11* and *out12* and we would see how the first MZI split the signal, but this figure is shown in the next section (section 3.5) because in this section we are more focused in the Matlab code than in the results of the simulation.

To complete the system we just need to define the transfer functions of each MZI and to multiply them with the outputs from the first MZI:

```

%Second MZI

%Setting length_dif2
    length_dif2 = c/(neff*FSR2);
    w2 = (2.*pi.*neff.*f.*length_dif2)/(c*2)
%

%MZI 2 T1
    T21 = sin(w2 - pi/4).^2;
%

%MZI 2 T2
    T22 = cos(w2 - pi/4).^2;
%

%Getting output21 and output22
    out21 = out11.*T21;
    out22 = out11 * T22;
%
%

%Third MZI

%Setting length_dif2
    length_dif2 = c/(neff*FSR2);
    w2 = (2.*pi.*neff.*f.*length_dif2)/(c*2)
%

%MZI 3 T1
    T31 = sin(w2).^2;
%

%MZI 3 T2
    T32 = cos(w2).^2;
%

%Getting output31 and output32
    out31 = out21.*T31;
    out32 = out22.*T32;
%
%

```

At this point we already defined the complete system with every input, mid, and output signals.

Right now, instead of evaluate the simulation results since we will do it later, we are going to define and program the non-ideal case.

3.4.2. Non-Ideal Simulation

To define the non-ideal simulation we will use most of the definitions of the previous subsection and we will change the transfer functions of the MZIs.

The previous step is to define the non-ideal constants a_i and b_i :

```
%Definitions
    %Couplers
    a1 = 0.51;
    a2 = 0.49;
    b1 = 0.55;
    b2 = 0.45;

    alpha=1;
    %
%
```

We just need to define 4 parameters since we are assuming that all MZIs have the same characteristics. Once defined those non-ideal parameters we are able to proceed with the transfer functions of each MZI:

```
%Constants
    AA = a1*a1*a2*a2;
    BB = b1*b1*b2*b2*alpha*alpha;
    2AB = 2*a1*a2*b1*b2*alpha;

    AB = a1*a1*b2*b2;
    BA = b1*b1*a2*a2*alpha*alpha;
    %

%MZI 1 T1
    T11 = A + B - AB*cos(2*w1);
    %

%MZI 1 T2
    T12= AB + BA + 2AB*cos(2*w1);
    %

%MZI 2 T1
    T21 = A + B - AB*cos(2*w2 - pi/2);
    %

%MZI 2 T2
    T22= AB + BA + 2AB*cos(2*w2 - pi/2);
    %
```

```
%MZI 3 T1
T31 = A + B - AB*cos(2*w2);
%
%MZI 3 T2
T32= AB + BA + 2AB*cos(2*w2);
%
```

Note that with this we have finished the non-ideal code since the rest of the definitions were independent of the non-idealities. It means that replacing these transfer functions we will have the non-ideal case simulation.

At this point we will go ahead to evaluate the obtained results. For more details about the code see the attached Matlab documents (Appendix 1 and Appendix 2)

3.5. Simulation Results

Both sections 3.4 and 3.5 are the main part of this chapter and after defining our system and to explain how we have done the simulation, we'll proceed with the results of that simulation.

Note that even in the non-ideal simulation, there are few things we don't consider using Matlab i.e. polarization effects and that means our simulation will be close to the real behavior but not equal.

3.5.1. Ideal Simulation Results

We will start analyzing the ideal simulation results. As mentioned before, in this simulation we don't consider the deviation of the couplers what means that the power division is equal to each channel (50%:50%) and there is no loss in the fiber.

Beginning with the first MZI which will separate the users 1 and 3 to the first arm and 2 and 4 to the second arm. In Figure 3.5 we can see the input signal and the transfer function of the first output of the first MZI. As shown in the figure we will select the users 1 and 3 while we will kill the users 2 and 4. The output signal in this case is shown in Figure 3.6.

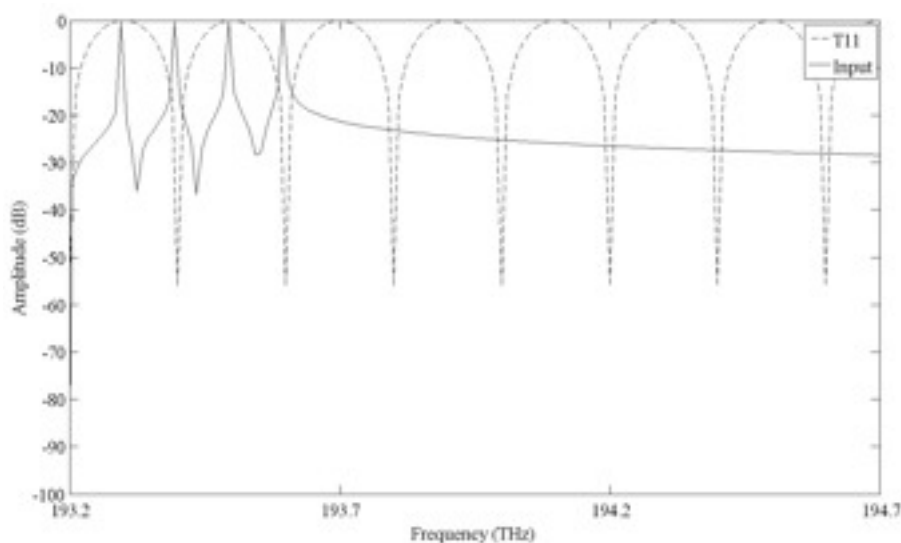


Figure 3.5. Input signal and first Transfer Function of MZI

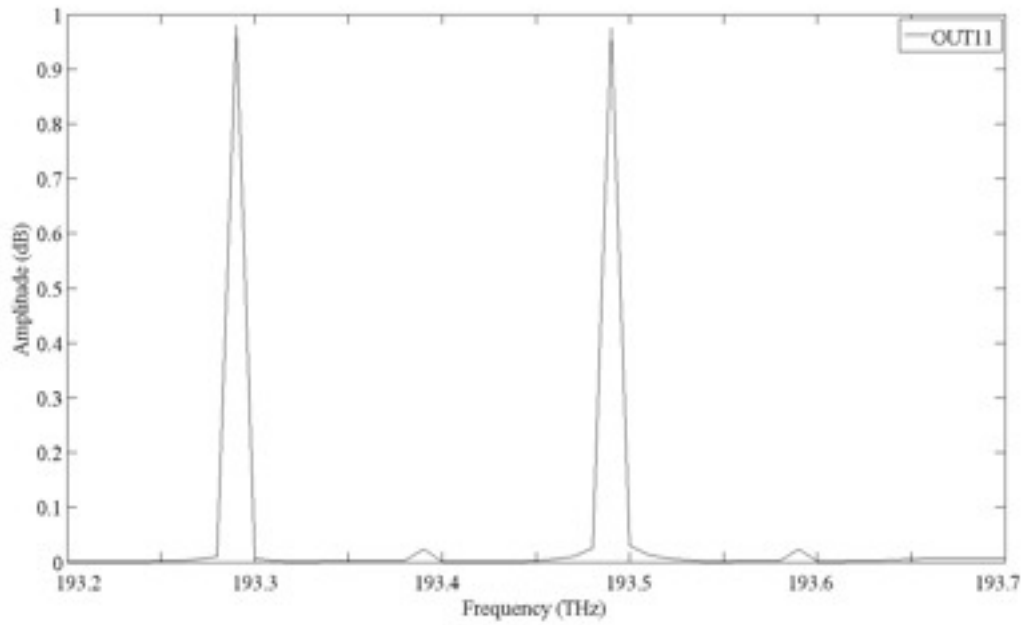


Figure 3.6. Output1 of the MZI1: Users 1 and 3

The same way we will show the second output and then we will analyze both:

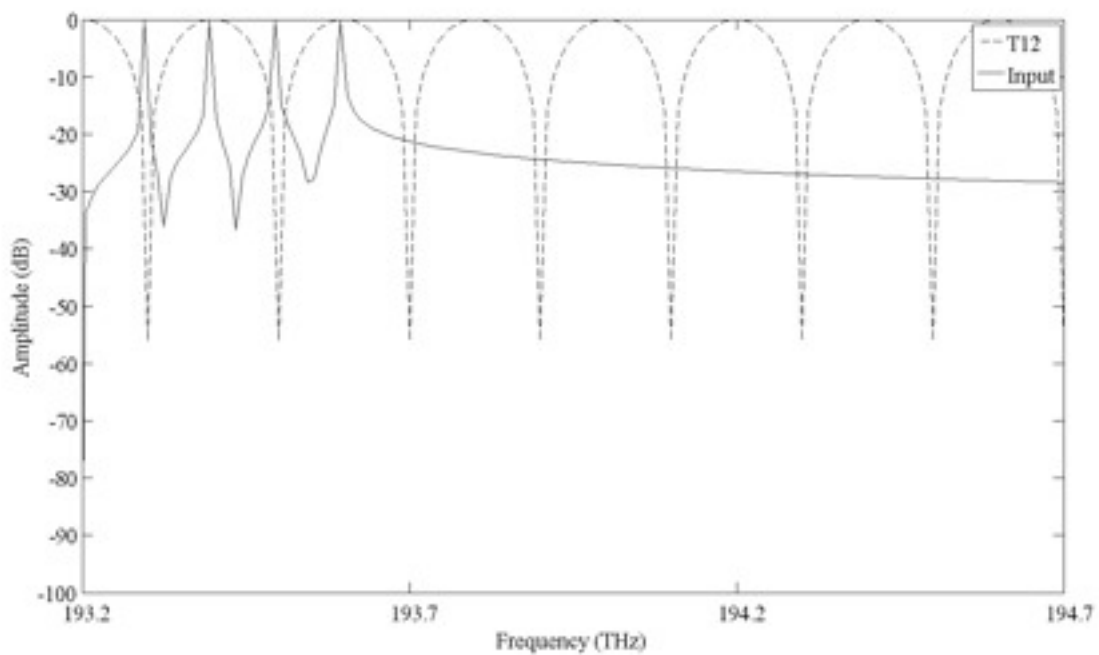


Figure 3.7. Input signal and second Transfer Function of MZI1

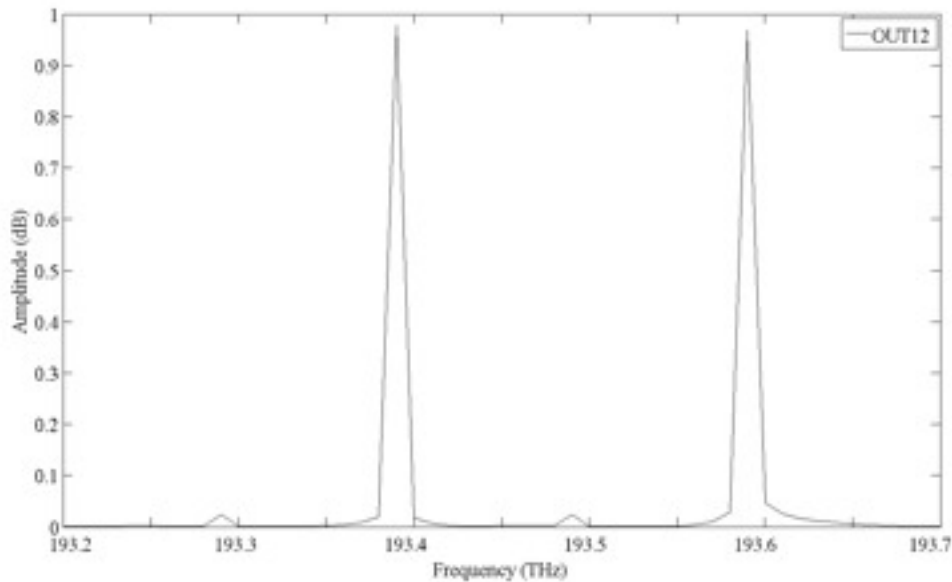


Figure 3.8. Output2 of the MZI1: Users 2 and 4

Now we are able to analyze that results. Note first that the input waveform looks different in Figures 3.5 and 3.7 because the Y-axis scale is in logarithmic (dB).

We will start stating that since is the ideal case the simulation is almost perfect, we can realize the amplitude of the outputs signals (Figures 3.6 and 3.8) are almost 1 what means there is not losses. Furthermore the Extinction Ratio is about 55 dB which produces almost the elimination of the non-desired signals each outputs: users 1 and 3 in the first output and users 2 and 4 in the second one.

The same way we will analyze the second MZI. Note that the third MZI is the same than the second with different phase so we will not discuss in details since would repeat the same.

The second MZI (and the third) will select just one channel or user in each output and in order to achieve that we need to raise the Free Spectrum Range to the double of the FSR of the first MZI. We can see this change in the Figures 3.9 and 3.11 below:

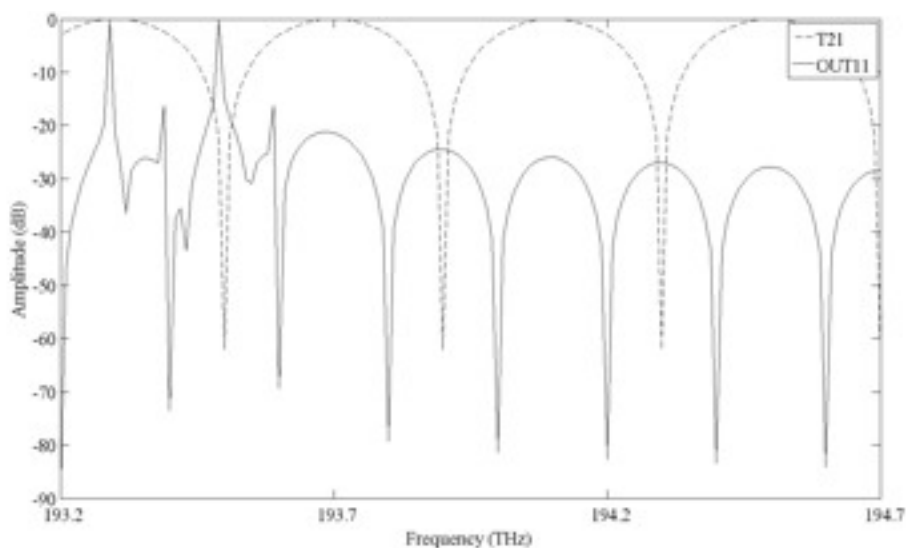


Figure 3.9. Output11 and first Transfer Function of MZI2

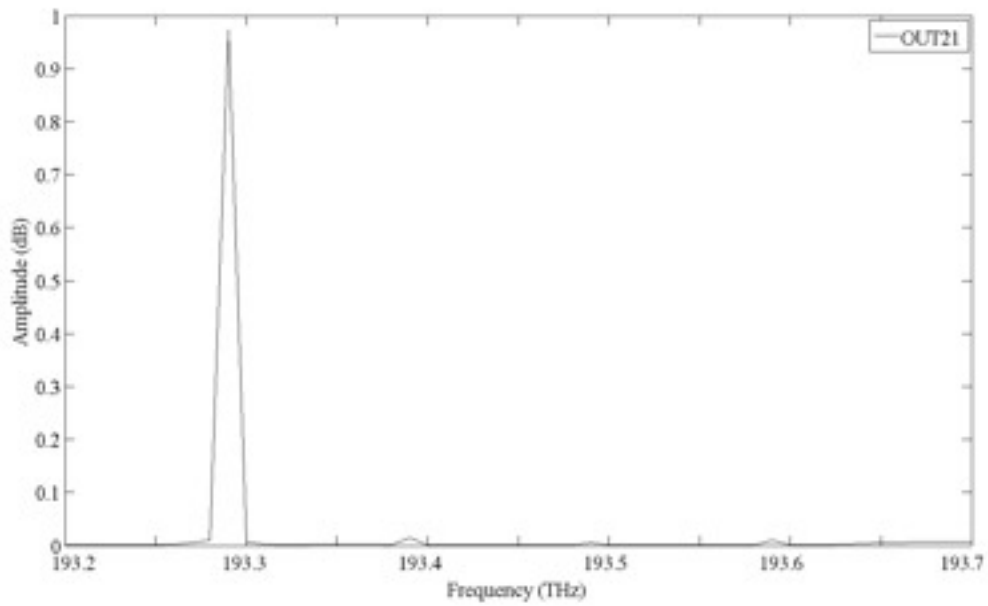


Figure 3.10. Output1 of the MZI2: User 1

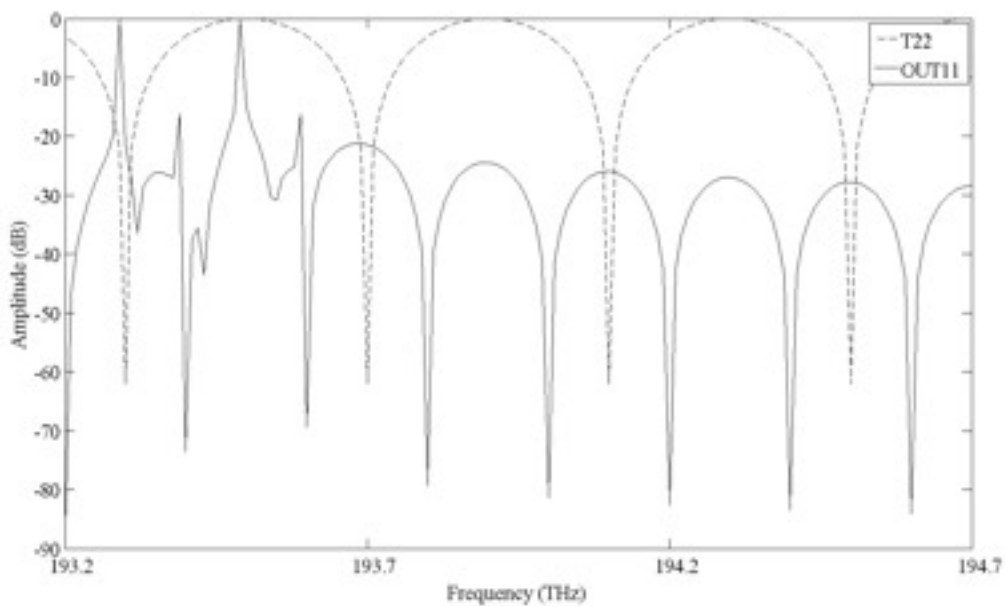


Figure 3.11. Output11 and second Transfer Function of MZI2

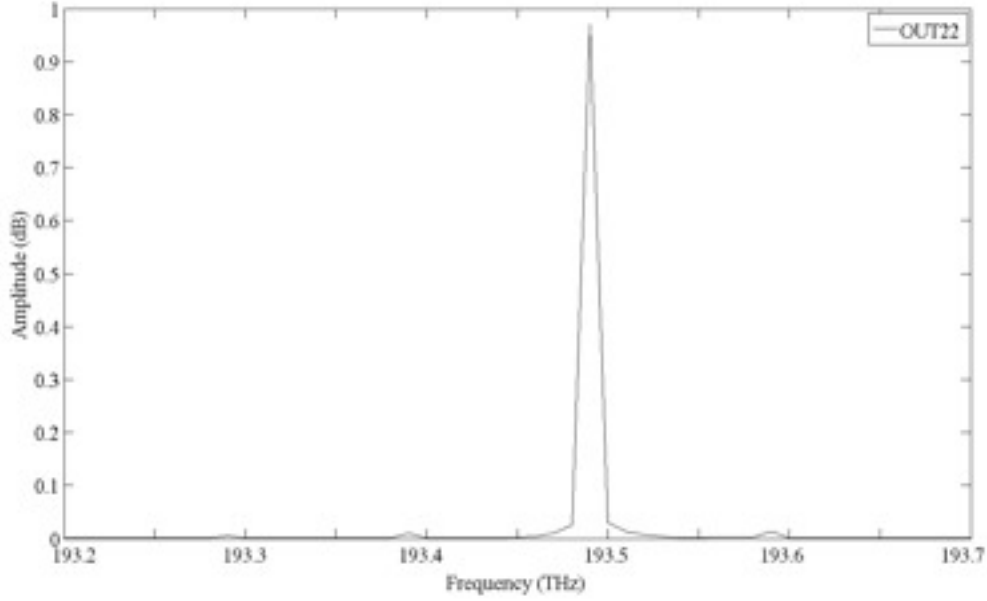


Figure 3.12. Output2 of the MZI2: User 3

At this point we can realize the only difference between MZI1 and MZI2 is just the FSR which allows us to select each channel individually. Again we have ideal conditions of no losses and high Extinction Ratio and a really clean signal at the end-output ports.

We will avoid to analyze the third MZI because it will not have any difference.

Below, the Figure 3.13, summarize this sub-section showing each output signal and the simulation of the complete system with the next two figures:

3.5.2. Non-Ideal Simulation Results

At this point, and in order to consider the system as closer as possible to the real device, we will proceed with the non-ideal simulations. In this case the couplers have different power division in each channel and the fiber introduces losses.

From now we will consider the couplers with the following parameters as we decided at the beginning of the Section 3.3:

$$a_1 = 51\%$$

$$b_1 = 49\%$$

$$a_2 = 55\%$$

$$b_2 = 45\%$$

Same than in the Section 3.5.1 the first MZI versus input signal (4 users) is show in the Figure 3.14 and Figure 3.15 which correspond to T1 (to select channels 1 and 3) and T2 (to select channels 2 and 4) respectively.

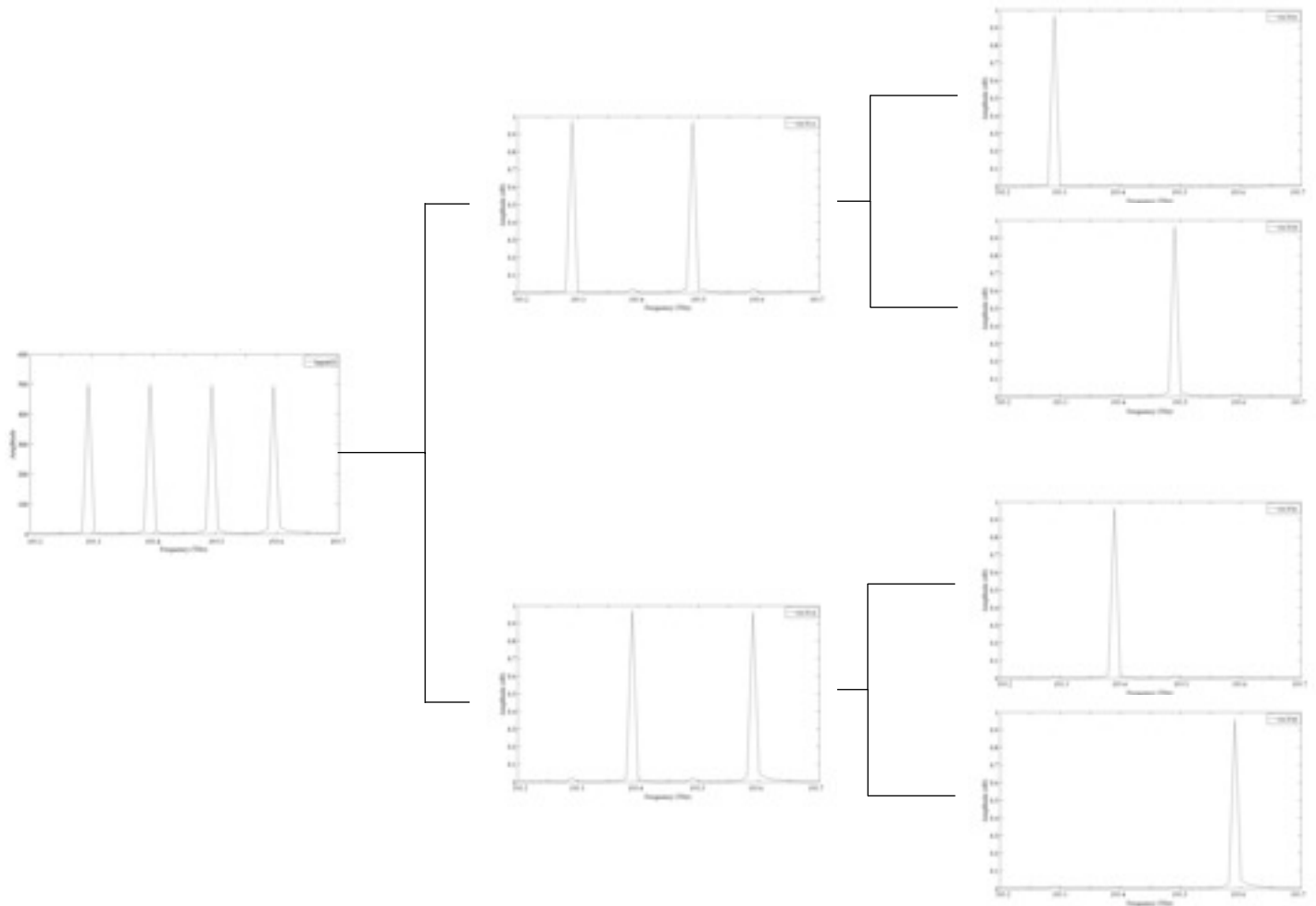


Figure 3.13. Complete System

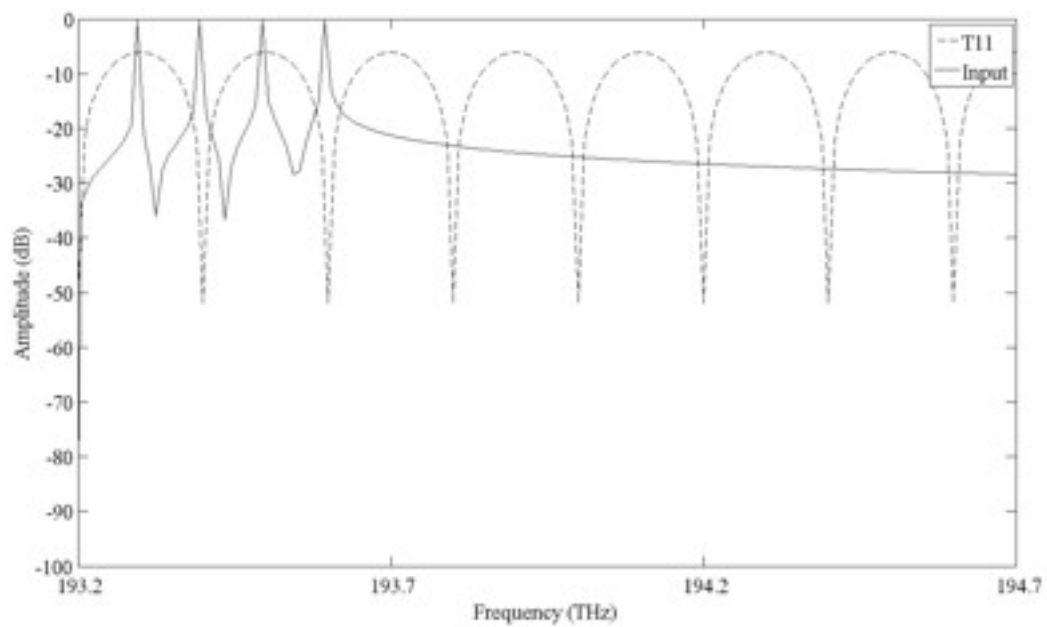


Figure 3.14. Input signal and first Transfer Function (T1) of MZ1

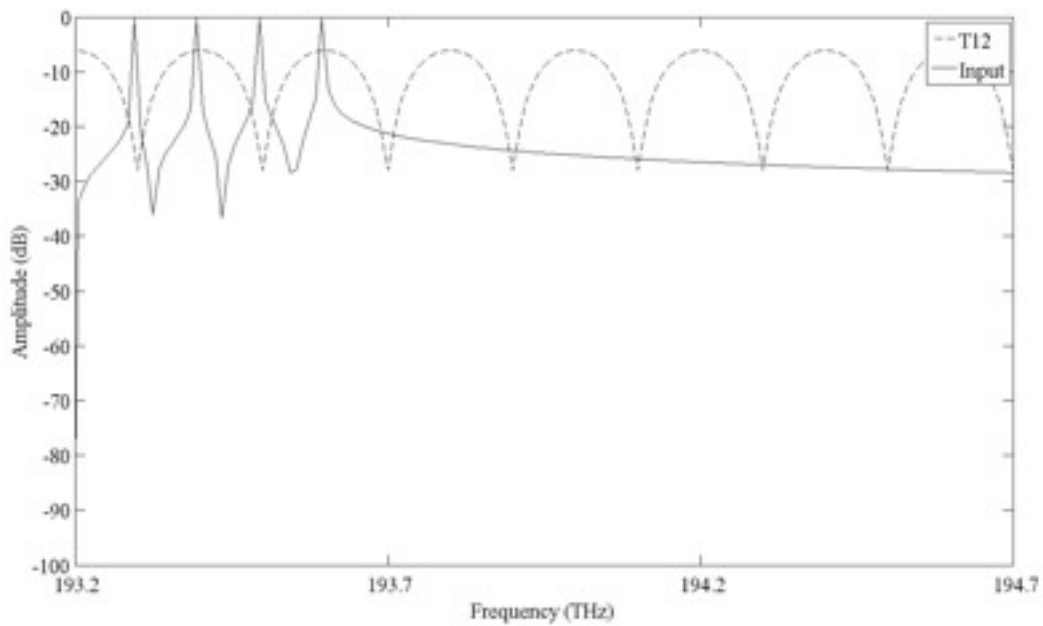


Figure 3.15. Input signal and second Transfer Function (T2) of MZI1

We can see in these two last figures how two important parameters of the MZI have been changed. We are talking about Insertion Losses and Extinction Ratio. In this case the IL are not 0 anymore like in the previous subsection but we have around 6dB of losses in each MZI.

That means, as known in the Section 3.3, each user will have approximately 12dB Losses since their signal will travel through 2 MZI in all cases.

The second parameter changed is the Extinction Ratio, now we don't have that ideal elimination of the non-desired channels but we can see in the following figures that even with this Extinction Ratio (around 20dB ~ 24dB) we are able to erase adequately the even channels in the case of T1 and odd channels in the case of T2.

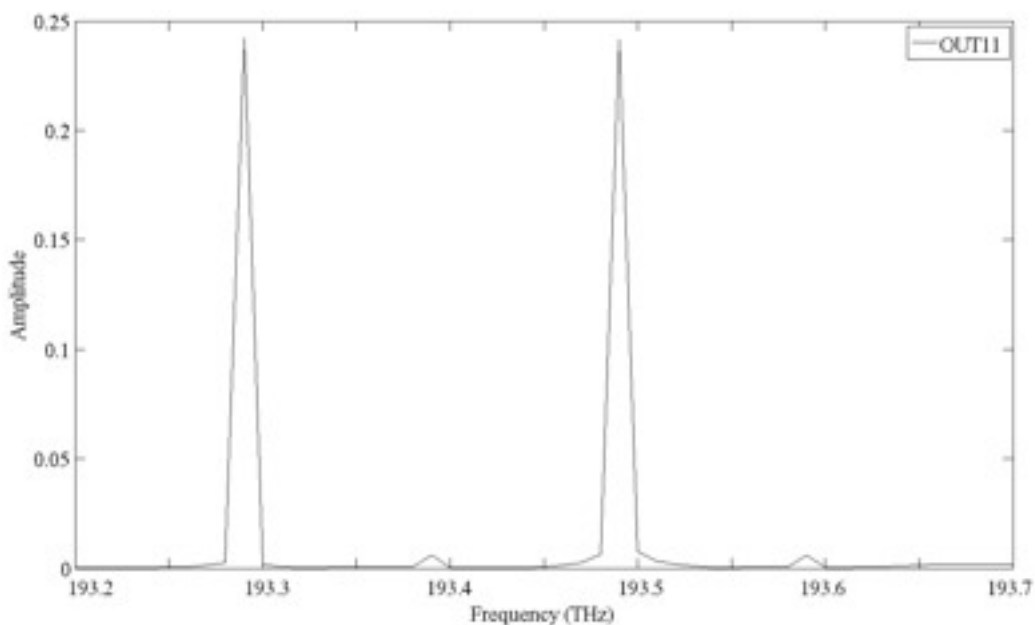


Figure 3.16. Output1 of the MZI1: Odd users

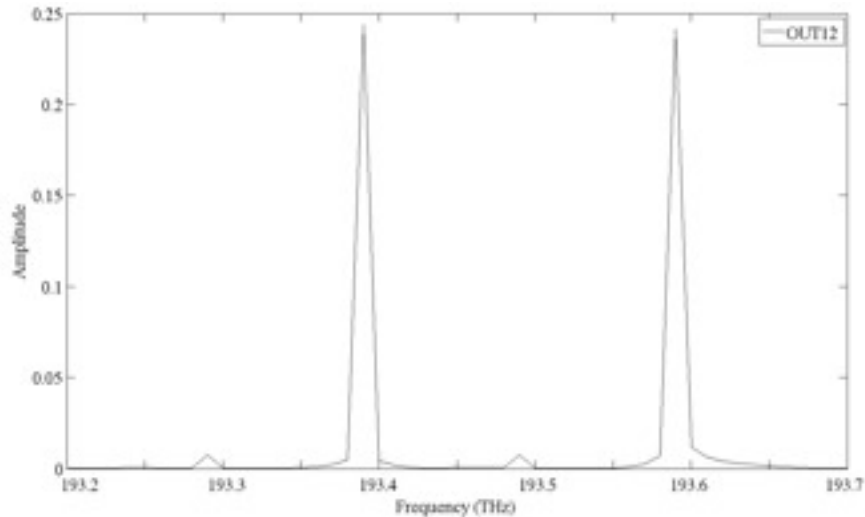


Figure 3.17. Output2 of the MZI1: Even users

At this point is important to realize than in Figure 3.16 and Figure 3.17 the output signal amplitude has been reduced to a quarter of the original. That corresponds to those 6dB of insertion losses and it is easy to proof:

$$10 \cdot \log\left(\frac{1}{4}\right) = -6.02 \text{ dB} \quad (3.16)$$

Now we will move forward to analyze the second MZI (again the third is not going to be analyzed since would be to repeat what we are going to see right now).

Again we are under non-ideal conditions and it means we should expect $IL > 0\text{dB}$ and reduced ER. Since we are using the same technology in each MZI (only changing the FSR) these parameter will not change than what we just saw.

Figures 3.18 and 3.19 show the MZI2 response versus the output signal from MZI1.

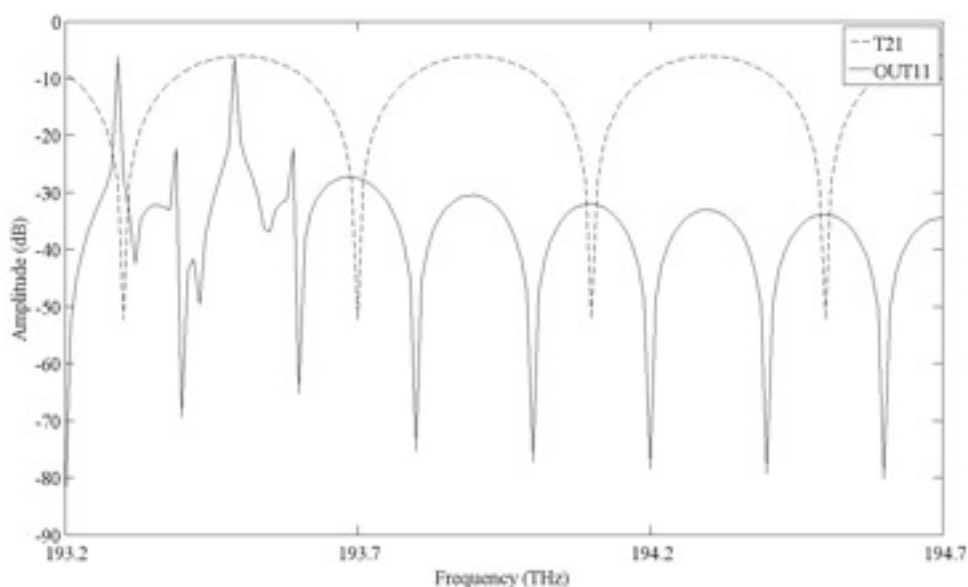


Figure 3.18. Output11 and first Transfer Function of MZI2

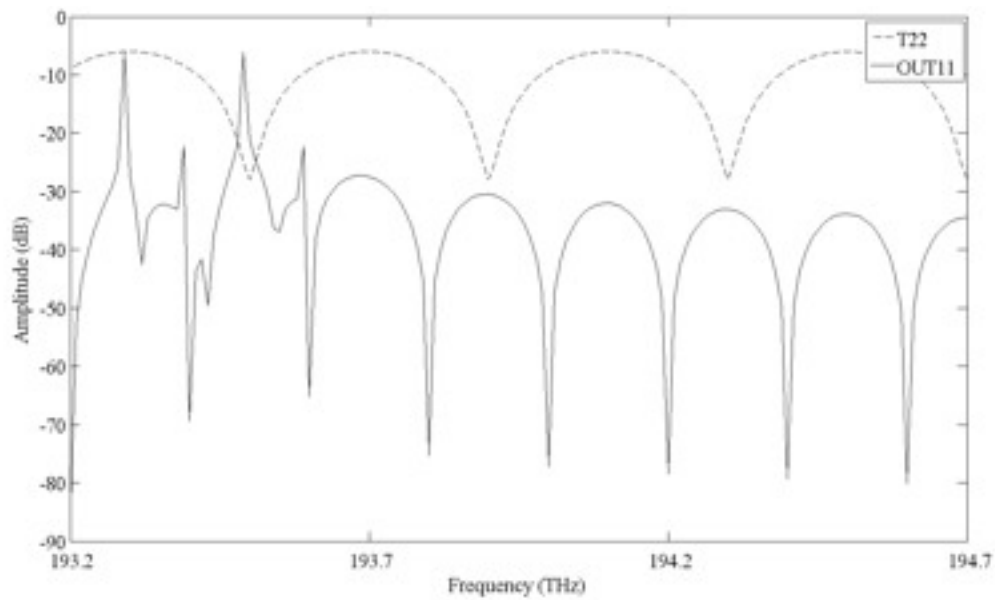


Figure 3.19. Output11 and second Transfer Function of MZI2

Meanwhile the Figures 3.20 and 3.21 show the output signals of the MZI2 corresponding to the users 1 and 3 respectively:

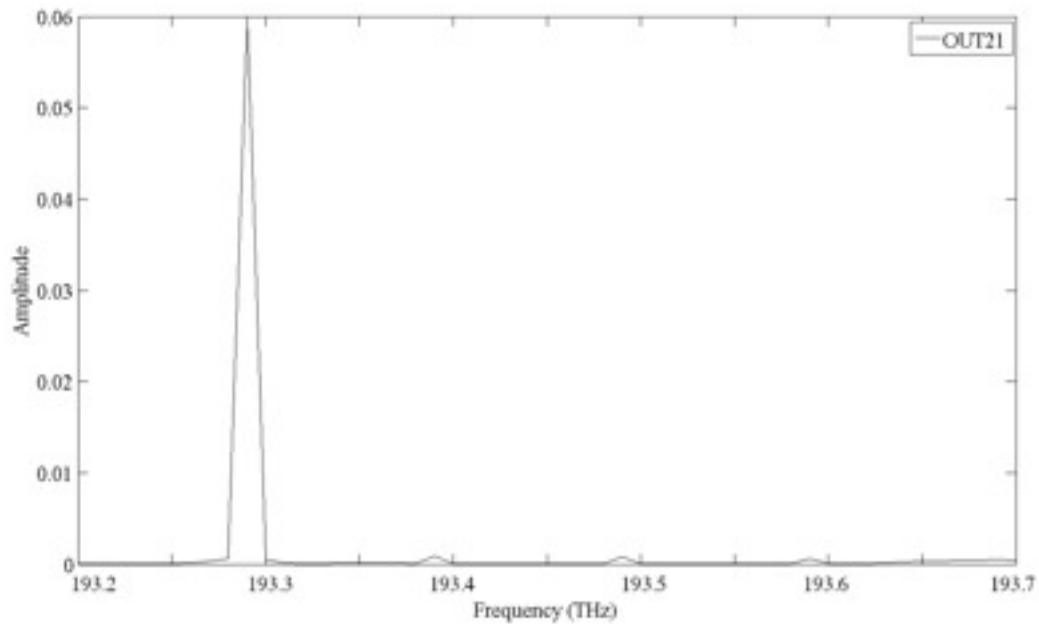


Figure 3.20. Output1 of the MZI2: User 1

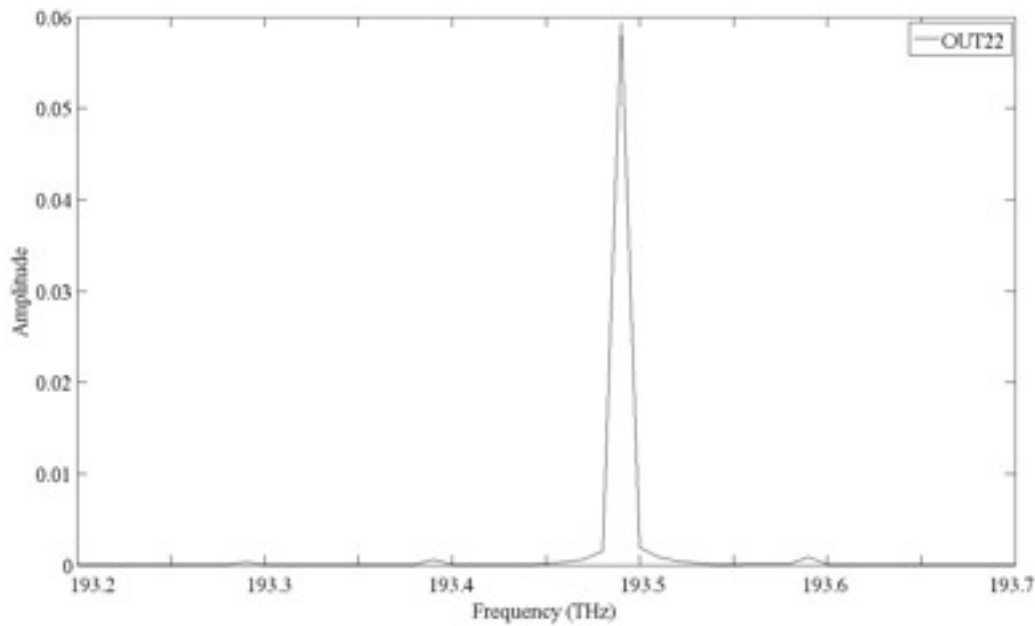


Figure 3.21. Output2 of the MZI2: User 3

Note again that the amplitude has been reduced to 0.06 which corresponds to 12.22dB of Insertion Losses as calculated in the Section 3.3:

$$10 \cdot \log(0.06) = -12.22 \text{ dB} \quad (3.17)$$

At this point we have already finished the simulation analysis and we are able to state the conclusion about that which makes us move to the next summary section to close this Chapter 3.

3.6. Summary

When developing a system there are 3 important steps to do and we have based on that this project: Theory, Simulation and Experiment.

We have simulated both cases (ideal and non-ideal) and we can already state the sensations are positive since the simulation results are pretty much the same than the numbers obtained in the theoretical calculations. That means we are following the correct path to reach our goal.

In order to definitely reach that goal we will close this Chapter 3 and open the most important chapter (Chapter 4) of this project where we will see the real experiment performed in the Optical Communications Group of the Polytechnic University of Catalonia (GCO - UPC) and the behavior of both MZI and Interleaver working as a user splitters for DWDM Networks.

CHAPTER 4

THE MAIN PARAMETERS IN-LAB EXPERIMENTATION

After the theoretical survey and the system simulation is the turn for the experimental research with real devices in order to proof and conclude that our initial purpose is feasible.

We should start stating that in this laboratory experience we have not tried to build the whole system as in the theory and simulation parts. We will simplify the system reducing it to one MZI (or Interleaver) and two users. After characterizing and to proof that it works we can assume that the simulated system would work the same way with the correct equipment.

In general the performed work is divided in two parts: Theoretical Review of Parameters and Experimental Affairs. According to the fact that the main reason to go with practical part was to use laboratory facilities and to do experiments and tests with a homemade-MZI in order to obtain deviation of expected parameters, therefore the majority of efforts were allocated to experimental affairs. The work has been briefly described as follows: chapter 4 focuses on experimental aspects of MZI characterization used as an Interleaver and commercial Interleaver.

The objectives of the practice are: first of all, the characterization of MZI and Interleaver parameters to compare both optical devices according to them. Also we will characterize the same system three times but using three different optical devices (coupler, MZI and Interleaver). The goal is to compare power and loss in the input with power and loss in the output in each case. Finally, we have built an OLT and Access WDM Network with purpose to observe the changes in the loss of the system in the real case.

To summarize we will test both devices in real conditions in order to proof that MZI could be the cheap alternative of the Interleaver for the Access Part of the DWDM-PON.

4.1. Theoretical Review

Even though all theoretical questions are answered in the previous sections we should note it can be recommended to review the important theoretical aspects in order to give enough self-sufficiency to this Chapter 4 and, at the same time, to show few new details of some parameters.

This part is divided by two subsections. First we pursued our field of interest that is Fiber-to-the-Home (FTTH), Passive Optical Network (PON) (access part) using DWDM technology and passive optical devices.

Second we did comprehensive review of parameters for MZI and commercial Interleaver, one of the main fields of research in GCO.

4.1.1. Review of the parameters for MZI and commercial Interleaver

As mentioned above we are going to review the parameters and the relation between them since it is requisite to have an adequate knowledge of optical devices. Note this subsection is repeating some already explained theoretical concepts in Chapters 2 and 3.

We will review the important parameters of a homemade MZI and Commercial Interleaver in order to analyze the quality and performance of the practical work have been done in laboratory. The main review was on Extinction Rate, Insertion Loss, Free Spectrum Range, Return Loss, Polarization Dependent Loss (PDL). Review and measurements were completed by various trying in order to get better results because of some parameters which not possible to control at all, like phase and polarization; for this reason it is necessary to implement methodology or strategy for this parameters.

Extinction Ratio (ER)

Usually in dB, is the measurement between the maximum amplitude of the frequency response and the minimum adjacent this maximum. When we are using MZI as a filter one user is going to be maximum and next in minimum.

$$ER(dB) = \max \{ H_{MZI}(\omega) |_{dB} \} - \min \{ H_{MZI}(\omega) |_{dB} \} \quad (4.1)$$

Free Spectrum Range (FSR)

Is the spacing in optical frequency or wavelength between two successive reflected or transmitted optical responses between two consecutive maximums (minimums) of an interferometer

The gap between the two branches needs to get the desired FSR, can be designed using the equation (2.11):

$$FSR = \frac{c}{\Delta L \cdot n_{eff}} \quad (4.2)$$

where ΔL is the length difference between the two branches and n_{eff} is refractive index (1.4682 for this simulation).

In this case FST is designed to obtain 60GHz since it is enough to work with technology DWDM.

FSR (GHz)	ΔL (mm)
10	20.4332
20	10.2166
30	6.8111
40	5.1083
50	4.0866

Table 4.1. Equivalence between FSR and ΔL

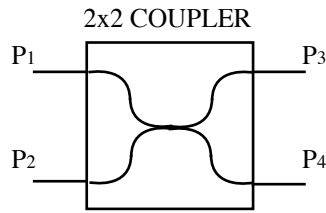
As you can see in the Figure 4.1. the calculation of the FSR is independent of loss and this will ensure that MZI works with desired requirements that guarantee FSR.

Insertion Loss (IL)

Refers to attenuation of a signal at an import port from another input port. IL is the decrease in transmitted signal power caused by the connector, measured as the light goes out from one fiber and goes into the next fiber.

The causes of the insertion loss are due to intrinsic and extrinsic mechanisms. Intrinsic mechanism caused due to differences between two fibers, for example, mismatch of the core area of the two fibers, mismatch of the numerical aperture of the two fibers, eccentricity of the cores of the fibers, mismatch of the refractive index profiles. Extrinsic mechanism caused due to the physical characteristics of the coupler, for example, lateral misalignment of the fibers, angular misalignment of the fibers, gap between the fibers and reflections at the fiber ends ($n_{\text{eff}} = 1.46$)

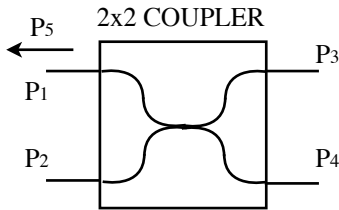
The attenuation of a coupler can depend on the environmental conditions as: temperature, vibration and etc. Each application requires a specific type of connector.



$$IL(dB) = 10 \log \left(\frac{P_1}{P_3} \right) \quad (4.3)$$

Return Loss (RL)

Also called Reflectivity, is the ratio of the optical power arriving at the coupler to the optical power reflected back.



$$RL(dB) = -10 \log \left(\frac{P_5}{P_1} \right) \quad (4.4)$$

Polarization-Dependent Loss (PDL or Influence of Polarization)

The electrical field in a plane transversal to the propagation vector defines the State of Polarization (SOP). Relation between X and Y components depends on module and phase mismatch. SOP describes the trajectory of Polarization Dependent Loss (PDL), [dB]: it measures the variation of the attenuation of the device as a function of the SOP (State of Polarization) usually two linear orthogonal polarizations of input signal (similar to a Polarizer effect).

Polarization states of optical field may change along the fiber because of the birefringence.

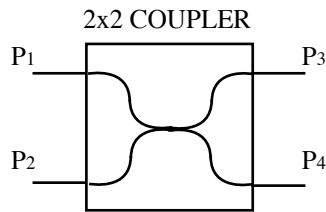
Another important source of MZI is polarization mismatch causing losses in the interferometer. For this reason it is important to study and simulate the behavior of interferometer which caused by the birefringence of the fiber (differ). In order to achieve the best performance, the state of polarization of waves for each of the paths must be the closest one to the other wave. The differences of two combined polarization ways is produced by the birefringence of the optical fiber.

Birefringence is also originated in the condition when an optical signal is propagated through a waveguide, in this case the refractive index of which is higher than the external. That is why, in the transverse plane, the waveguide can present problems when the section in this plane is not perfectly symmetric, this being the reason why the linear polarization component parallel to the axis of this section is propagated at a different velocity than the parallel component. This difference in propagation speeds, due to non-idealities in the geometry of the fibers which is called as birefringence of the fiber. The physical effect of the differences in propagation velocities is that each component represent a different refractive. The difference between the two speeds is possible to quantify birefringence using the local refractive index in the fiber.

These non-idealities in fiber is cause of penalty in MZI response and it is interesting to characterize the confidence margin. Also we should state that one of our limitations is the ER since the device is already built (homemade) and we can not change that parameter nor any internal construction of the MZI in order to improve it.

Directivity

Also named as Isolation refers to the signal attenuation at one of the input ports different from the one at which signal is being injected.



$$Directivity(dB) = 10 \log \left(\frac{P_1}{P_2} \right) \quad (4.5)$$

4.2. Experimental Affairs

As mentioned in the introduction of this Chapter 4 we are going to measure all important parameters of both devices, we will compare them and also we will see the behavior of both devices in front of the desired input signal.

The tests performed could be classified in few different categories:

- i. The first one will focus on the measurement of MZI parameters.
- ii. Then we will proceed to evaluate this result and to try to compensate limitation in instrumentation.
- iii. In the third Section we will do the same with the Interleaver.
- iv. Compare and conclude Interleaver and MZI.
- v. Propose new techniques to improve the multistage system to control polarization and phase response.

4.2.1. Preparing the acquisition system

In order to test the optical system of our experiment we are going to isolate the MZI from any external deviation to create the stability. This regulation is performed by packaging the MZI device in an aluminum surface and foam from both sides in order to isolate external vibration.

First, for demonstration purposes we consider only a single-stage MZI filter using two standard 3-dB couplers, where the two output ports of one coupler are fused with the two input ports of a second one in order to maximize the isolation and with an optical path difference corresponding to the required 100GHz free spectral range (FSR).

For the experimental part, it is necessary to inject the light emitted by tunable laser into one of the inputs of the directional coupler. The measurements will be done at one of the outputs port of coupler into the optical spectrum analyzer (OSA) in the optical domain. To do that, it will be necessary to use a fiber optical cable having connection with Laser and with one of the input of MZI device, at the other side, the same kind of connectors as the one from the output ports of the coupler with the OSA.



Figure 4.1. Some examples of real GCO-UPC Laboratory configurations

4.2.2. Equipment Used

We will proceed describing each instrument and device used in the laboratory. In order to simplify the rest of the report we will assume after reading this subsection that all devices and instruments are known.

Mach-Zehnder Interferometer device

It is already known that the MZI used is not a commercial one but a homemade build in the laboratory (GCO, in 2013). It is composed by 2 couplers and fibers between them with known length.

Since it is not either commercial nor professional device we should mention that it has a huge instability to any physical perturbation (movements, temperature changes, knocks...) and the measurements are subject to many ungovernable parameters. For this reason the measurements we are changing every day depending on all conditions.

However we were able to improve the stability of this device by placing (as mentioned above) foam surface on both sides of the MZI and this way we could get results with acceptable quality.

In Figure 4.3a is shown the symbol used for this MZI.

Interleaver

The interleaver used (see Figure 4.2) is the commercial 50GHz Interleaver from Oplink Communications Inc. The manufacturer specifications are attached in the Appendix 3 in order to compare the results provided by Oplink and our laboratory measured results.

It includes, as expected, 3 fibers corresponding to the common, even and odd ports. As we already know we will use the common port as the input and the even and odd ports as the outputs to split the users. In Figure 4.3b we show the Interleaver symbol used.



Figure 4.2. 50GHz Oplink Interleaver

Optical Spectrum Analyzer (OSA)

This device is one of the main instruments used to characterize the MZI and Interleaver. We will use it to obtain the optical and electrical spectrum. In the GCO Laboratory we have two different OSA which are HP 70951A with 600nm to 1700nm bandwidth and the Anritsu MS9710B with 600nm to 1750nm bandwidth.

All parameters are obtained using this two instruments with the exception of the Power that also has been obtained using the Power Meter.

See the Figure 4.3c to know the OSA symbol used in this report.

Electrical Spectrum Analyzer (ESA)

As well as the OSA, this Electrical Spectrum Analyzer helps us to obtain the response and the values of the electrical-domain parameters. We are using also HP ESA and the symbol will be the same than the OSA since they have the same physical appearance (Figure 4.3c).

Power Meter

The GTPM-3T Optical Power Meter is used to get easily the power in each output or input of the devices. The sensitivity of this devices is -70dBm and is able to measure signals up to +10dBm, this values will be more than enough in our case. The power meter symbol is shown in Figure 4.3d.

Laser

Lasers are our one of the two light sources used in this project. Note we don't use just one kind of laser but up to 3. We will use two commercial Instrumental Lasers (Agilent 8164B and JDS Uniphase SW15101) which are tunable and stable, a DFB and a current laser developed also in GCO for previous projects.

We will use these lasers and the their added signal to create and simulate the OLT users in a DWDM Passive Optical Network. The symbol is shown in Figure 4.3e.

EDFA

The other light source used in this project is the commercial EDFA IRE-POLUS EAD-40 16 dBm Erbium Amplifier with wide spectrum in order to excite a broad range of the devices (MZI or Interleaver) to get their complete response.

See Figure 4.3f to know the EDFA symbol used in the next figures.

Circulator

In our case the circulator is a 3-port device (there are also with more ports) where the going path is different than the return one following the order of the numbers. It means the power inserted in port 1 will leave the circulator by the port 2, but the signal coming from the 2nd port will go by the 3rd port and same from 3 to 1 ports.

With this device we can measure the return power without any interference of the input signal.

The circulator symbol is shown in the Figure 4.3g.

Polarizer

Polarization of the light is a really complex and hard to dominate parameter. In order to simplify this job we use the Polarizer which allows us to turn the fiber in different ways and axis in order to change the polarization. Figure 4.3h shows the polarizer symbol.

Coupler

The Mach-Zehnder Interferometer has couplers inside but we also use couplers in order to mix or divide signals out of the Mach-Zehnder Interferometer. Since it is a bidirectional device and there are many different types we can see in our figures different representation of the couplers. However the Figures 4.3i and 4.3j show the used coupler symbols.

Fiber and connectors

To end with the device descriptions we will mention the fibers and connectors were are shown as a line shape and avoided respectively in the figures.

Is important to know that each length of the fiber introduces losses as well as the connectors introduce loses and reflections.

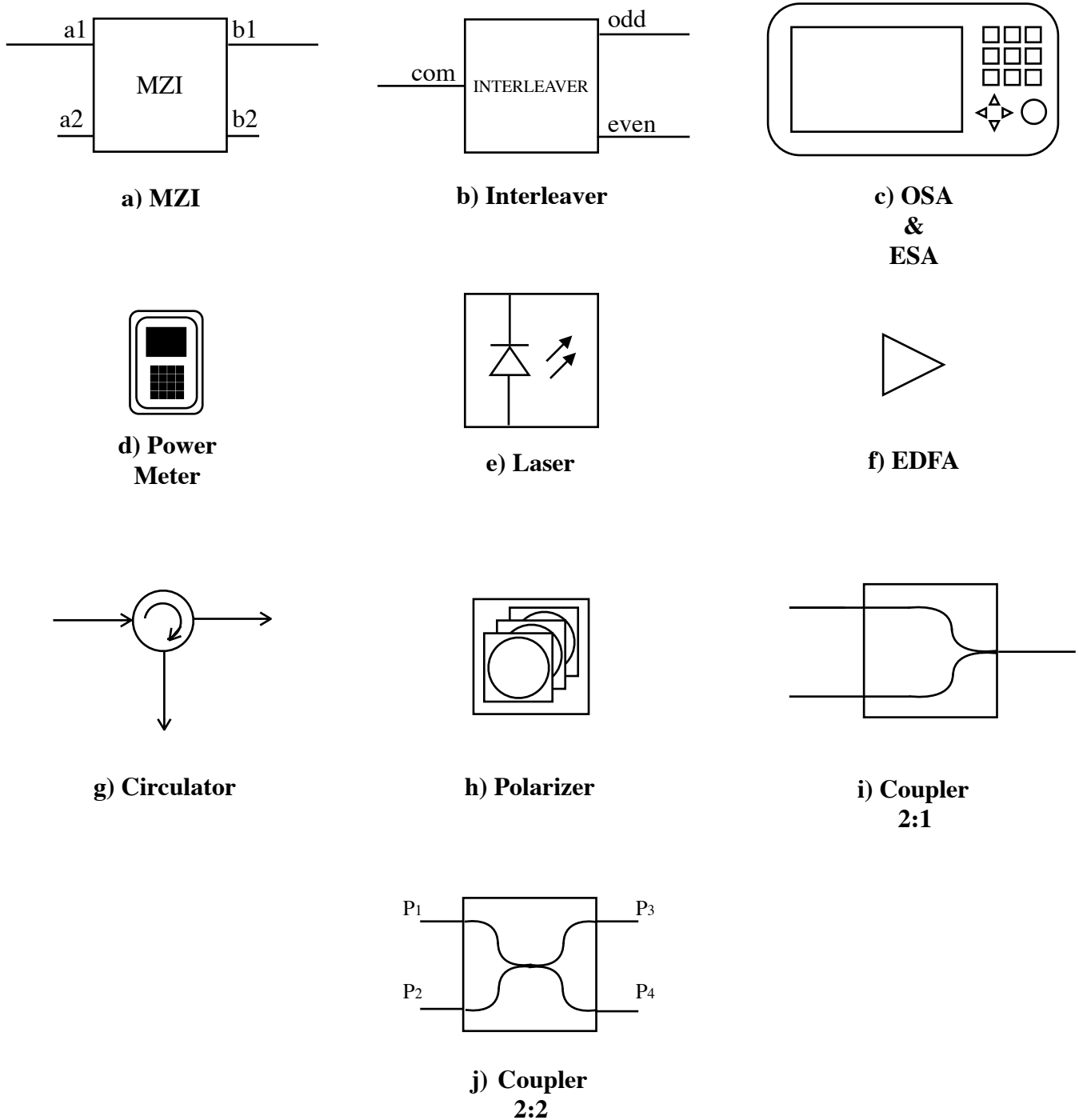


Figure 4.3. Symbol gallery

4.2.3. MZI Measurements

The idea of this experiment is to measure ER and FSR. In order to achieve it Figure 4.4 shows the system built in the laboratory.

We inject the light emitted by an EDFA into input A1 of the MZI. The measurement will be done at the output B2 of the MZI into the optical spectrum analyzer. To do that it will be necessary to use connectors which we used to connect between Laser and with one of the input, of MZI, and another connector we used between one of the outputs of MZI and OSA.

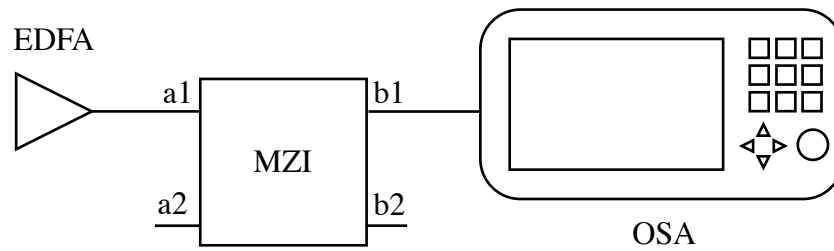


Figure 4.4. Schema of the response obtainment from input a_1 to output b_2

Extinction Ratio obtainment

To obtain the Extinction Ratio we have to identify the maximum and the minimum of the MZI response. Once we have the response shown in the OSA screen (Figure 4.5) it is easy to identify these two values.

In the Figure below we can see both response of the MZI: in green is shown b_1 output and in yellow the b_2 output, in both cases using the EDFA as input as Figure 4.4 shows.

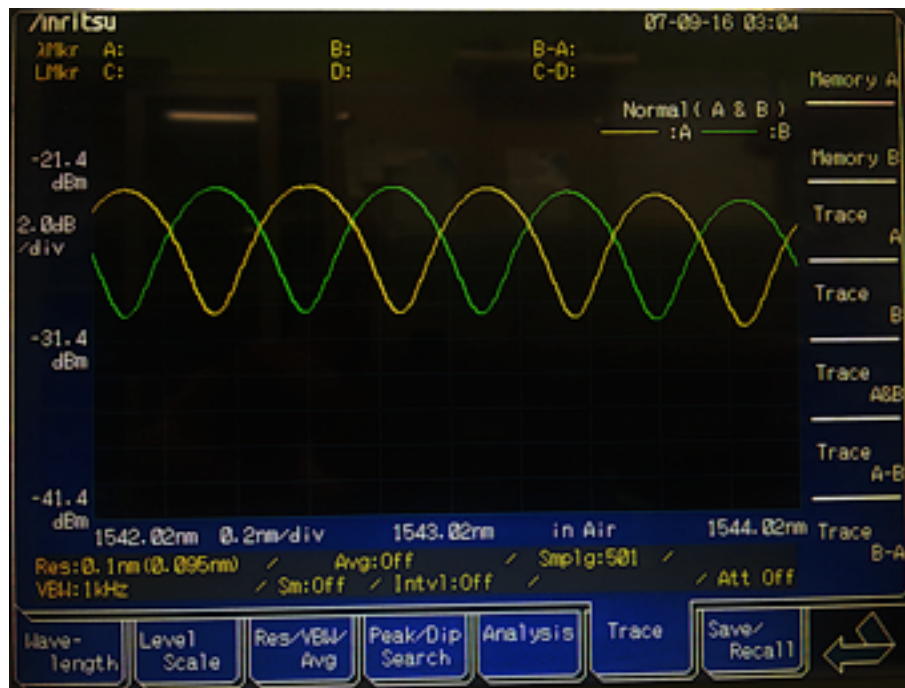


Figure 4.5. Frequency response of MZI shown in OSA screen

In the following MATLAB figures we have in blue color (left) the a_1 to b_1 response and the measurement of the ER. In the other hand in the red color we have the a_1 to b_2 response and also the ER obtainment.

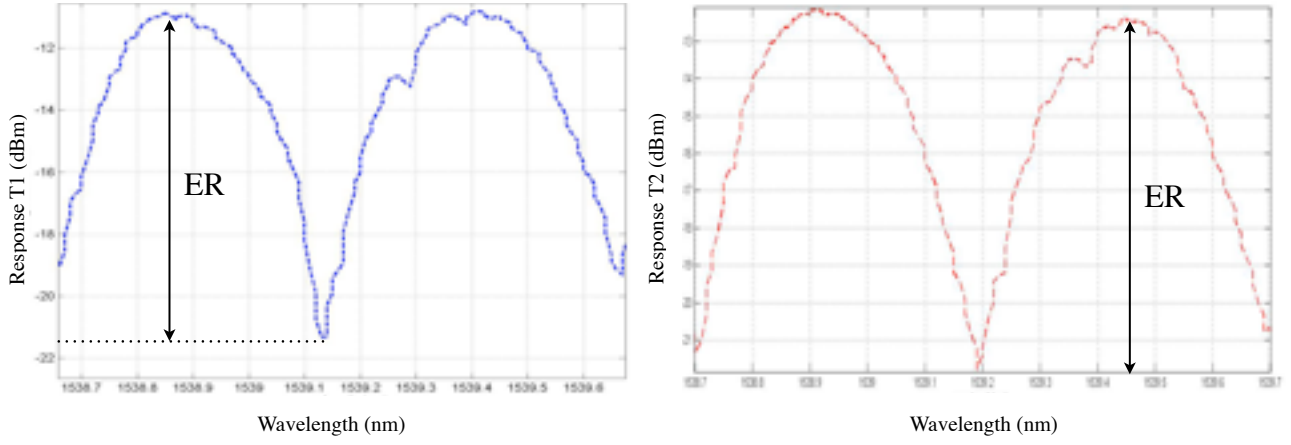


Figure 4.6. ER obtainment. Left: input a_1 to output b_1 . Right: input a_1 to output b_2

Both response combined are shown in the figure below: again in blue color the a_1 to b_1 response and in red color the a_1 to b_2 response.

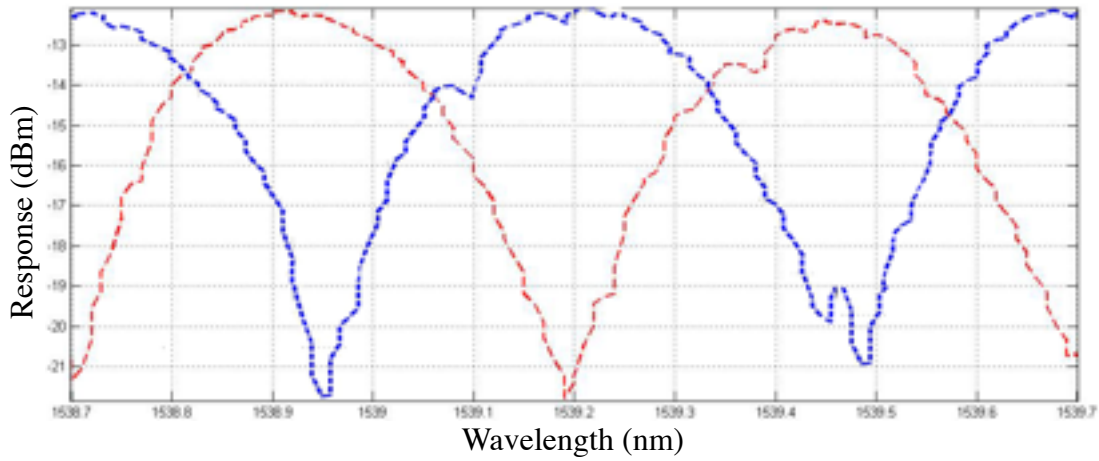


Figure 4.7. Both frequency response of MZI captured with MATLAB

In our case and shown in Figure 4.6 the ER values are:

$$ER_{a1 \rightarrow b2} = 10.32 \text{ dB} \quad (4.6)$$

$$ER_{a2 \rightarrow b2} = 12.36 \text{ dB} \quad (4.7)$$

FSR Measurement

From the same Figures above (4.5 and 4.6) we can obtain the FSR, we just need to measure the distance between two maximum points of the response (λ_0 and λ_1) and apply the following expression:

$$FSR = \frac{c}{\lambda_0} - \frac{c}{\lambda_1} \quad (4.8)$$

Also, and according to the Figure 4.8, we also can calculate the FSR as follows:

$$FSR = \frac{c}{\lambda_0} - \frac{c}{\lambda_0 + \Delta\lambda} \quad (4.9)$$

Now, we can calculate the Free Spectrum Range:

$$FSR = \frac{c}{1550nm} - \frac{c}{(1550 + 0.5)nm} = 62.41GHz$$

Using the same graphs than in Figure 4.6 we can also calculate the FSR as it shows the Figure 4.8 below.

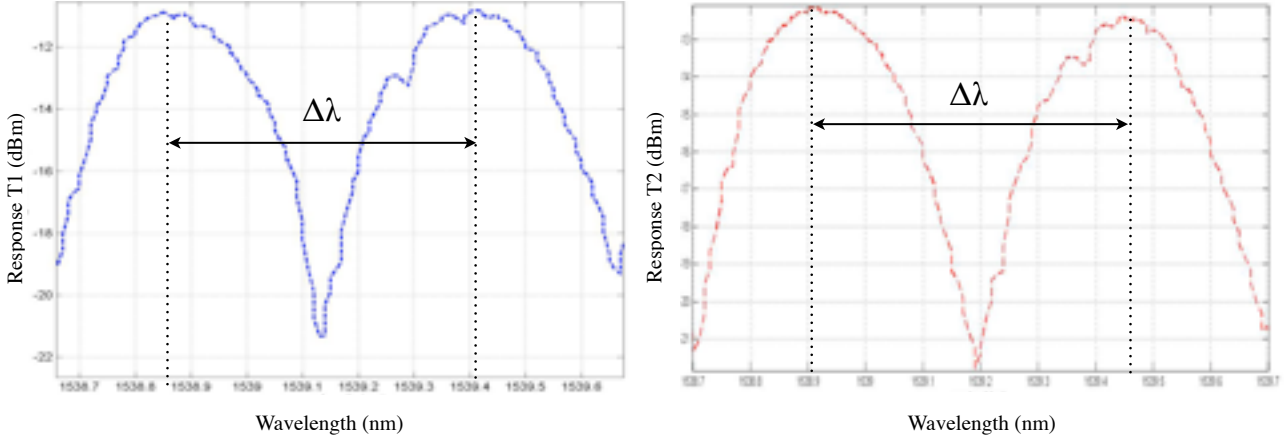


Figure 4.8. FSR obtainment. Left: input a2 to output b1. Right: input a2 to output b2

Insertion Losses procurement

The goal of this section is to be able to qualify the MZI. To do that, the attenuation of the connectors of fiber cables will be measured, in both transmission directions. The optical source (tunable laser) and the power meter will be used to know the power injected into the cable under test. Note we have changed the measurement system of the previous two measures: in this case, to measure the IL we need to know the difference between the powers at the input and at the output. That difference will be the IL. In order to achieve that we will measure the output of the laser and then we will connect it to the MZI for, later, measure the output power.

In order to obtain Insertion Loss, Input and Output Powers have been measured with power meter.

First we considered input a1 with the following values measured:

$$\begin{aligned} P_{IN_LASER} &= -8dBm \\ IL_1 &= P_{IN_LASER} - P_{OUT_1} = 1.3dB \\ IL_2 &= P_{IN_LASER} - P_{OUT_2} = 1.5dB \end{aligned}$$

Second we take a look at the output b₁:

$$P_{IN_LASER} = -8dBm$$

$$IL_1 = P_{IN_LASER} - P_{OUT_1} = 1.5dB$$

$$IL_2 = P_{IN_LASER} - P_{OUT_2} = 0.9dB$$

Then we considered input a₂:

$$P_{IN_LASER} = -8dBm$$

$$IL_1 = P_{IN_LASER} - P_{OUT_1} = 1.2dB$$

$$IL_2 = P_{IN_LASER} - P_{OUT_2} = 0.7dB$$

And finally we measured the output b₂:

$$P_{IN_LASER} = -8dBm$$

$$IL_1 = P_{IN_LASER} - P_{OUT_1} = 1dB$$

$$IL_2 = P_{IN_LASER} - P_{OUT_2} = 1.1dB$$

The goal of the Table 4.2 is to summarize this measurements.

Input	Output	IL (dB)
a ₁	b ₁	0.9
a ₁	b ₂	1
a ₂	b ₁	1.2
a ₂	b ₂	0.7

Table 4.2. Summary of experimental IL Results

According to the Table 4.2 we can see that the IL of MZI is very close to the IL of Interleaver (See Section 4.2.4).

Return Loss acquirement

Again to measure the return loss we must change the system in the laboratory. In order to get the Return Loss we have performed what Figure 4.9 indicates.

Following the schema (Figure 4.9) we can see that to achieve our goal we inject the light from the laser to a circulator. This light is going through the circulator toward the port 2, which is connected to a coupler.

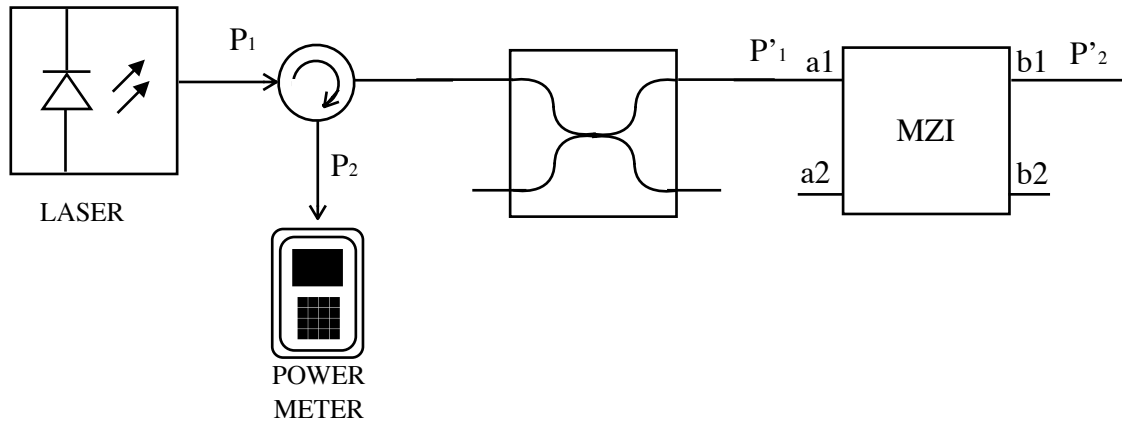


Figure 4.9. Return Loss measurement schema

The return power (or reflections) will travel from port 2 to port 3 of the circulator which is connected to out power meter. This way we can measure the Return Loss without any interference using the Equation mentioned in the Section 4.1.1.

And the values measured:

$$\begin{aligned}
 L_{DS \rightarrow 4.3} &= 4.3dB \\
 L_{US \rightarrow 4.3} &= 4.3dB \\
 P'_1 &= P_1 - L_{DS} = -1.25dBm - 4.3dB = -5.55dBm \\
 P'_2 &= P_2 - L_{DS} = -57.7dBm + 4.3dB = -53.4dBm \\
 RL &= P'_1 - P'_2 = 47.85dB
 \end{aligned}$$

Where, as we can see in Figure 4.9, P_1 and P_2 are the input and the output power of the circulator respectively, while P'_1 and P'_2 refers to the input and the output of the MZI respectively. Moreover L_{DS} are the losses trace DS (Downstream) port to MZI input and L_{US} are the losses trace US (Upstream) port to MZI input.

According to this schema shown in the Figure 4.6 we need to compensate these 4.3dB losses depending on which signal (input or output) we are measuring, in one case we will need to subtract these 4.3dB and in another case we will have to add them.

After obtaining these results it is recommended to state that it is tough to control this critical value and we can not compensate to improve geometry.

Polarization Dependent Loss measurement

The last parameter to measure is the Polarization Dependent Loss which could be critically important for the characterization of optical components: MZI and Interleaver.

Polarization dependent loss has become a standard measurement when characterizing passive optical components: MZI and Interleaver. In optical networks, where polarization is not constrained and changes randomly, the PDL of components can accumulate in an uncontrolled manner. This effect can degrade the network transmission quality and even lead to network failure.

Polarization dependent loss (PDL) is a measure of the peak-to-peak difference in transmission of an optical component or system across all possible states of polarization. It is the ratio of the maximum

and minimum transmission of an optical device with respect to all polarization states. The PDL is defined as:

$$PDL_{dB} = 10 \log \left(\frac{T_{\max}}{T_{\min}} \right) = (T_{\max})_{dBm} - (T_{\min})_{dBm} \quad (4.10)$$

Where T_{\max} and T_{\min} denote the maximum and minimum transmission through the MZI and Interleaver, respectively.

Now we will use an EDFA and a Polarizer to control the polarization of the wide light emitted by the EDFA. After that we will measure the power at a2 port of the Mach-Zehnder while we are seeing the b1 output in the OSA screen.

The Figure 4.11 describes the system built in the laboratory.

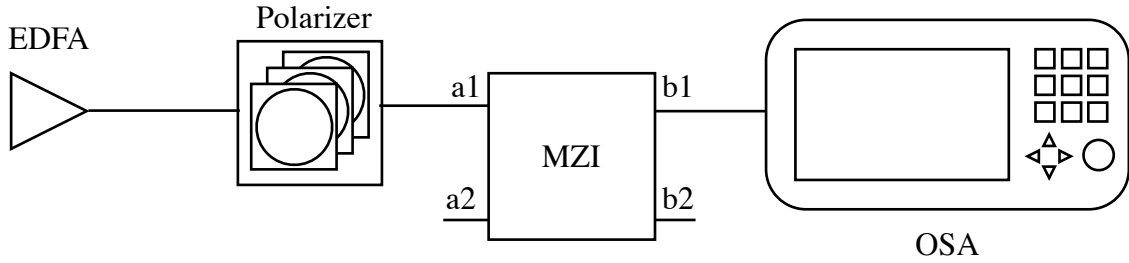


Figure 4.10. Polarization Dependent Loss measurement schema



Figure 4.11. Polarization Dependent Loss measurement In-Lab configuration

We decided to use EDFA because of the non-stability of the MZI response phase. For this reason we can obtain all response quickly without necessity to return the system when the environmental condition is changing.

Practically every component exhibits a polarization dependent transmission. As polarization of the transmission signal is not constrained in fiber optic networks, the insertion loss of a component varies over polarization. The effect can grow in an uncontrollable manner along a transmission link with severe consequences for the transmission quality because the polarization changes randomly along a fiber, in the case of MZI and Interleaver PDL have a negligible influence which we can see in the figure below.

As commented in Figure 4.12 we have the T_{\max} (right) and T_{\min} (left) are determined by marker C. We must note that we have chosen the left lobe because it is the highest one.

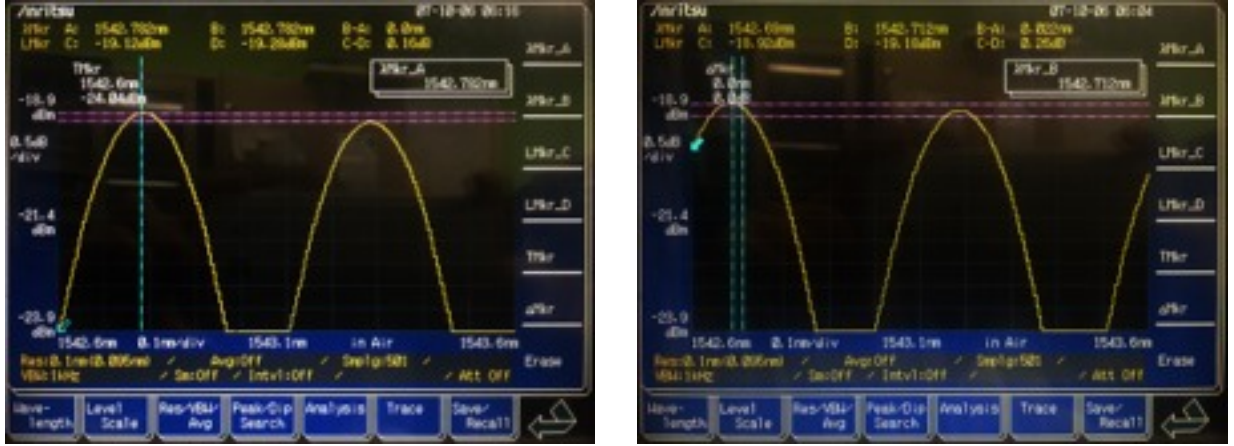


Figure 4.12. PDL of MZI from input a_1 to output b_1

According to the equation (4.10) and the results shown in Figure 4.12 we can calculate the PDL as follows:

$$PDL_{dB_{a_1 \rightarrow b_1}} = -18.92dBm - (-19.12dBm) = 0.2dB$$

Using the same strategy we will measure the PDL from input a_1 to output b_2 . In the figure below we have the T_{\max} (right) and T_{\min} (left) are determined by marker C.

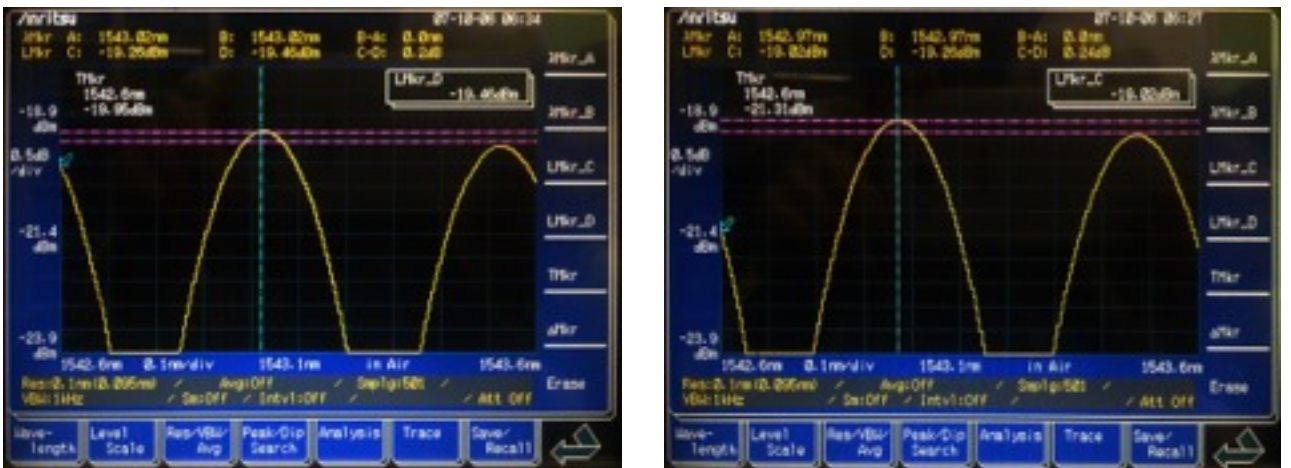


Figure 4.13. PDL of MZI from input a_1 to output b_2

According to the equation (4.10) and the results shown in Figure 4.13 we can calculate the PDL as follows, which was the worse case we could reproduce:

$$PDL_{dB_{a_1 \rightarrow b_2}} = -19.02dBm - (-19.26dBm) = 0.24dB$$

Polarization it is particular parameter for MZI device. It is random process which makes important limitation of the system because it can reduce properties of the device.

If we are working in the optimal conditions we have two possibilities to improve the system:

- i. To maintain two ways (winding) of the same symmetry inside of MZI. For that reason it is important to guarantee symmetry between two optical waves.
- ii. To compensate with external polarizer. In this case we can affect external polarizer outside of the MZI and by seeing it we can try to minimize bad effect of geometry but although it is very complicated to fix the behavior of MZI, using external polarizer it is possible to improve a little bit response.

4.2.4. Interleaver Parameters Measurement

At this point, and with all the MZI parameters obtained, we should take a look to the Interleaver ones in order to compare both devices. We will proceed equally as with the MZI:

Extinction Ratio obtainment

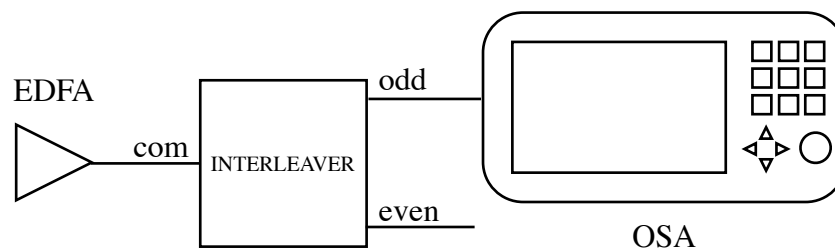


Figure 4.14. Schema of the Interleaver odd response obtainment

One more time, from the Figure 4.15 below we can identify the maximum and the minimum values of its response. Also in the same figure are shown both Interleaver responses: in yellow color is the odd response and in green color is the even.

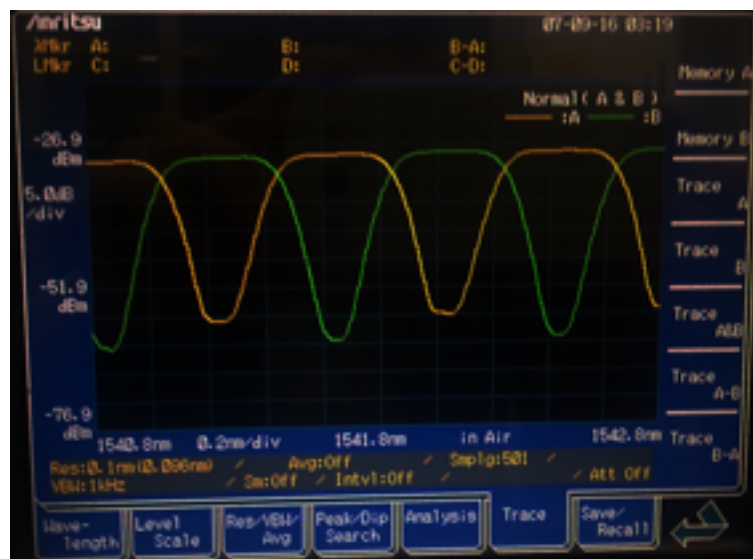


Figure 4.15. Frequency response of Interleaver shown in OSA screen

Now, in the Figure 4.16 we can see in the blue color is the odd response and in the red color is the even. Moreover we can see the measurement of the ER using the lower lobe since it is the most restrictive case.

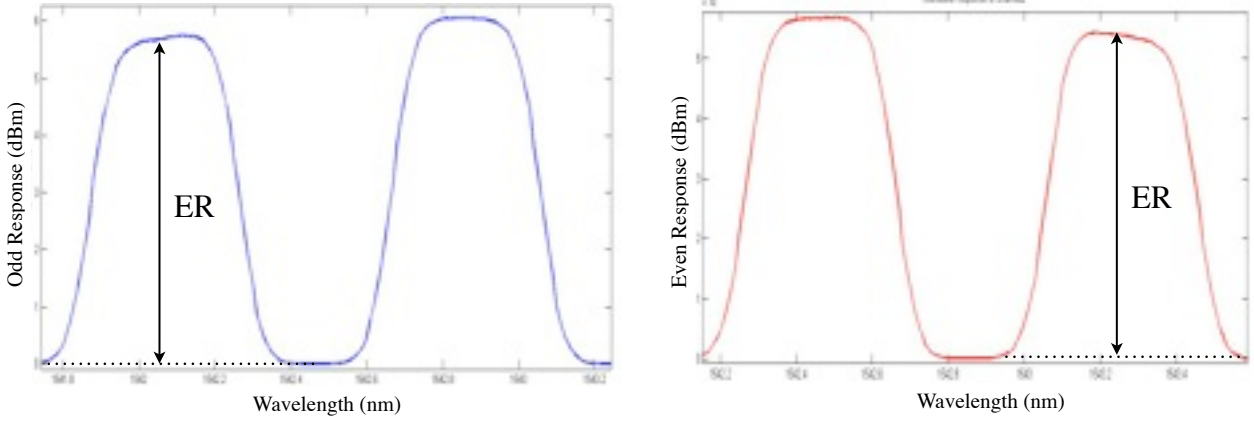


Figure 4.16. ER obtainment in Interleaver response

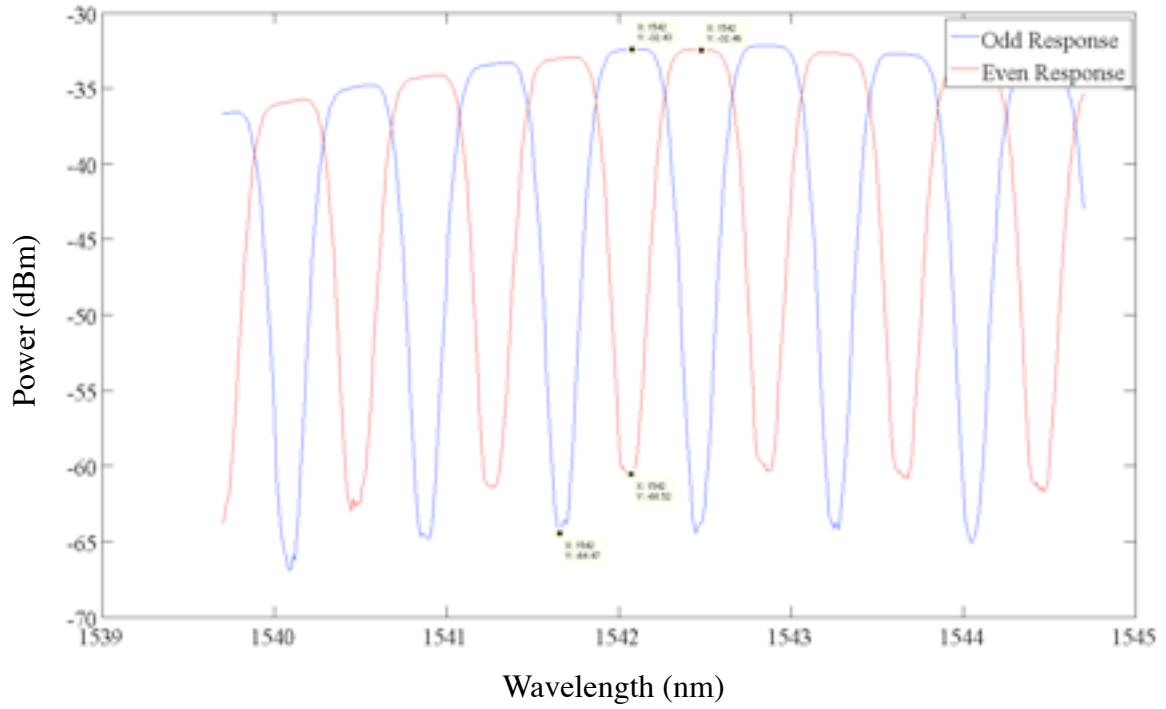


Figure 4.17. Frequency response of Interleaver captured with MATLAB

As we can see in the figures the ER equal to:

$$ER_{odd} = -32.42 \text{ dBm} - (-64.47 \text{ dBm}) = 32.05 \text{ dB}$$

$$ER_{even} = -32.46 - (-60.52) = 28.06 \text{ dB}$$

FSR Measurement

In the Figure 4.18 we can see the measurement of the FSR Interleaver where, one more time, the blue graph corresponds to the odd response and the red one corresponds to the even response. Also below there is the accurate result using again the equation (4.9):

$$FSR = \frac{c}{1550nm} - \frac{c}{(1550+0.8)nm} = 99.84GHz$$

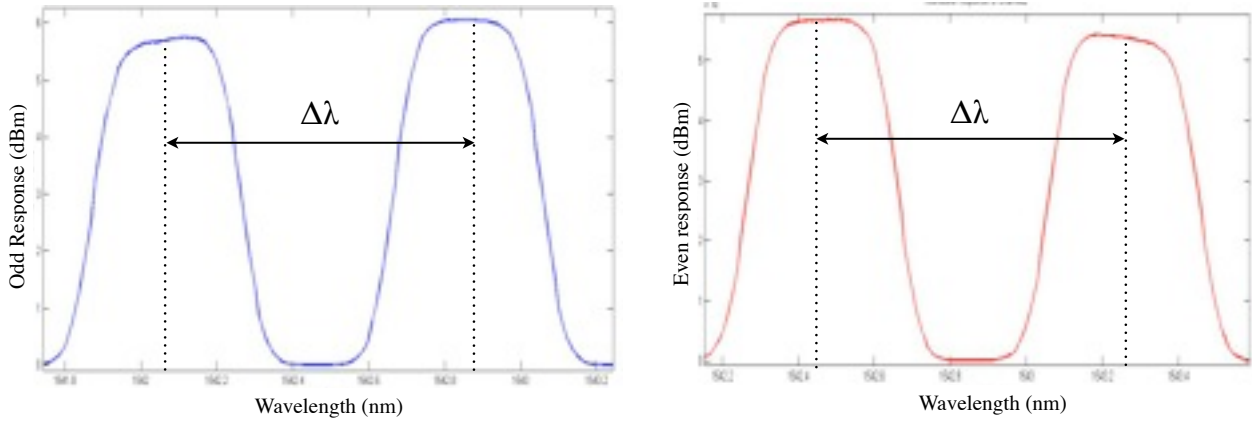


Figure 4.18. FSR obtainment of the Interleaver

Insertion Losses procurement

To measure the Insertion Losses of the Interleaver we will use the Power Meter to know the input and the output power of the Interleaver. In the laboratory we have obtained the following results:

$$IL_{odd} = P_{IN} - P_{OUT_odd} = -3.4dBm - (4.3dBm) = 0.9$$

$$IL_{even} = P_{IN} - P_{OUT_even} = -3.4dBm - (4.6dBm) = 1.2dB$$

Return Loss measurement

As in the MZI measurements, the Return Loss obtainment is done using a circulator and a Power Meter.

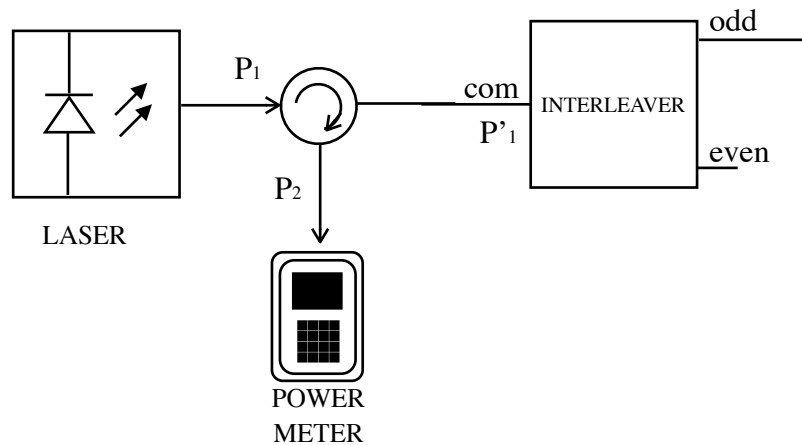


Figure 4.19. RL measurement of the Interleaver schema

This is good moment to remember the RL formula:

$$RL(dB) = -10 \log \left(\frac{P'_2}{P'_1} \right) \quad (4.10)$$

And in our experiment we have measured the following results of Return Loss:

$$L_{DS \rightarrow 4.3} = 4.3dB$$

$$L_{US \rightarrow 4.3} = 4.3dB$$

$$P'_1 = P_1 - L_{DS} = -1.5dBm - 4.3dB = -5.8dBm$$

$$P'_2 = P_2 - L_{DS} = -60dBm + 4.3dB = -55.7dBm$$

$$RL = P'_1 - P'_2 = 49.9dB$$

Polarization Dependent Loss acquirement

Same than with the MZI, in order to obtain the PDL, we will connect the interleaver after the polarizer and we will excite them using the EDFA.

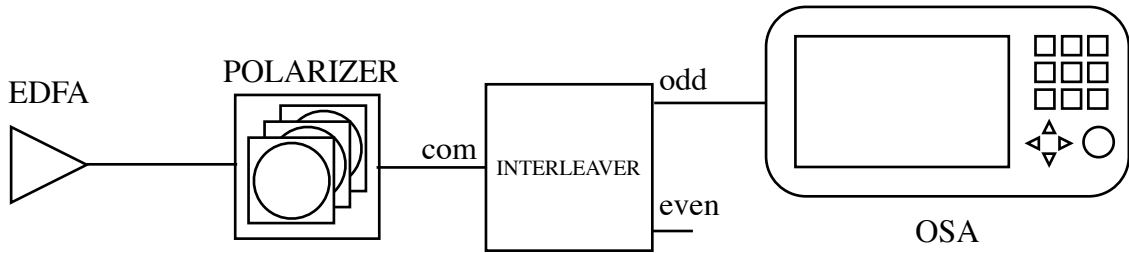


Figure 4.20. Polarization Dependent Loss measurement schema for Interleaver

Now we have the T_{\max} (right) and T_{\min} (left) are determined by marker C. We must note that we have chosen the centered lobe because it is the highest one.

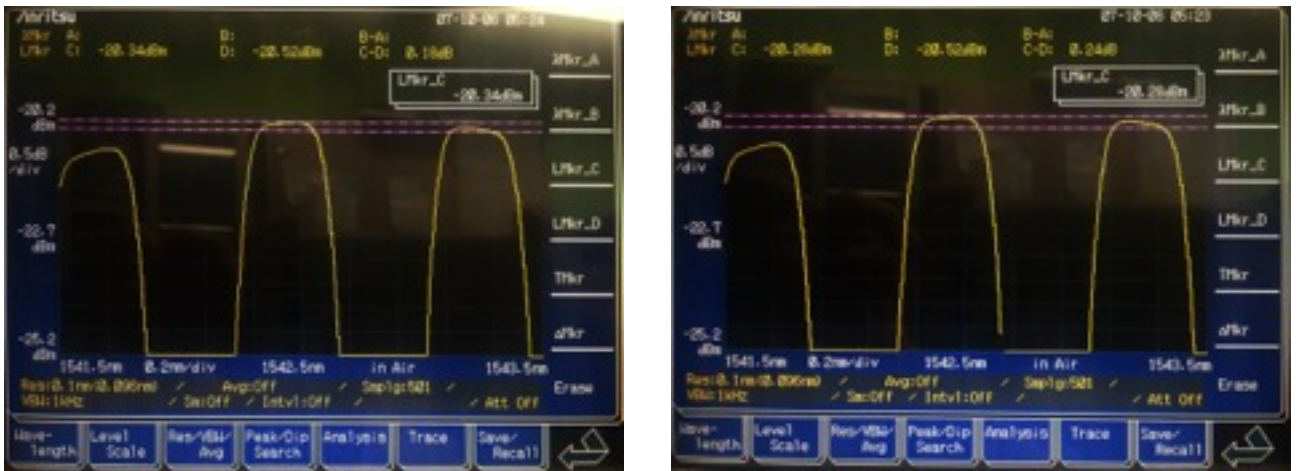


Figure 4.21. PDL of MZI from input a_1 to output b_1

According to the equation (4.10) and the results shown in Figure 4.21 we can calculate the PDL as follows:

$$PDL_{dB} = -20.28dBm - (-20.34dBm) = 0.06dB$$

To summarize the results: polarization dependent loss for both arms of MZI are $PDL_{MZI_a1_b1} = 2.4dB$, $PDL_{MZI_a1_b2} = 2dB$ and in interleaver case $PDL_{INTERLEAVER} = 0.06dB$, in this case we can tell, PDL of interleaver is smaller than in the MZI case, somehow in both cases we got insignificant PDL, thereby small changes was not influence in the response.

4.2.5. Downstream system: behavior of MZI and Interleaver

In this subsection, and however is the most important one, we will build the complete set up for the Downstream simulation in our laboratory for both devices which have been compared before (MZI and Interleaver).

In order to simulate a possible signal from the Internet Service Provider (ISP) or the Optical Line Terminal (OLT) we will use two tunable lasers and we will mix them using a coupler which we will characterize before.

The idea of this experiment is to maintain two set up: with MZI and with Interleaver devices in order to see the splitting of two users in their outputs and to make a comparison between the results. To compare them we will obtain the powers at the input and output ports to see the Insertion Losses and the Extinction Ratio.

MZI Set up

The idea of this experiment to measure the power in the outputs of MZI. In order to achieve it the Figure 4.22 shows the system built in the laboratory and the Figure 4.23 the corresponding schema.

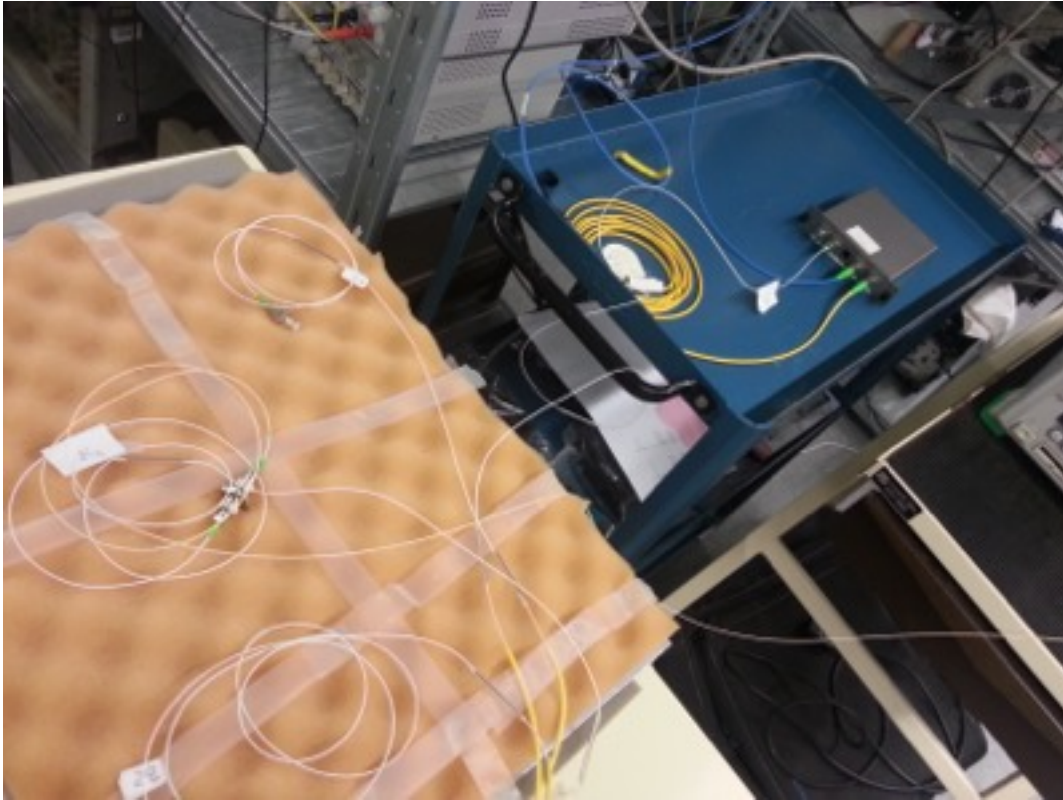


Figure 4.22. Set up with MZI in the GCO Laboratory

The goal of the project is to split two channels and to see results in the output that is why we need a coupler to combine two lasers in order to generate the OLT signal. Then we will introduce this signal to the MZI to see the states of the lasers in the output b_1 and in the output b_2 .

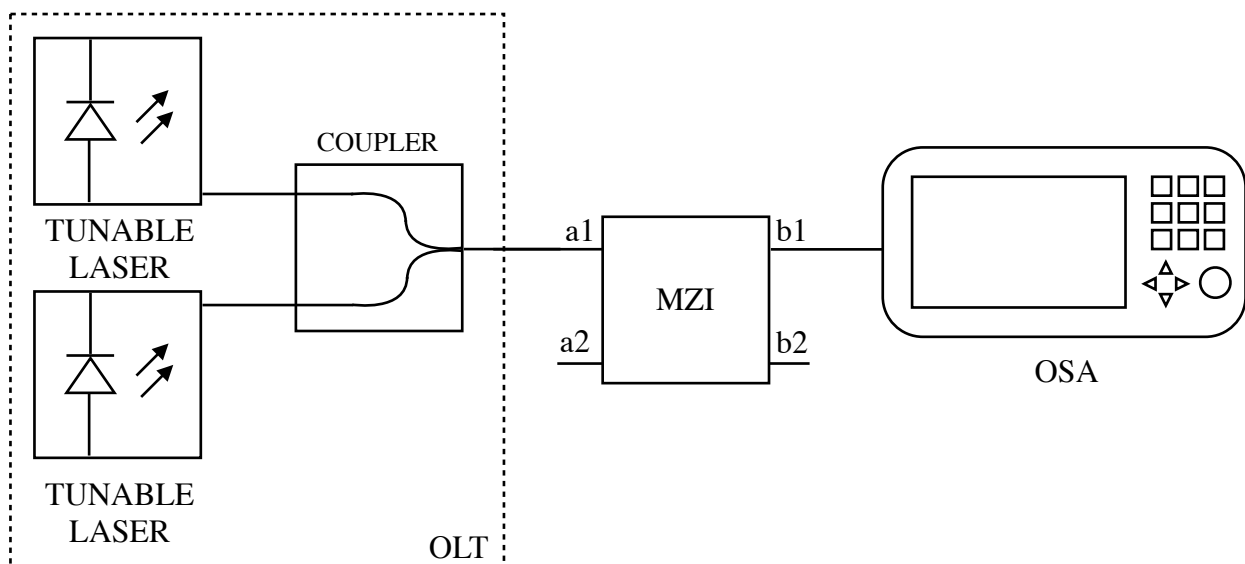


Figure 4.23. Schema of the MZI Set up

We inject the light emitted by first tunable laser into first input of coupler and the second tunable laser into the second input of coupler. The measurement will be done, first connecting to the output b_1 of MZI directly into the optical spectrum analyzer (OSA) and then the same with the output b_2 .

At this point we could change the schema to the following one since is what we are trying to simulate in the lab:

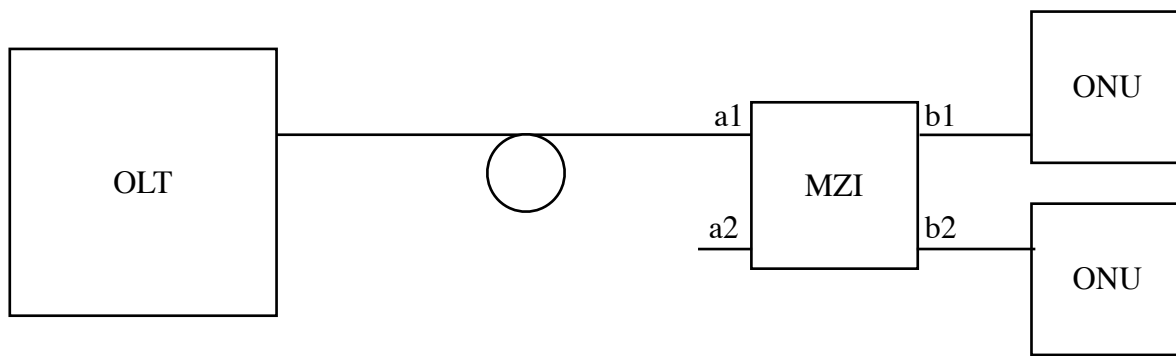


Figure 4.24. Schema of the simulated situation

That means, as explained in previous chapters, that we are trying to split 2 carriers coming together from the OLT in order to send each carrier to each ONU.

The results we got are the following (see Figure 4.25):

$$P_1 = P_2 = -10.3 \text{ dBm}$$

$$\lambda_1 = 1549.76 \text{ nm}, \lambda_2 = 1550.0 \text{ nm} \rightarrow \Delta\lambda \approx 0.25 \text{ nm}$$

The Figure 4.25 shows the generated signal with 2 carriers with the same power.

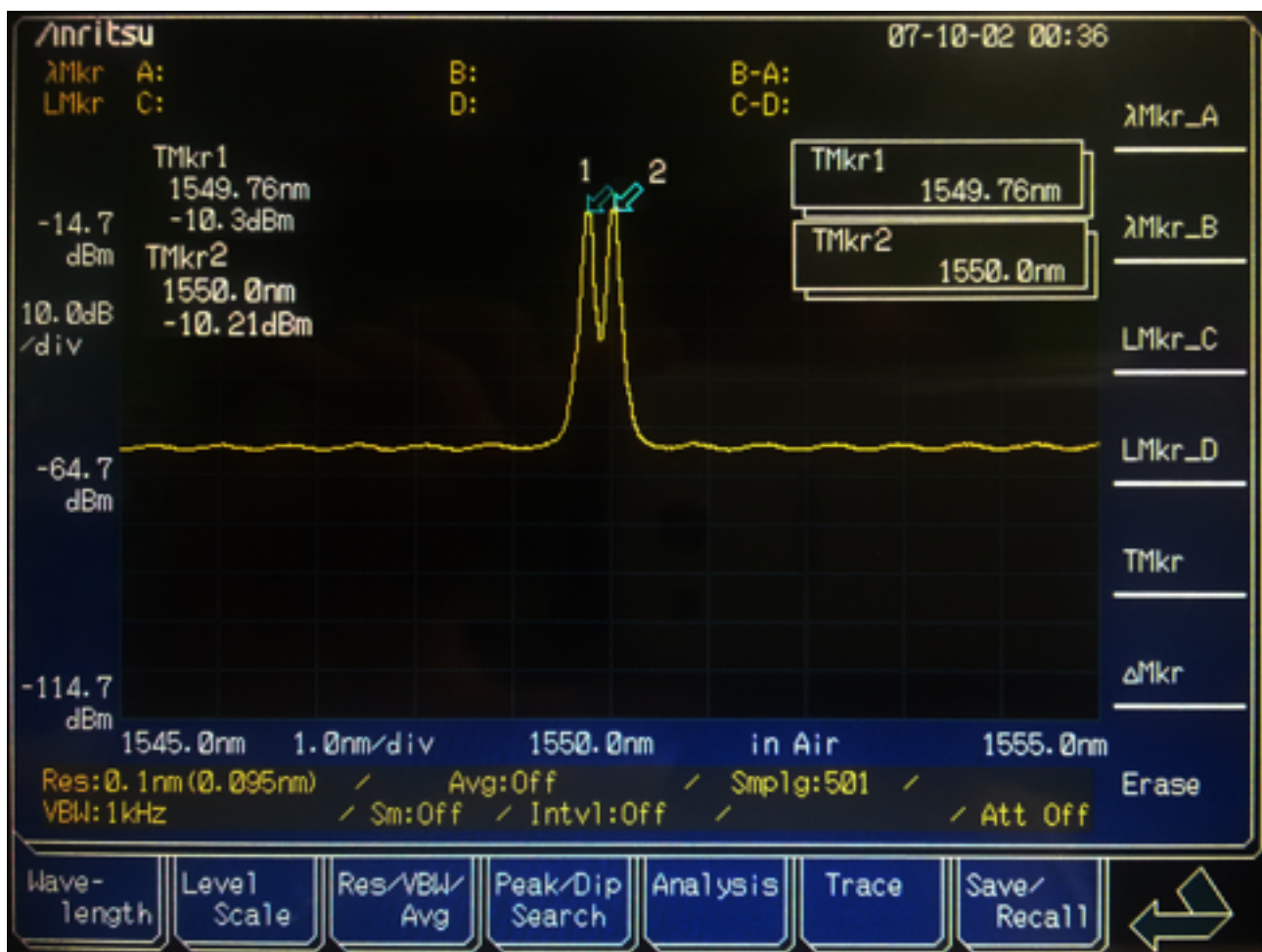


Figure 4.25. Signal generated with two lasers and coupler

We also should understand why both lasers are so close to each other. As we calculated in the previous subsections, the MZI has a FSR = 0.5nm, that means we are able to split users when the distance between them is a multiple of half FSR.

$$\Delta\lambda = k \cdot \frac{FSR}{2} \quad k = \mathbb{Z}^+ \quad (4.11)$$

So we have to generate the signal with two lasers separated $\Delta\lambda = 0.5/2 = 0.25\text{nm}$ in order to show how to split them. To calculate the spacing in frequency domain we have just to apply the formula:

$$\Delta f = \frac{c}{\lambda} - \frac{c}{\lambda + \Delta\lambda} = 31.22\text{GHz} \quad (4.12)$$

Then, connecting this input to our MZI a_1 port we can capture the signal of the Figure 4.26 at the output b_1 and the signal of the Figure 4.27 at the output b_2 .

In Figure 4.26 two channels are shown in the output b_1 of the MZI; one of this two channels have maximum power, this is mean the high pick which is equal 13,03 dBm filtered by MZI in the output b_1 and this is what we supposed to see. And the obtained results are as follows:

$$\begin{aligned} P_1 &= -13.03\text{dBm}, P_2 = -19.97\text{ dBm} & \rightarrow & \Delta P = 6.94\text{dB} \\ \lambda_1 &= 1549.76\text{nm}, \lambda_2 = 1550.0\text{nm} & \rightarrow & \Delta\lambda \approx 0.25\text{nm} \end{aligned}$$

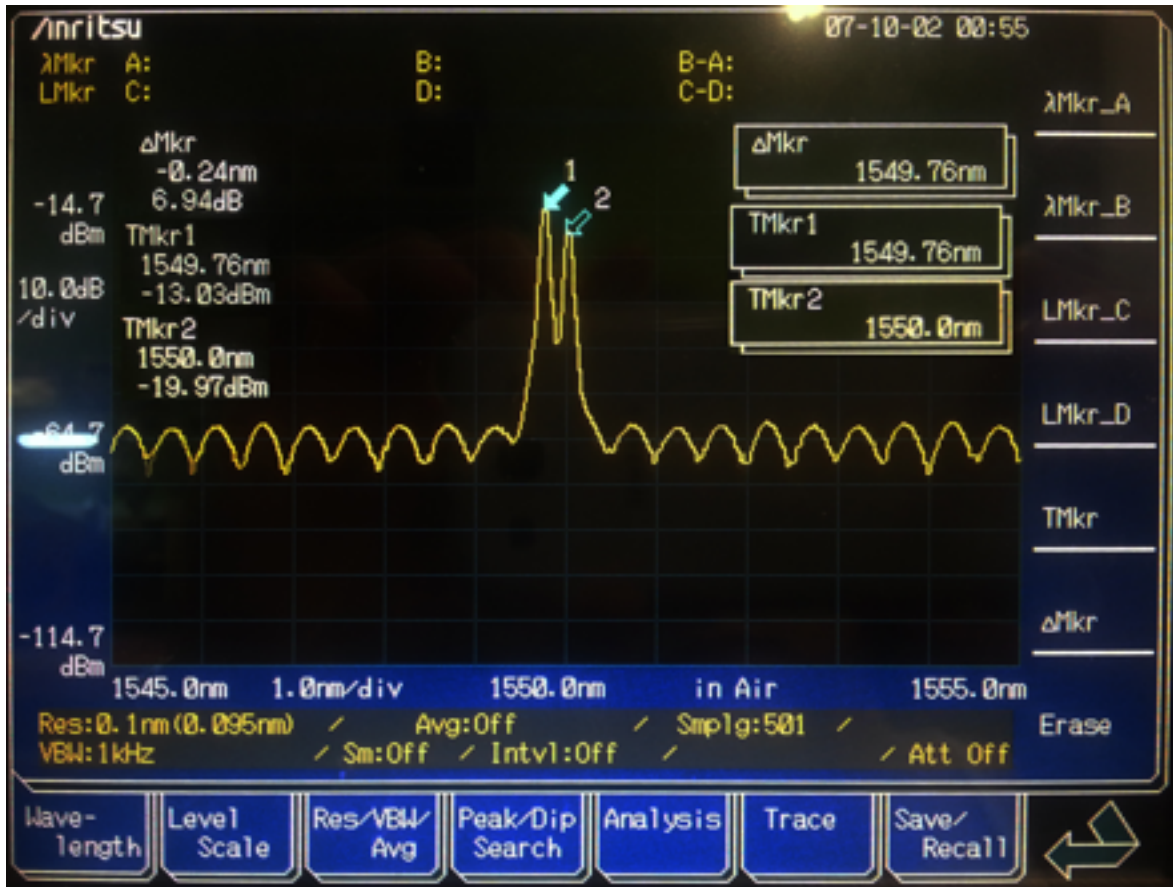


Figure 4.26. Output b_1 of the MZI

In Figure 4.27 the same view is shown but in the output b2 of the MZI; in this case the maximum power is 13.11 dBm filtered by MZI in the output b2 (blue arrow 2 is showing it). The summary of the results are below:

$$P_1 = -25.81 \text{ dBm}, P_2 = -13.11 \text{ dBm} \rightarrow \Delta P = 12.7 \text{ dB}$$

$$\lambda_1 = 1549.76 \text{ nm}, \lambda_2 = 1550.0 \text{ nm} \rightarrow \Delta \lambda \approx 0.25 \text{ nm}$$

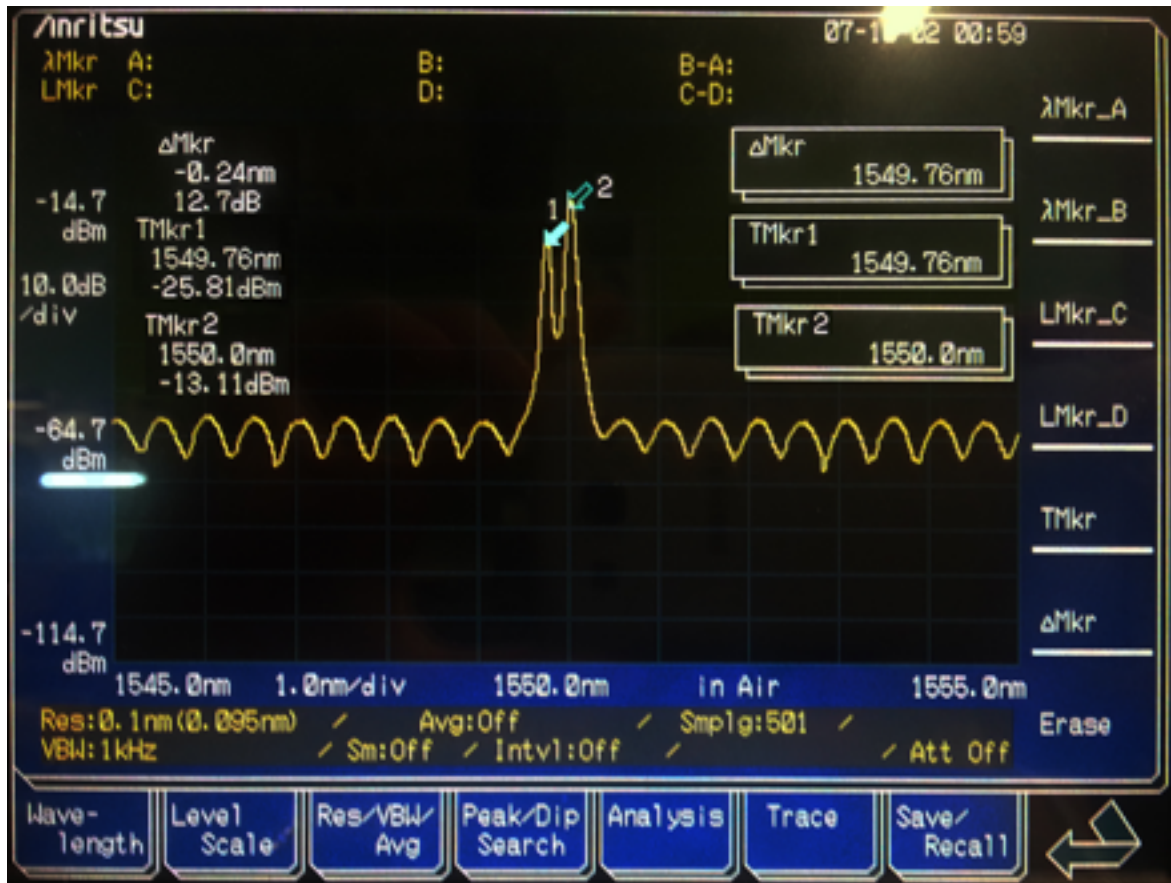


Figure 4.27. Output b₂ of the MZI

In those two figures we could see directly the power of each laser in both outputs as well as the ER of each arm what is the difference between the powers.

Moreover, using the Figure 4.25 again, we can calculate the IL in each arm of the MZI. Below the table is showing the results of this experiment in the worse case.

	Input MZI	Output b ₁	Output b ₂
Laser 1 Power	-10.3 dBm	-13.03 dBm	-25.81 dBm
Laser 2 Power	-10.21 dBm	-19.97 dBm	-13.11 dBm
ER	-	6.94 dB	12.7 dB
IL	-	2.73 dB	2.81 dB

Table 4.3. Final results of MZI

Note we have more or less the same IL in both outputs, but almost double ER in output b_2 in comparison with b_1 this could be because the MZI has a really poor stability and the response is changing constantly and it is tough to capture the best result. In our capture we could get those 6.94 dB but in the reality, if we could stabilize the MZI, we could achieve the 12.7 dB measured in the second output.

Interleaver Set up

Same than with the MZI we will proceed with the Interleaver. We will use the same coupler and two lasers to generate the signal expected from the OLT but now we have to know that the wavelengths will be changed since the Interleaver has a different FSR. Specifically, in our case, the Interleaver has a $\text{FSR} = 0.8 \text{ nm}$ what will force is to set up two lasers with $\Delta\lambda = 0.8/2 = 0.4 \text{ nm}$ of distance.



Figure 4.28. Interleaver set up in GCO Laboratory

Below is the corresponding schema of this set up. Note that is exactly the same than in the Figure 4.23 but with the Interleaver instead of the MZI.

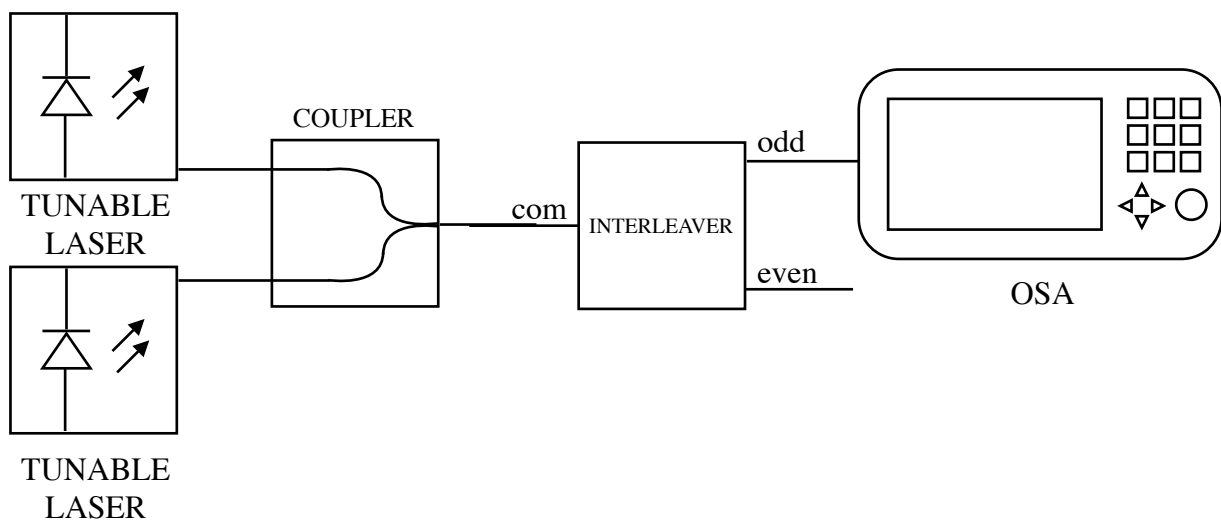


Figure 4.29. Schema of the Interleaver Set up

Again after generating the signal with two users we are introducing it from the common input of the Interleaver and then we are measuring the signal in both outputs (odd and even).

First we will show the input signal, the one generated with two lasers and the coupler:

$$P_1 \approx P_2 \approx -13 \text{ dBm}$$

$$\lambda_1 = 1549.6\text{nm}, \lambda_2 = 1550.0\text{nm} \rightarrow \Delta\lambda = 0.4\text{nm}$$

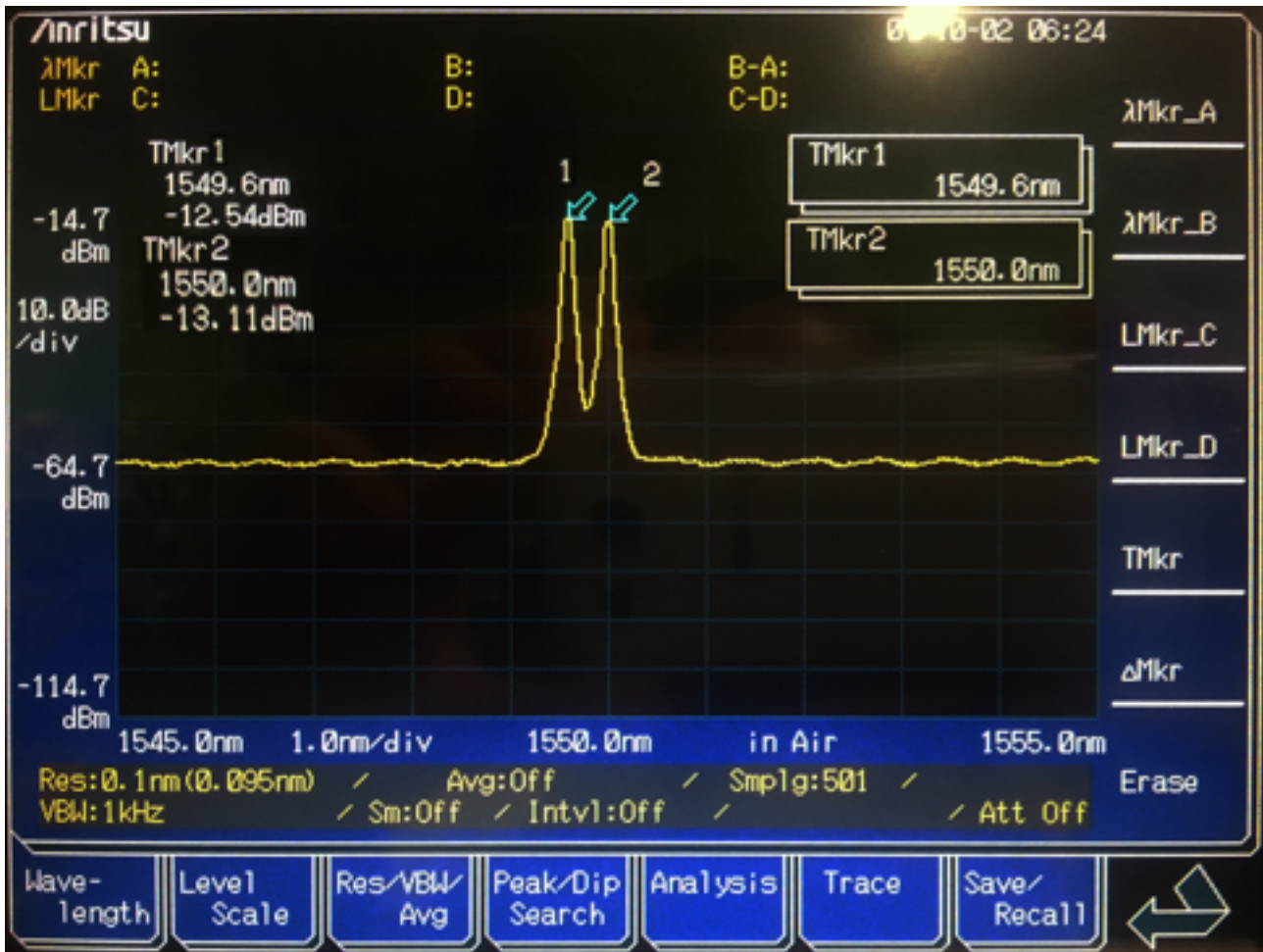


Figure 4.30. Signal generated with two lasers and coupler

Once we have the input signal generated we are able to introduce it into the Interleaver and to see both outputs.

The Figures 4.31 and 4.32 below show the output signals and powers of the Interleaver.

The same comment we will introduce in the case of interleaver, In Figure 4.31 two channels are shown in the output Odd of the MZI; one of this two channels have maximum power, this is mean the high pick which is equal 14.72 dBm filtered by MZI in the output Odd and this is what we supposed to see in the Interleaver case. In Figure 4.33 the same view is shown but in the Even output of the MZI; in this case the maximum power is 14.98 dBm filtered by MZI in the Even output. The results we got in this case are:

$$P_1 = -14.72 \text{ dBm}, P_2 = -13.11 \text{ dBm} \rightarrow \Delta P = 29.15 \text{ dB}$$

$$\lambda_1 = 1549.6\text{nm}, \lambda_2 = 1550.0\text{nm} \rightarrow \Delta\lambda = 0.4\text{nm}$$

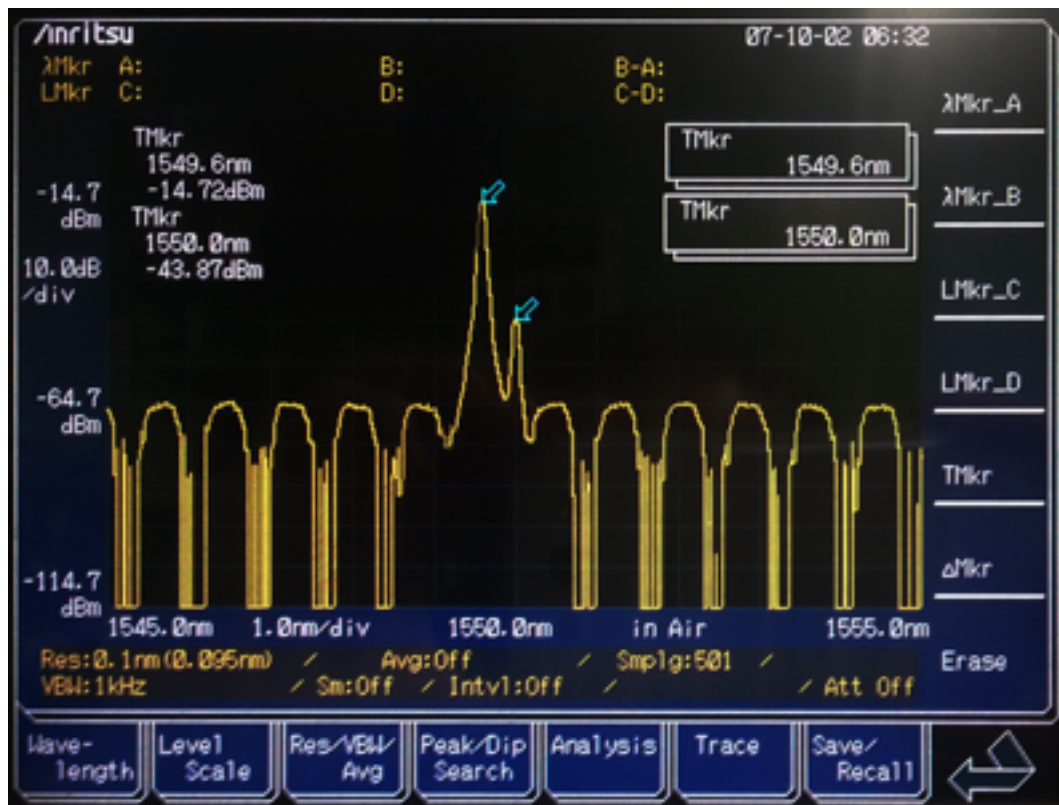


Figure 4.31. Odd output of the Interleaver

The results we got in this case are:

$$P_1 = -50.27 \text{ dBm}, P_2 = -14.98 \rightarrow \text{dBm } \Delta P = 35.29 \text{ dB}$$

$$\lambda_1 = 1549.6 \text{ nm}, \lambda_2 = 1550.0 \text{ nm} \rightarrow \Delta \lambda = 0.4 \text{ nm}$$

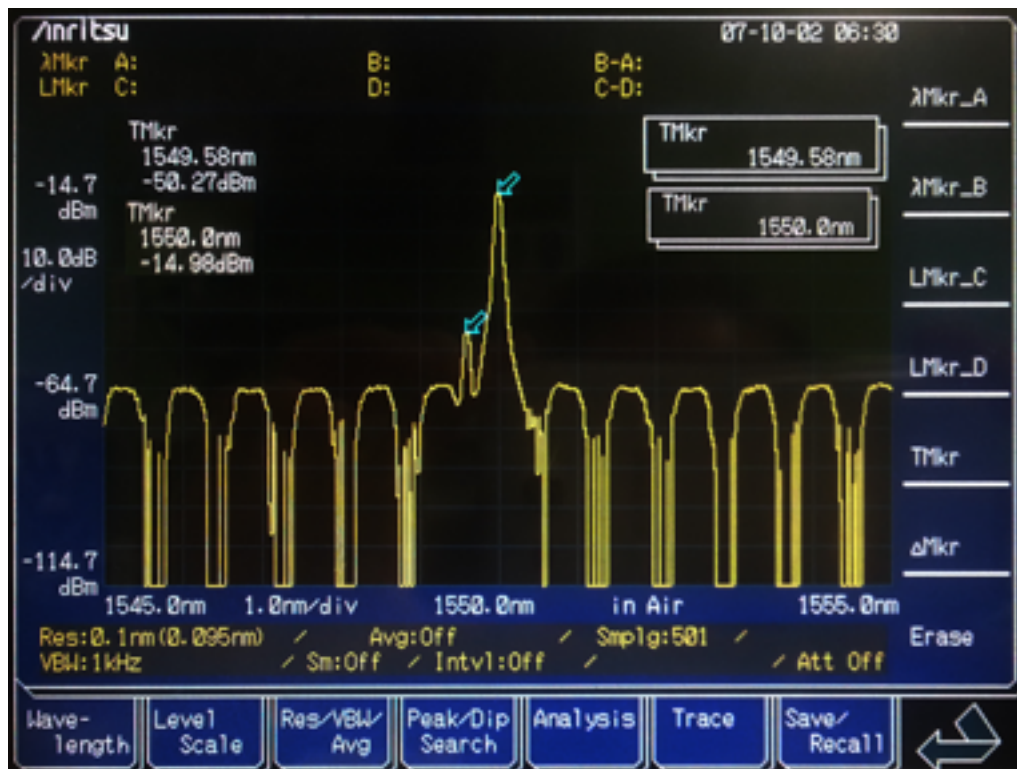


Figure 4.32. Even output of the Interleaver

At this point we can summarize the results of the Interleaver using the same table format than before.

	Input Interleaver	Odd Output	Even Output
Laser 1 Power	-12.54 dBm	-14.72 dBm	-50.27 dBm
Laser 2 Power	-13.11 dBm	-43.87 dBm	-14.98 dBm
ER	-	29.09 dB	35.29 dB
IL	-	2.18 dB	1.87 dB

Table 4.4. Final results of Interleaver

Comparison

At this point we have finished the analysis of both sets up and using the best results we can compared them as follows:

	MZI	Interleaver
ER	12.7 dB	35.29 dB
IL	2.73 dB	1.87 dB

Table 4.5. Comparison between MZI and Interleaver in Downstream set up

As we can see the Interleaver has better results than MZI, although the MZI results are not bad either, even with its non-stability.

4.2.6. Upstream system: behavior of three devices (MZI, Interleaver and coupler)

Now we will compare three different Upstream sets up. Two of them we already know: MZI and Interleaver. And the third possible set up for the Upstream is using the coupler. We are able to introduce the coupler in this case because for the Upstream we just need to combine the signal coming from the different ONUs to a single one. The coupler is able to do this but in the ideal case (50:50) it will introduce at least 3dB of IL to each ONU (assuming we just have two of them).

Coupler analysis

To simulate the case of the ONUs sending data up to the OLT we will use two lasers and we will combine them using a coupler. We want to know the IL as the most important parameter in order to compare it with MZI and Interleaver.

To measure the IL we will build the schema shown in the Figure 4.33 where we are injecting the light from the lasers directly to the coupler and then we are measuring the output of that coupler.

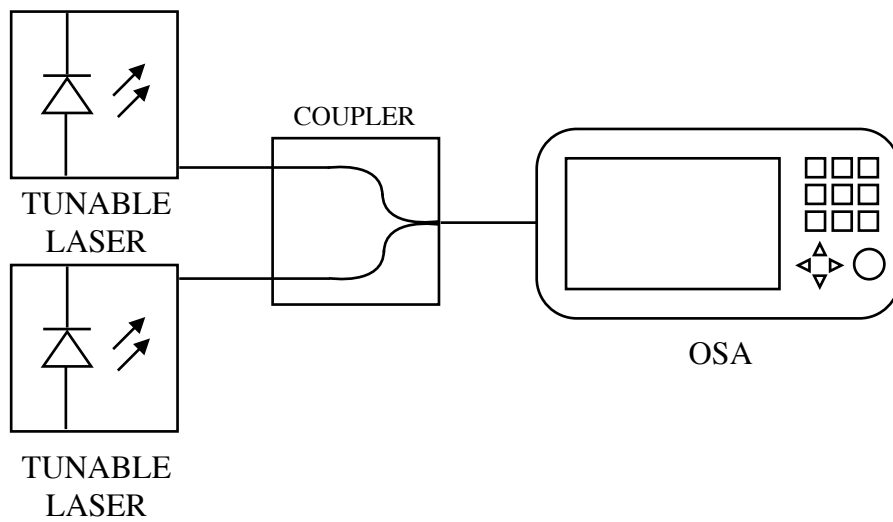


Figure 4.33. Set up with coupler in GCO Laboratory

To calculate the IL of each input we need to measure both signals and the same with the output.

The Figures 4.34, 4.35 and 4.36 show this three measurements of this set up.

In the Figure 4.34 we can see the first output with the following parameters:

$$P_1 = -7.93\text{dBm} \quad \lambda_1 = 1549.76\text{nm}$$

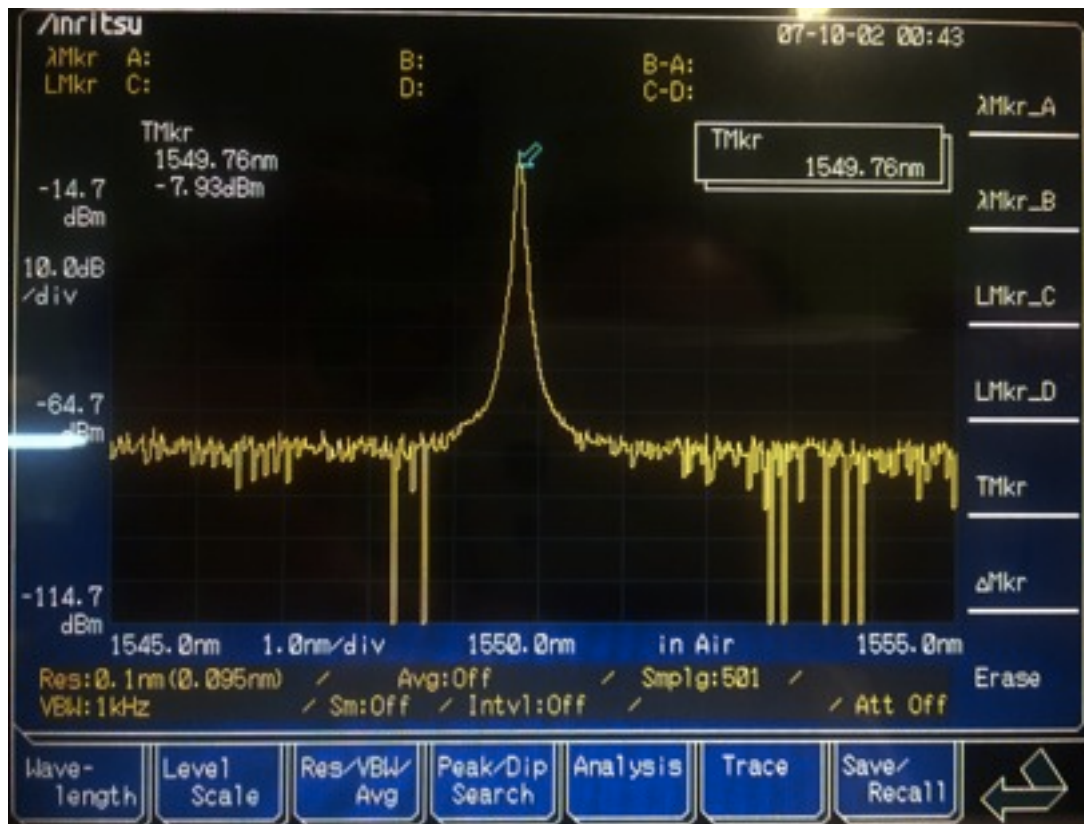


Figure 4.34. Laser 1 signal

In the Figure 4.35 we can see the second output with the following parameters:

$$P_2 = -8.953 \text{ dBm} \quad \lambda_2 = 1550.0 \text{ nm}$$

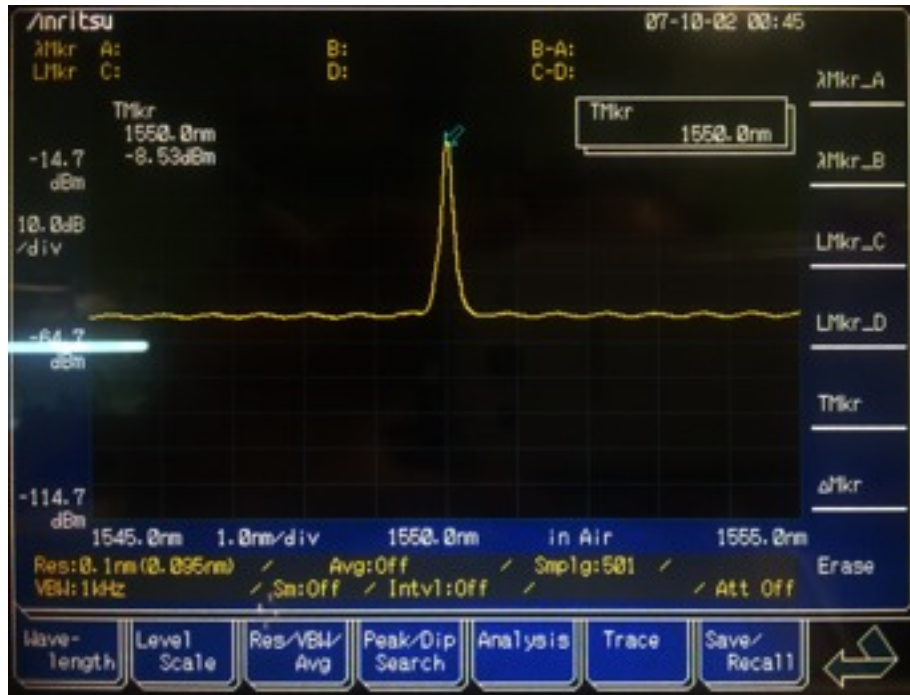


Figure 4.35. Laser 2 signal

The results we got in this case are:

$$\Delta P_1 = -2.37 \text{ dBm}, \Delta P_2 = -1.68 \text{ dBm}$$

$$\lambda_1 = 1549.76 \text{ nm}, \lambda_2 = 1550.0 \text{ nm} \rightarrow \Delta \lambda \approx 0.25 \text{ nm}$$

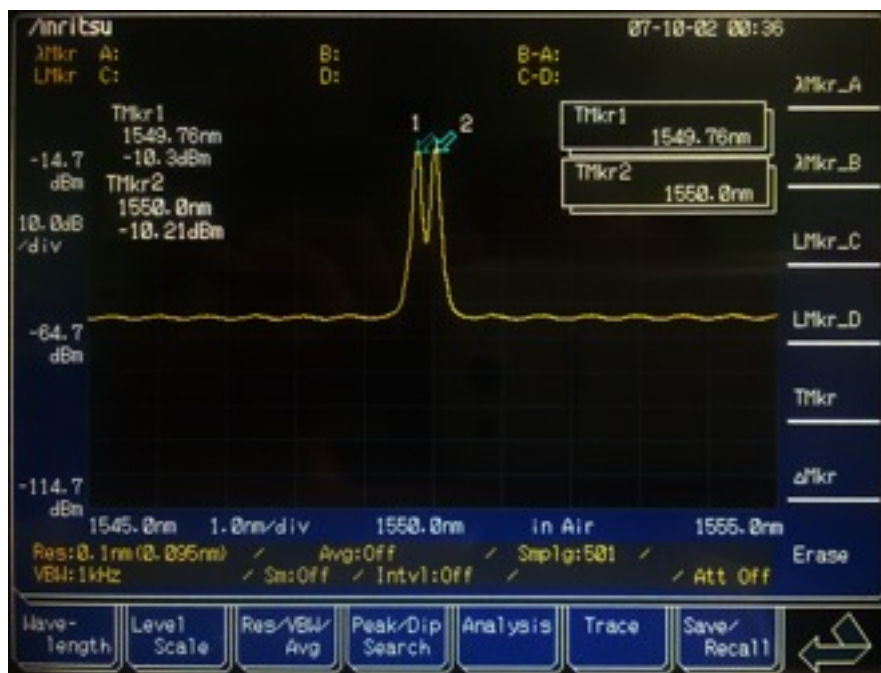


Figure 4.36. Coupler output signal

Note that the Figure 4.36 is the same than the Figure 4.25 since the first part of the MZI set up was also to combine two lasers using the coupler.

To get the Insertion Losses of the coupler we must look at the powers. With this powers we can fill the following table out:

	Power before coupler	Power after coupler	IL
Laser 1	-7.93 dBm	-10.3 dBm	2.37 dB
Laser 2	-8.53 dBm	-10.21 dBm	1.68 dB

Table 4.6. Coupler measurements

Comparison

Although we will not explain the same set up for MZI and for Interleaver (to join the users) we are able to compare all them since both MZI and Interleaver are bidirectional. However, we have done that measurements but we will avoid them since the results are pretty much the same than in Downstream case due to that bidirectionality.

	MZI	Interleaver	Coupler
IL	2.73 dB	1.87 dB	1.68 dB

Table 4.7. IL Comparison between MZI, Interleaver and Coupler

In the Table 4.7 we can see we got almost the same results for all tested optical devices.

4.2.7. Behavior of both devices in Downstream with data

Now, in this Subsection 4.2.7 and 4.2.8 we will repeat the experiment of the previous Subsections 4.2.5 and 4.2.6 but adding data to the signal. That is from now our lasers will be modulated using a pattern generator and we will see and compare the behavior of the MZI and the Interleaver.

MZI Set up filtering data

Starting with the MZI, the schema is almost the same but adding the modulator and the pattern control for each laser. Finally the experiment performed in the GCO Laboratory looked like the Figure 4.37.

To create a closer signal to the real one we will modulate the lasers (include data in the light) using modulators and the Pattern Generator. The light from the lasers is going through the modulator which also receive the RF signal from the Pattern generator and include the signal into the light coming from the lasers. Then this modulated light of each laser are combined using the coupler to be later separated again by the MZI.

One more time we will show the signal of each laser already modulated, the signal after the coupler and both outputs of the MZI.

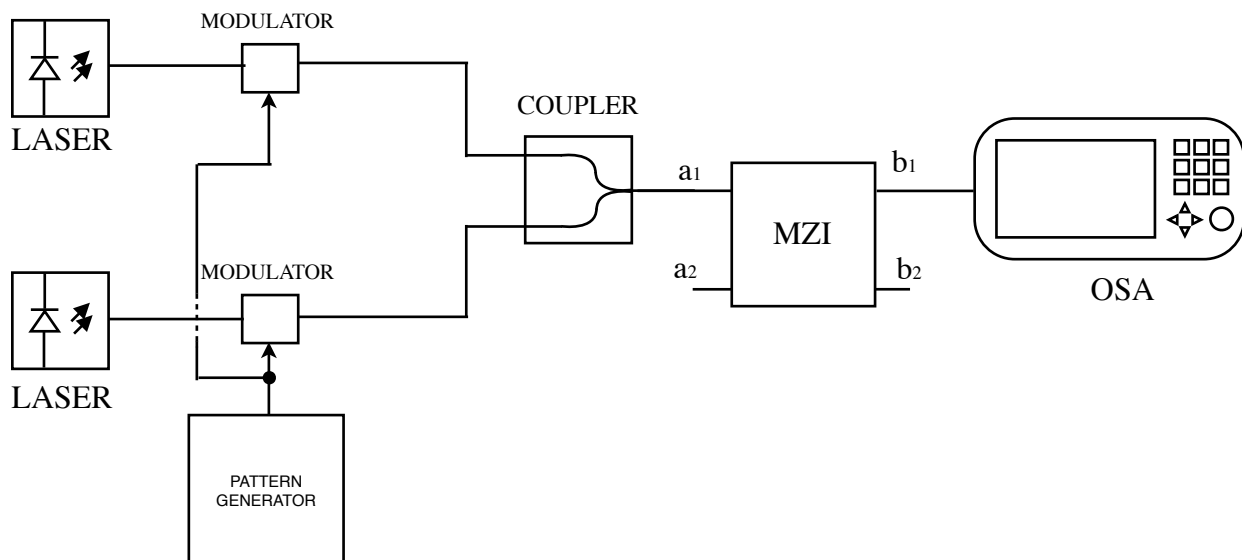


Figure 4.37. Schema of the MZI Set up modulating the lasers

The lasers modulated (and already combined) look like the Figure 4.38 below, in this case:

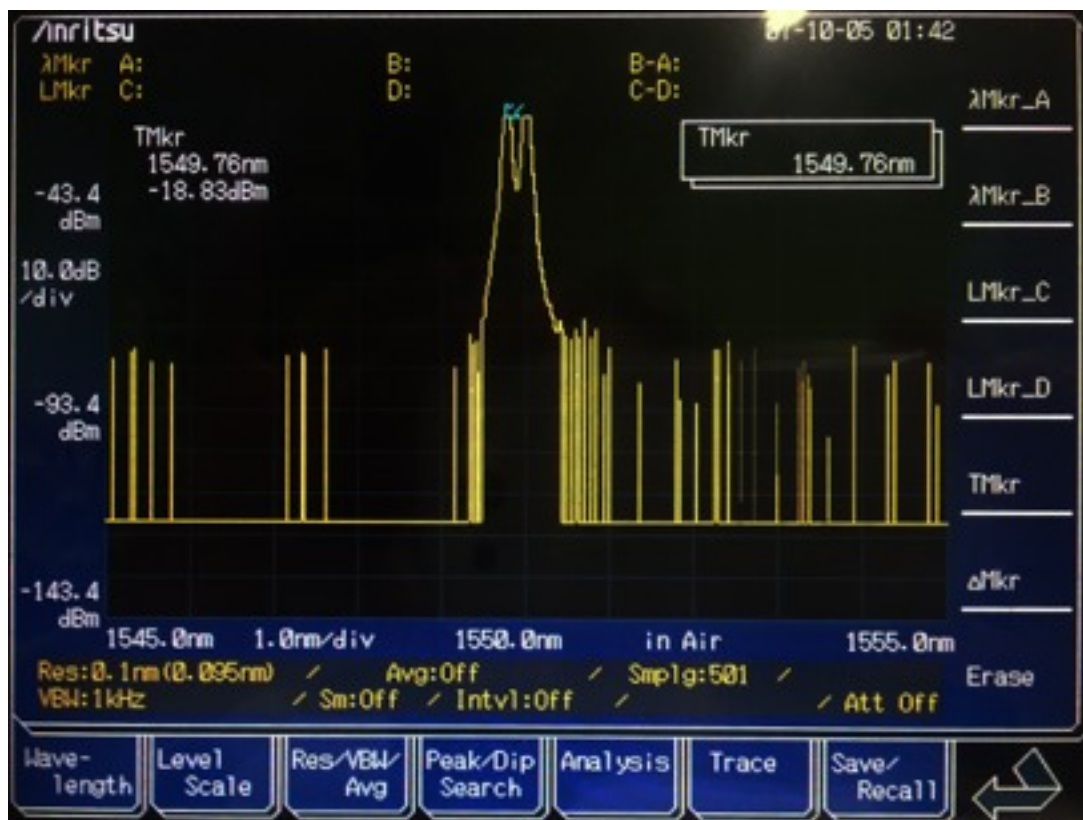


Figure 4.38. Signal generated with two lasers modulated and coupler

With powers equal to -18.83 dBm in case of the first laser and -18.52 dBm for the second one we can see how the signal is when it includes data although the changes are not enough to change completely the behavior of our devices. Again we should note the distance between them is $\text{FSR}/2 = 0.25\text{nm}$ to split them using our MZI.

The Figures 4.39 and 4.40 show the output b_1 and b_2 respectively in this case.

The results we got in this case are:

$$P_1 = -23.68 \text{ dBm}, P_2 = -34.52 \text{ dBm} \rightarrow \Delta P = 10.93 \text{ dB}$$

$$\lambda_1 = 1549.76 \text{ nm}, \lambda_2 = 1550.0 \text{ nm} \rightarrow \Delta \lambda \approx 0.25 \text{ nm}$$

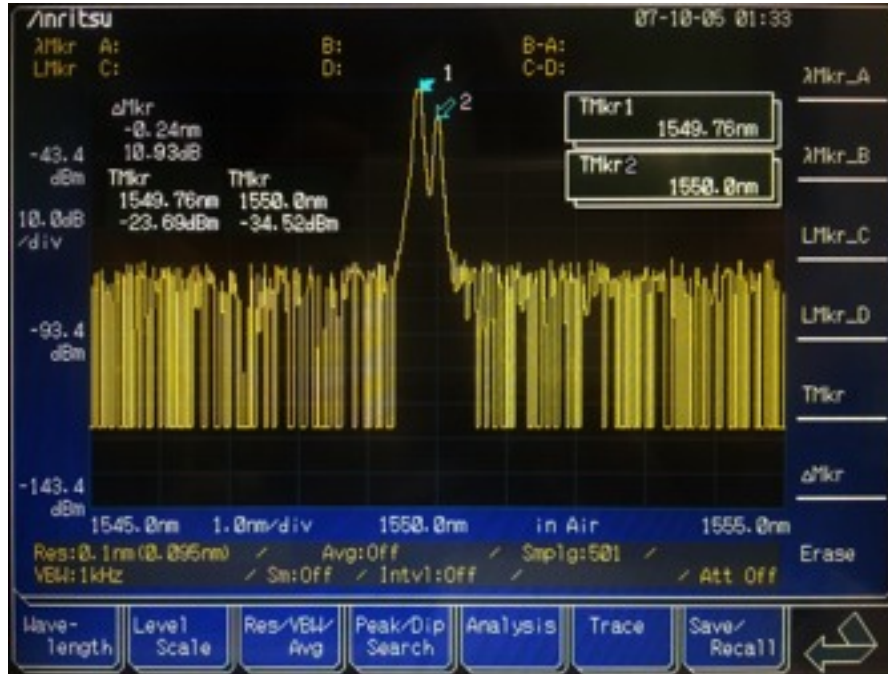


Figure 4.39. Output b_1 of the MZI

The results we got in this case are:

$$P_1 = -30.83 \text{ dBm}, P_2 = -29.96 \text{ dBm} \rightarrow \Delta P = 9.87 \text{ dB}$$

$$\lambda_1 = 1549.76 \text{ nm}, \lambda_2 = 1550.0 \text{ nm} \rightarrow \Delta \lambda \approx 0.25 \text{ nm}$$

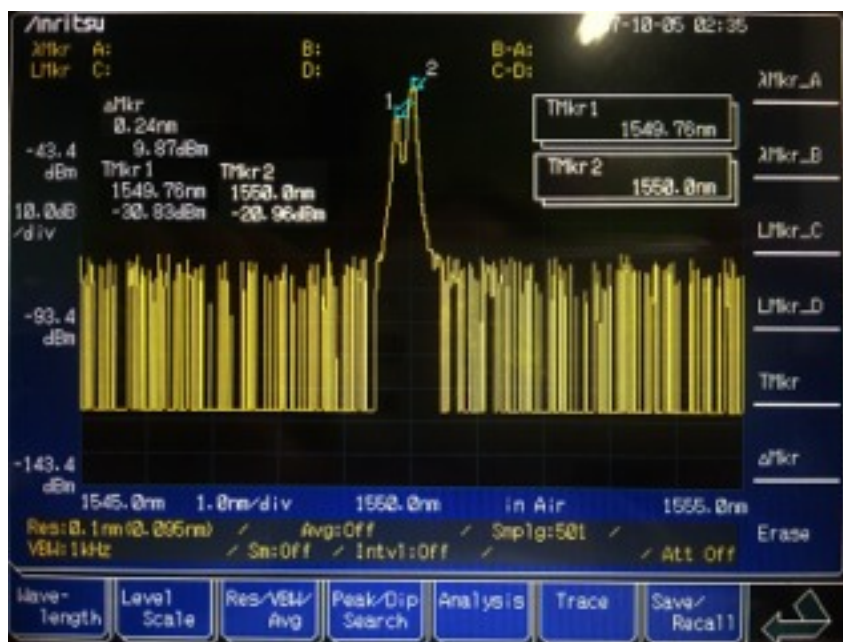


Figure 4.40. Output b_2 of the MZI

To summarize the results shown above here is the Table 4.12 where we can see the powers and the ER and IL obtained.

	Input MZI	Output b ₁	Output b ₂
Laser 1 Power	-18.83 dBm	-23.69 dBm	-30.83 dBm
Laser 2 Power	-18.52 dBm	-34.52 dBm	-20.96 dBm
ER	-	10.83 dB	9.87 dB
IL	-	4.86 dB	2.44 dB

Table 4.8. Final results of MZI

We can see how the results are more or less the same than with data since the signal, in the optical domain and with our resolution do not change that much.

Moreover note that the IL in the output b₁ is bigger than expected and it is due to the deviations and non-stability of the MZI.

Interleaver Set up filtering data

Now we will do the same with the Interleaver. One more time the schema of the Figure 4.40 shows how he modulate the lasers but we will avoid to explain one more time the same than in the previous part with MZI.

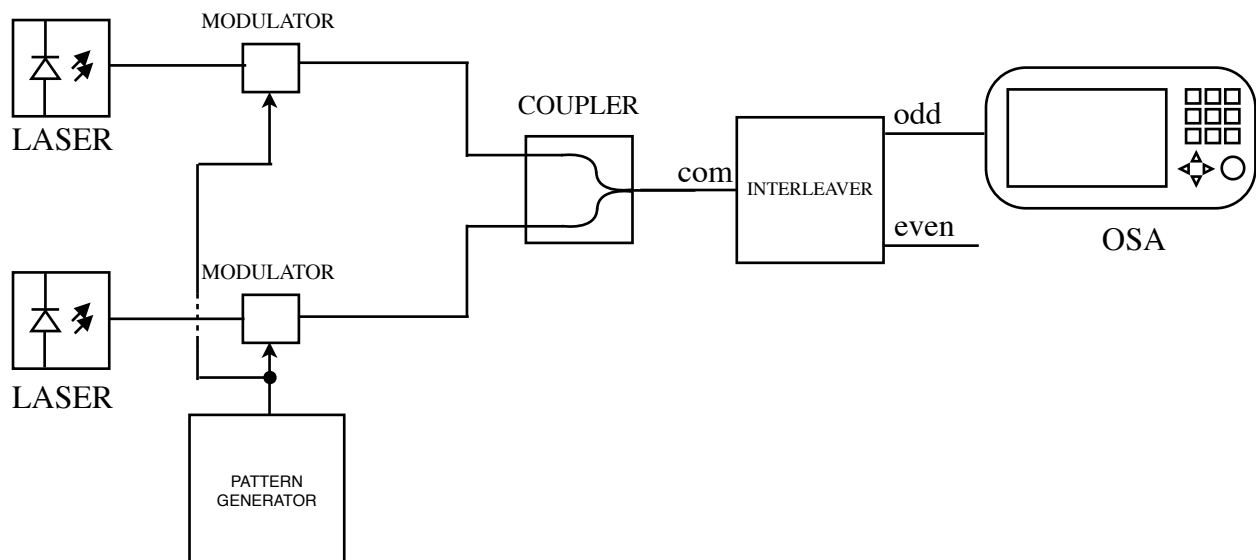


Figure 4.41. Schema of the Interleaver Set up modulating the lasers

Once we have the set up ready, we proceed the same way, first obtaining the signal generated with the lasers, the modulators and the coupler. And then we will see how the Interleaver works to split the users in each of its outputs.

Now we will see, in the Figure 4.42, the signal generated one more time with the lasers, the modulators and the coupler.

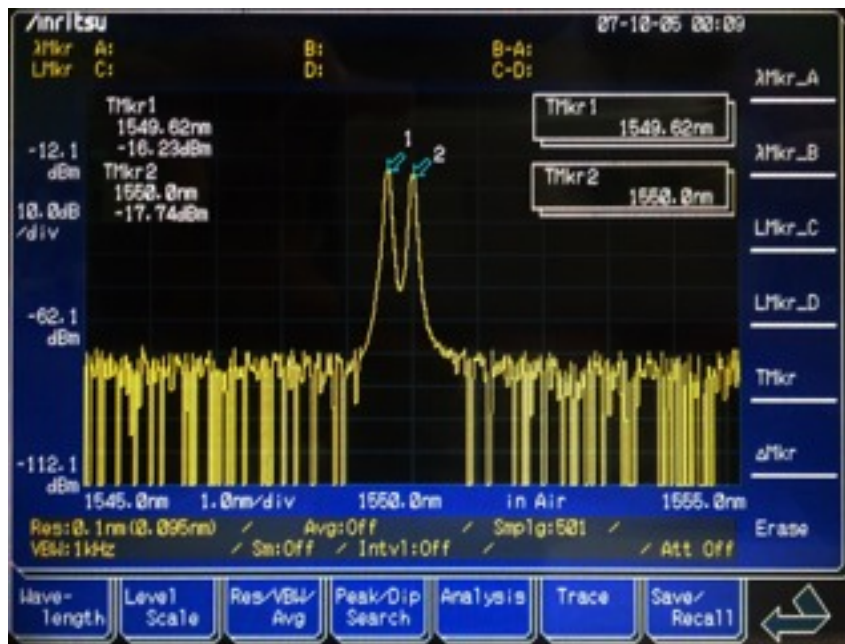


Figure 4.42. Signal generated with two lasers modulated and coupler

In the figure above we see the both modulated signals with powers of -16.23 dBm and -17.74 dBm in this case. Again the signal is not changing a lot.

The Figures 4.43 and 4.44 show the even and the odd output respectively when using data.

The results we got in this case are:

$$P_1 = -17.17 \text{ dBm}, P_2 = -46.74 \text{ dBm} \rightarrow \Delta P = 29.6 \text{ dB}$$

$$\lambda_1 = 1549.6 \text{ nm}, \lambda_2 = 1550.0 \text{ nm} \rightarrow \Delta \lambda = 0.4 \text{ nm}$$

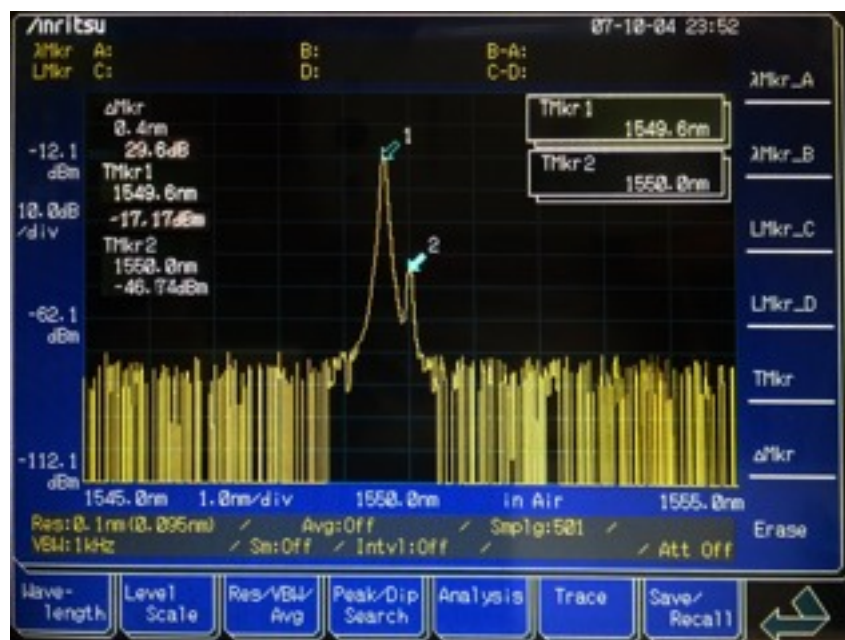


Figure 4.43. Even Output of the Interleaver

The results we got in this case are:

$$P_1 = -53.08 \text{ dBm}, P_2 = -18.52 \text{ dBm} \rightarrow \Delta P = 34.56 \text{ dB}$$

$$\lambda_1 = 1549.6 \text{ nm}, \lambda_2 = 1550.0 \text{ nm} \rightarrow \Delta \lambda = 0.4 \text{ nm}$$

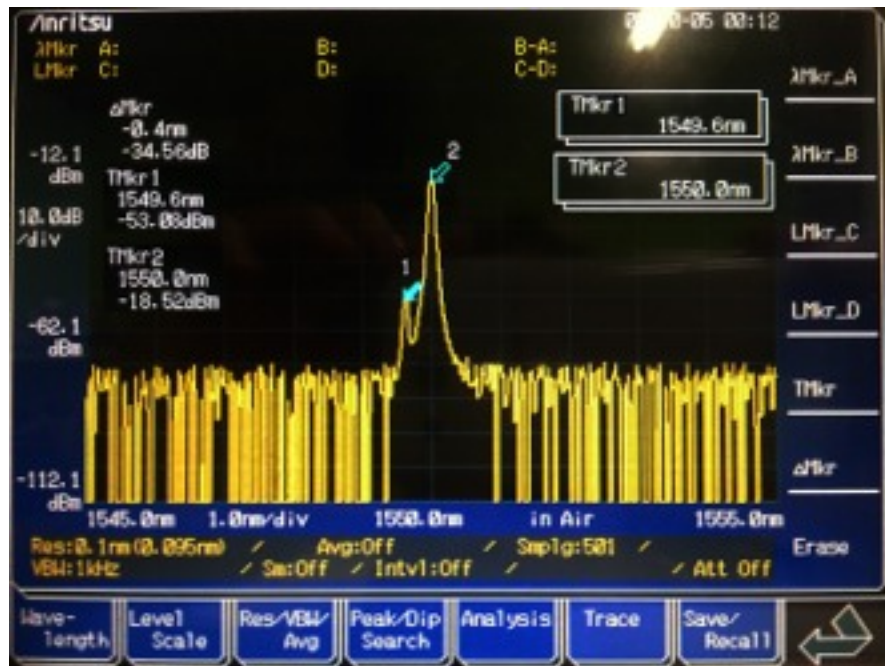


Figure 4.44. Odd Output of the Interleaver

At this point we can summarize the results of the Interleaver with modulated signal using the same table format than before.

	Input Interleaver	Odd Output	Even Output
Laser 1 Power	-16.23 dBm	-17.17 dBm	-53.08 dBm
Laser 2 Power	-17.74 dBm	-46.74 dBm	-18.52 dBm
ER	-	29.57 dB	34.56 dB
IL	-	0.94 dB	0.78 dB

Table 4.9. Final results of Interleaver with data

We want to highlight the results obtained right now with the Interleaver since they have been improved the IL results considerably in the case with data.

Comparison

At this point we have finished the analysis of both set ups and using the best results we can compared them as follows:

	MZI	Interleaver
ER	10.83 dB	34.56 dB
IL	2.44 dB	0.78 dB

Table 4.10. Comparison between MZI and Interleaver in Downstream set up

In the Table 4.10 the final results are shown: we can see the best result in the Interleaver case, although MZI has enough good result for such non-stability.

4.2.8. Behavior of three devices in Upstream with data signals

To end with this Section 4.2 we will compare three different Upstream set ups using modulated lasers as a input signal. Two of them we already know: MZI and Interleaver. And the third possible set up for the Upstream is using the coupler. We are able to introduce the coupler in this case because for the Upstream we just need to combine the signal coming form the different ONUs to a single one. The coupler is able to do this but in the ideal case (50:50) it will introduce at least 3dB of IL to each ONU (assuming we just have two of them).

Coupler analysis

To simulate the case of the ONUs sending data up to the OLT we will use two lasers with modulator (and pattern generator) and we will combine them using a coupler. We want to know the IL as the most important parameter in order to compare it with MZI and Interleaver.

To measure the IL we will build the schema shown in the Figure 4.45 where we are injecting the light from the lasers directly to the coupler and then we are measuring the output of that coupler.

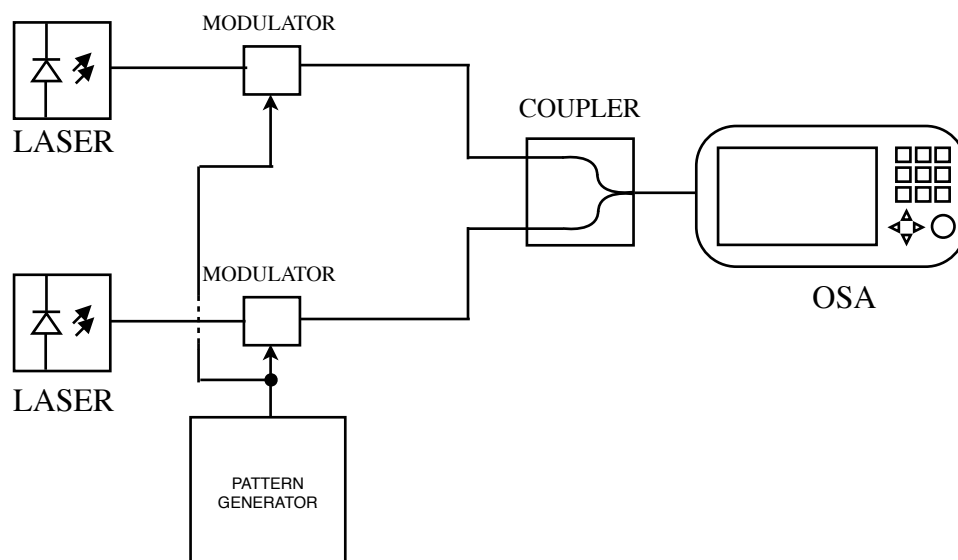


Figure 4.45. Set up with coupler and modulated signal in GCO Laboratory

To calculate the IL of each input we need to measure both signals and the same with the output.

The Figures 4.46, 4.47 and 4.48 show these three measurements of this set up.

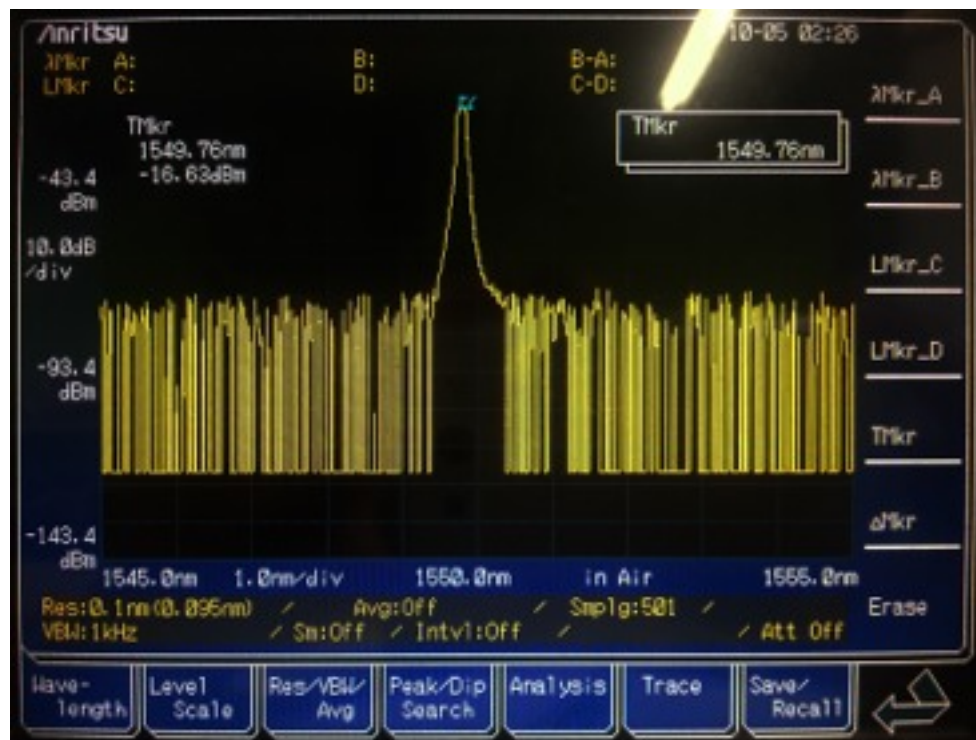


Figure 4.46. Modulated Laser 1 signal

Figure 4.46 shows the laser 1 signal and the Figure 4.47 the second laser

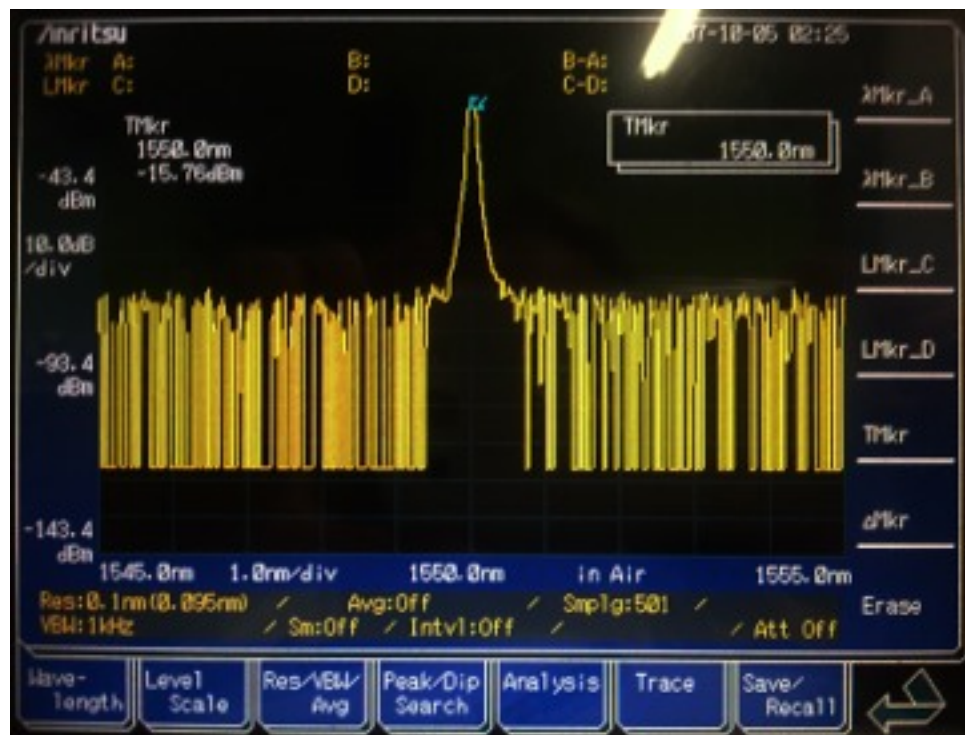


Figure 4.47. Modulated Laser 2 signal

The results we got in this case are:

$$P_1 = -16.63 \text{ dBm}, P_{1_OUT} = -18.83 \text{ dBm} \rightarrow \Delta P_1 = 2.2 \text{ dB}$$

$$P_2 = -15.76 \text{ dBm}, P_{2_OUT} = -18.52 \text{ dBm} \rightarrow \Delta P_2 = 2.76 \text{ dB}$$

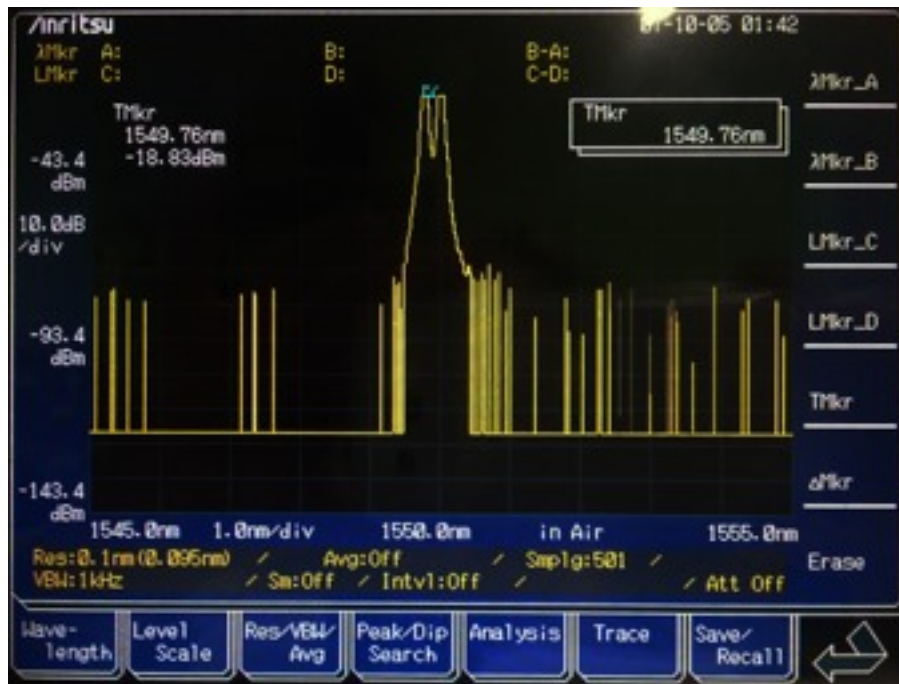


Figure 4.48. Output modulated signal of the Coupler

Note that the Figure 4.48 is the same than the Figure 4.38 since the first part of the MZI set up was also to combine two lasers using the coupler.

To get the Insertion Losses of the coupler we must look at the powers. With this powers we can fill the following table out:

	Power before coupler	Power after coupler	IL
Laser 1	-16.63 dBm	-18.83 dBm	2.2 dB
Laser 2	-15.76 dBm	-18.52 dBm	2.76 dB

Table 4.11. Coupler measurements with data signal

Comparison

Same than in the subsection 4.2.6 we will not explain and detail the measurements of the upstream using the MZI and the Interleaver because those are bidirectional devices and we can work with the results in the downstream case to compare them with the coupler.

	MZI	Interleaver	Coupler
IL	2.44 dB	0.78 dB	2.2 dB

Table 4.12. IL Comparison between MZI, Interleaver and Coupler

The measurements show the best result in interleaver case and in the case of MZI and coupler the Insertion Losses are similar.

4.2.9. OLT and Access WDM Network. Test and Measurement

In the last section of this project we are going, finally, to test different configurations under the OLT detection. We will build the Access WDM Network as well as the OLT detector (where we will get the Bit Error Rate, BER, value) using both devices measured before: the MZI and the Interleaver.

Due to the difficulty of the system, we will test just using one user to simplify it.

The built system follows the schematic shown in the Figure 4.49.

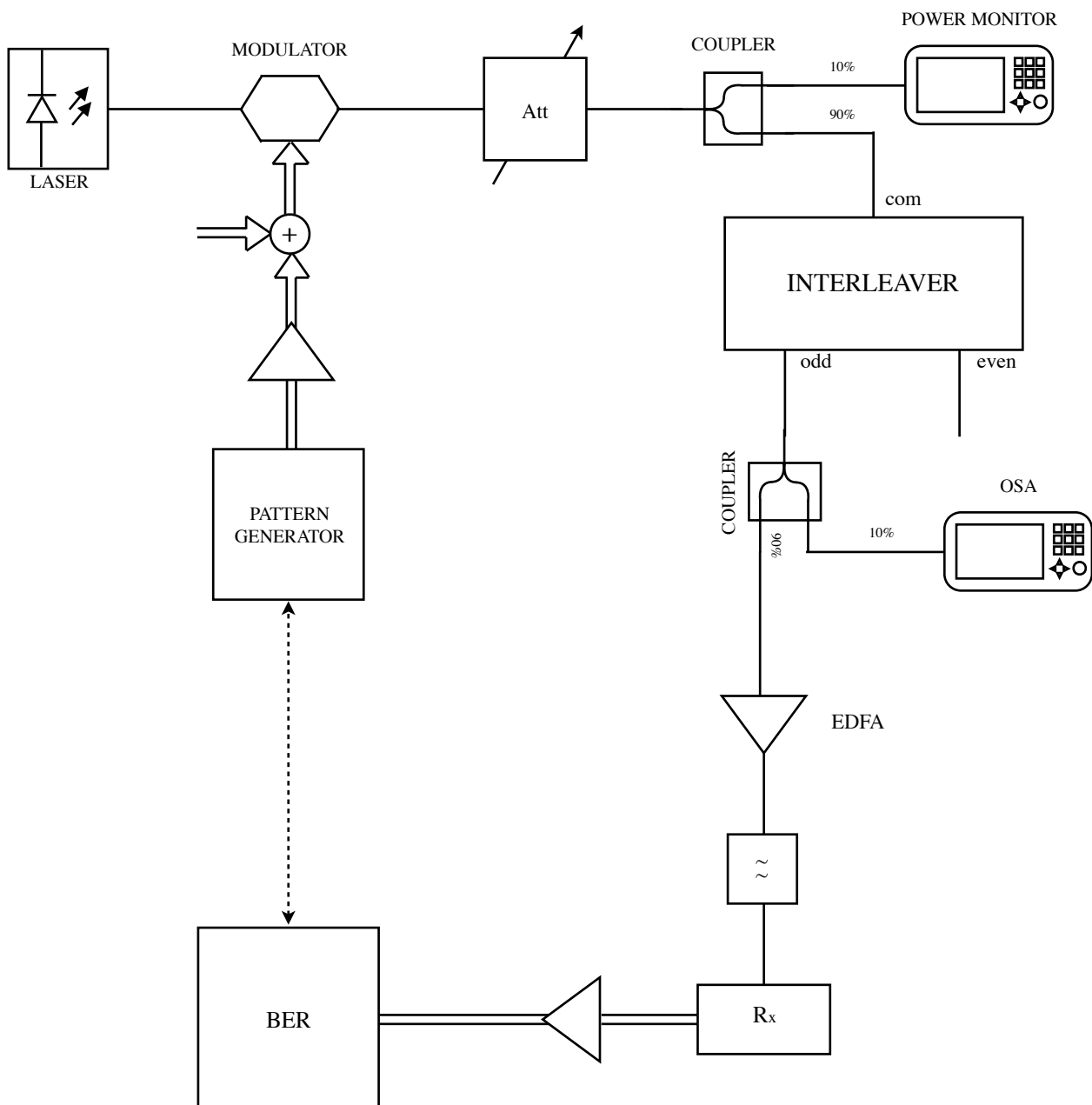


Figure 4.49. Access Network + OLT Detector schematic under Interleaver use

To start with this complex network we have to explain how we generate the signal which is supposed to come from the ONU: first we need to modulate a laser. In order to do that we will use a modulator and a pattern generator connected to it. The light coming from the laser will be modulated according the pattern generated and that will be our ONU signal. After that we will simulate the length of the fiber with an attenuator which effect will be the same than few kilometers of fibers.

At this point we have achieved the Access Part of our network. We will use couplers 90:10 to monitor the network and losing the less power possible. Here our device (Interleaver or MZI) comes in and then we will monitor the network one more time. Note we have monitored the signal power at the input and the output of our device. With this we will be able to obtain the IL for each Bit Error Rate (BER) case.

Following the schematic now we have an amplifier since the power of the signal has been decreased considerably. Then we can see a filter and at this point we will get the receiver or OLT. We will use an amplifier after the receiver to connect to the Pattern Generation in order to obtain the BER value.

Now we can understand that what we are going to do is to obtain the variation of the Insertion losses with different BER's and in different points of the spectrum, i.e. in different wavelengths.

The experiment was made following the steps below:

1. We have set the wavelength of the laser at the center of the channel
2. Then we have adjust the Optical Attenuator in order to get $BER = 10^{-x}$ (where x is on 3, 6 or 9)
3. After that we measured the power in both input and output signals
4. Then we increased the wavelength $+0.04\text{nm}$ and we repeated the process form the step 2 until 4, up to nine times in order to get the end of the channel (See Appendix 4).
5. We repeated this process for each BER and we could determine the IL for each BER.

After the schematic is good point to see our real experiment built in the GCO-Lab. The pictures below show the configuration in the Interleaver case.



Figure 4.50. In-Lab configuration with Interleaver

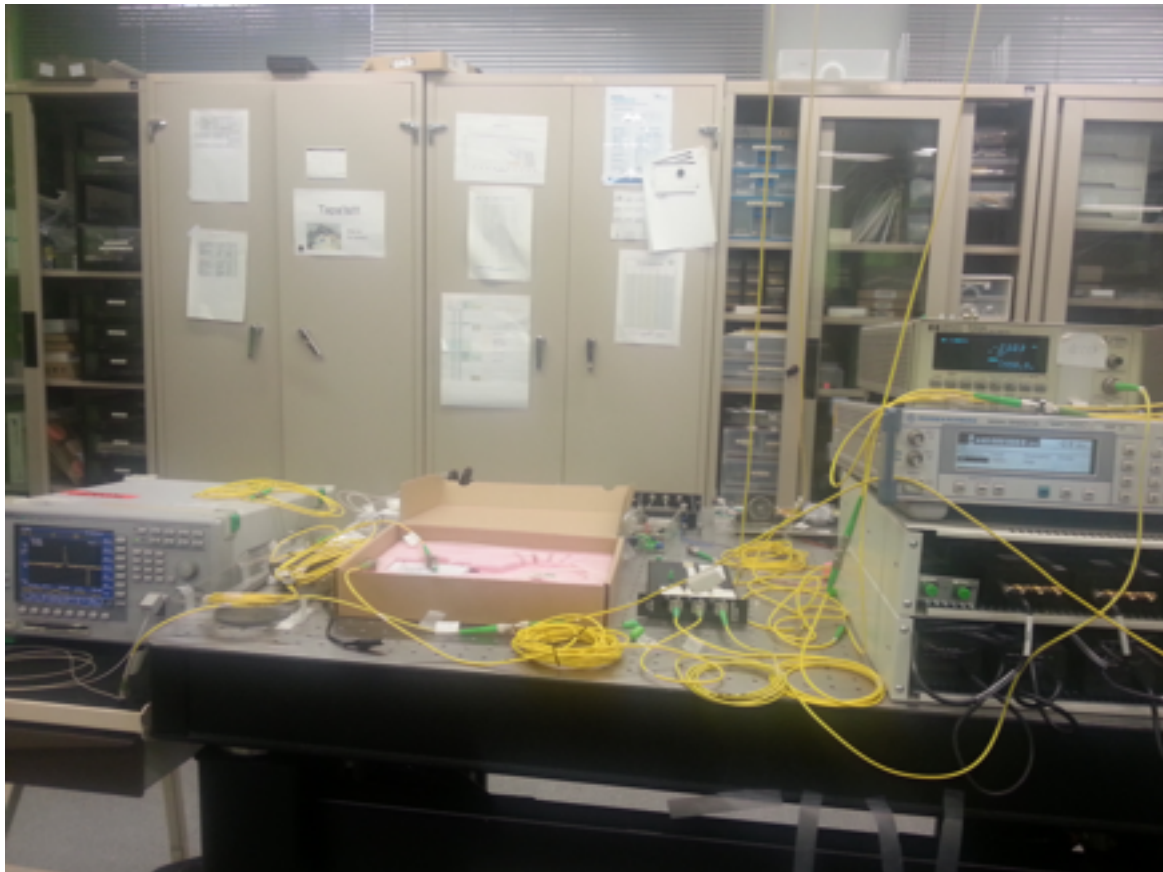


Figure 4.51. In-Lab configuration with Interleaver



Figure 4.52. In-Lab configuration with Interleaver

Once we understand the experiment above we can show the results obtained.

In the case of the Interleaver the results are pretty much the same than in the Ideal case when the IL are following the envelope of the transfer function of this device. Figure 4.53 shows this behavior in all cases ($\text{BER} = 10^{-9}$; $\text{BER} = 10^{-6}$; $\text{BER} = 10^{-3}$).

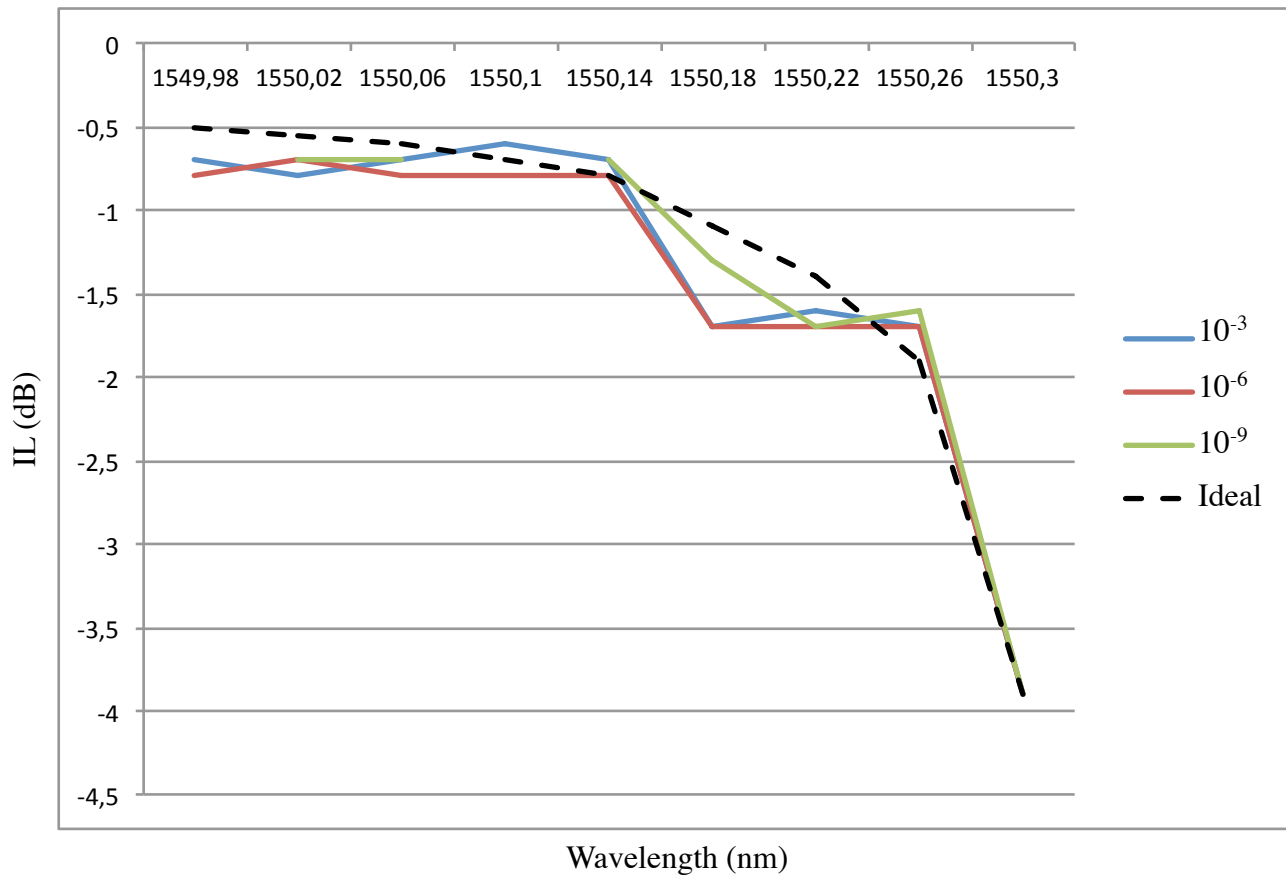


Figure 4.53. IL vs Wavelength in 3 real BER cases and in the ideal case for Interleaver device

After showing the results of the Interleaver case and before to comment them we will reproduce the same schematic and configuration but using the MZI instead of the Interleaver. Figure 4.54 shows the schematic for the MZI case.

Same way we show the real In-Lab configuration in the laboratory at Universitat Politècnica de Catalunya.

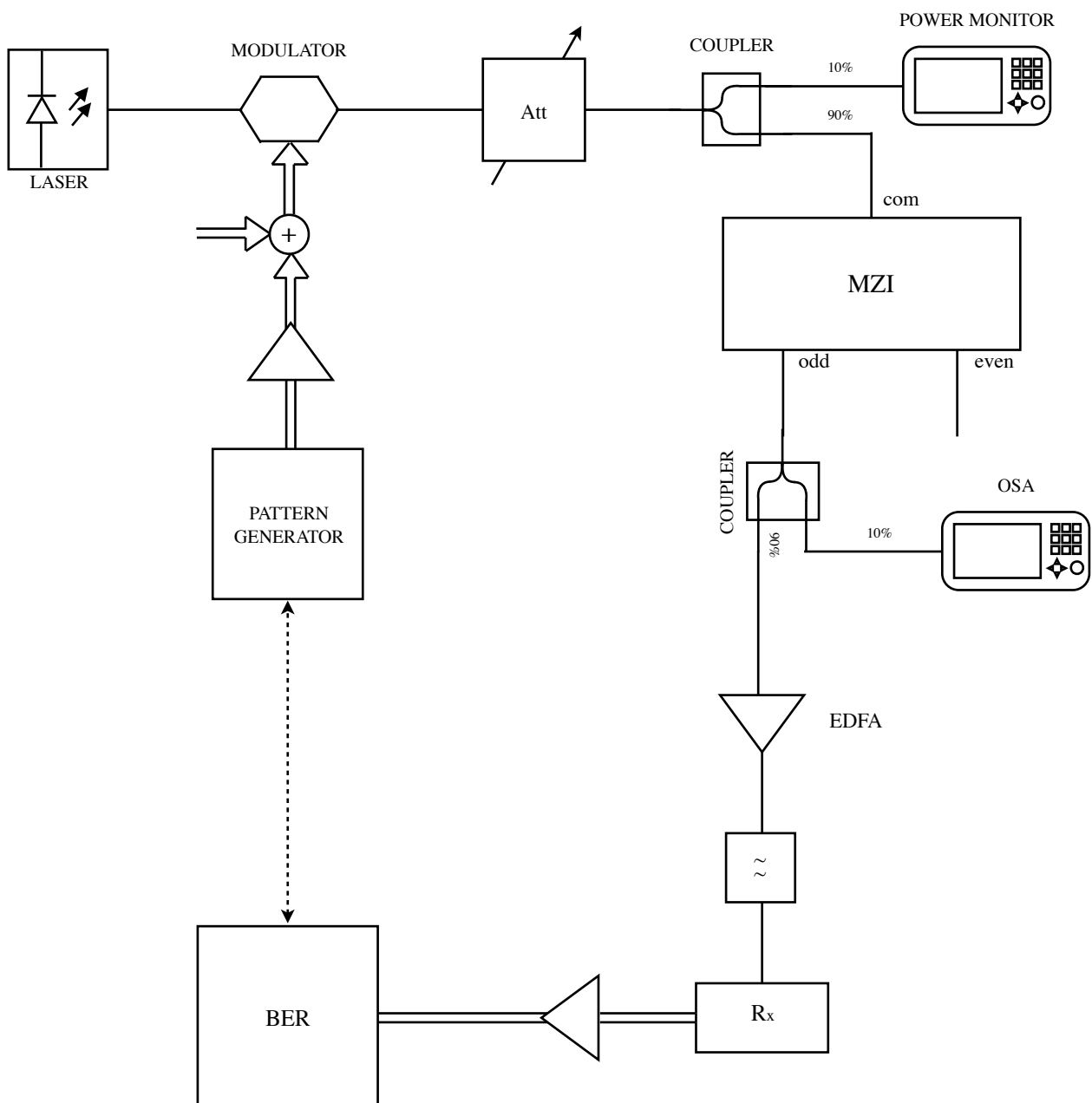


Figure 4.54. Access Network + OLT Detector schematic under Interleaver use



Figure 4.55. In-Lab configuration with MZI



Figure 4.56. In-Lab configuration with MZI



Figure 4.57. In-Lab configuration with MZI

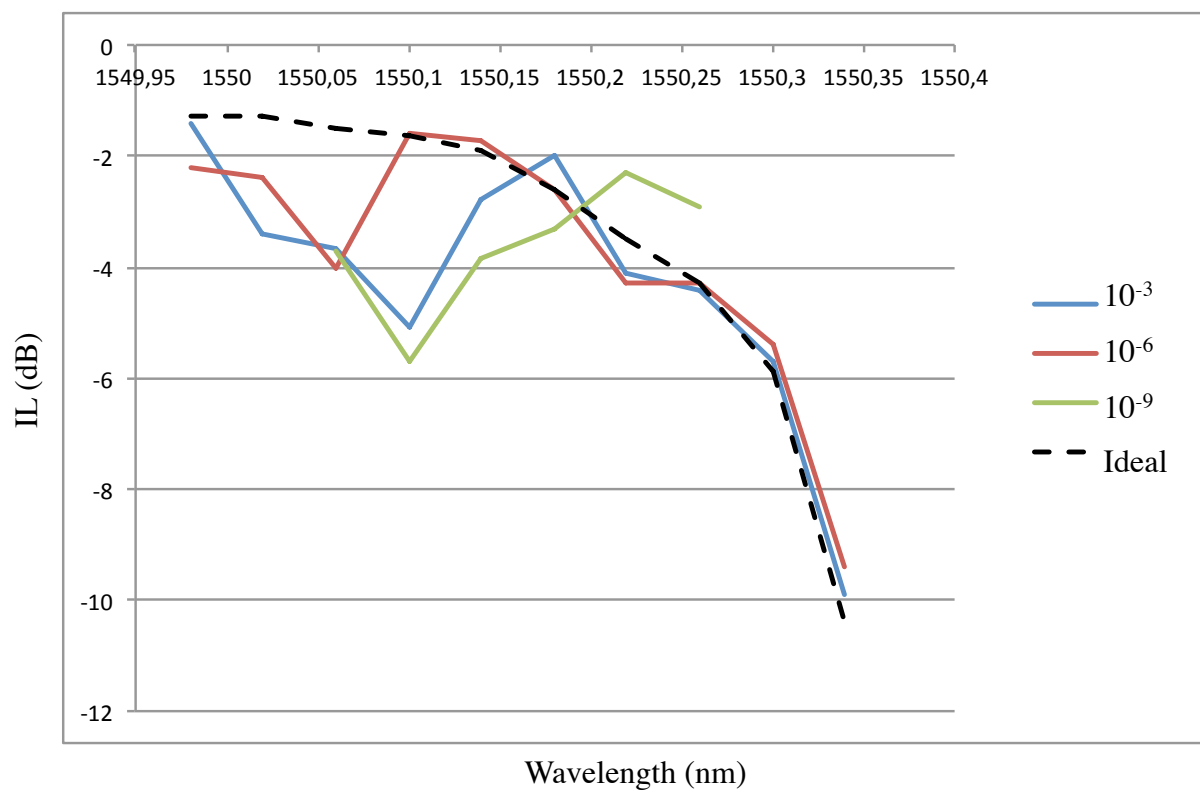


Figure 4.58. IL vs Wavelength in 3 real BER cases and in the ideal case for MZI device

The objective of this specific case is to evaluate the changes of the loss in each wavelength.

As depicted in Figure 4.53 and Figure 4.58, the two optical devices have been compared. Actually, with these options, we would justify the loss changes in each channel.

Insertion Loss is the one of the most critical performance parameter in this project which has been evaluated for making comparison between two optical devices: MZI and Interleaver. The final acceptance test consists of characterizing the complete optical network, which would be used in a real case, i.e. when the OLT and the user are fully connected, sending and receiving signal.

By installing full optical network: OLT (considering only one channel), ONU and access part (Interleaver or MZI) we performed the measure of the IL along the channel width.

First of all we should mention that we are not considering the full width of the channel due to its symmetry from the central point. That is why we will measure only half of it. Figures 4.53 and 4.58 show this half channel for both cases.

One of the technical options in access part of network it is Interleaver, as we can see in Figure 4.53 the behavior of its response is close to the ideal case. Thereby it will be possible to separate the users, which is the principal goal of the whole thesis. Moreover we can conclude that the response is not changing as a function of the BER since all three curves are following the same pattern.

In the other option, the MZI results (see Figure 4.58), although we could suspect its response is harder to see it similar to the ideal case. We have supposed that this behavior is due to the instability of the MZI along the time since the measurements are not instantly but take time. In this period of time between measurements the MZI changes its response and that is why the results are erroneously modified.

Figure 4.59 below shows our own conclusion to justify that results by the changes of the MZI response. One more time we can realize that the BER here is not playing an important role since the form of the response is not changing.

To conclude, at first sight, the scenario with Interleaver is a good trade-off of the issue in the deployment point between OLT and ONU. It allows seeing separation of the channels in the required wavelength. According to the MZI device, as a result, it could be possible to reach our target, after this first visibility, by providing stabilization to the MZI.

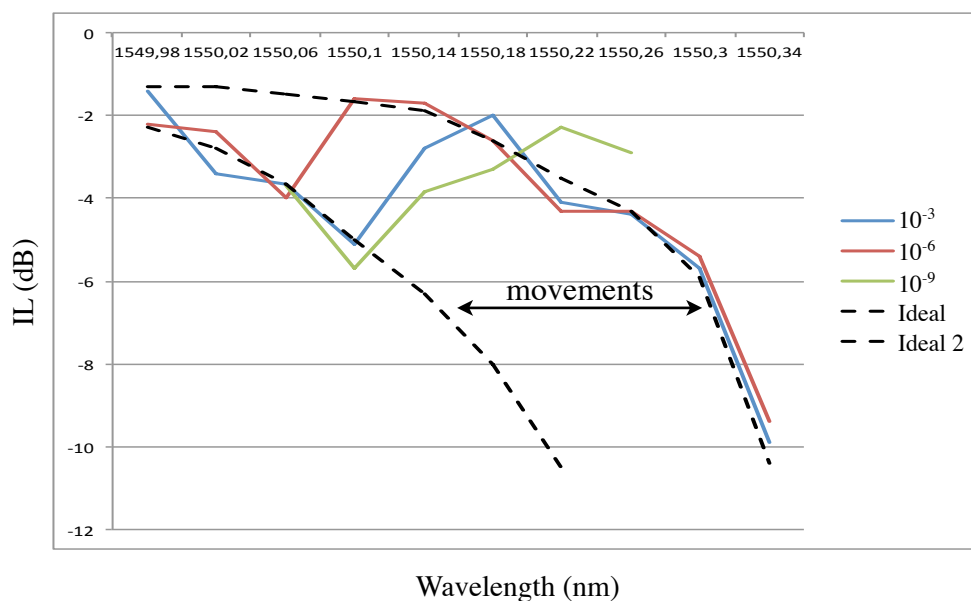


Figure 4.59. Frequency response movements of the MZI along the time

4.3. Summary

As it was observed in the practical part, ER in the MZI (9.87dB at least) is smaller than in Interleaver case (29.57dB at least). This means that when we were working with MZI as a filter, suppression of the adjacent channel is worse than working with the Interleaver. This undesired behavior is coming from non-idealities of the constructive process: non-balanced optical ways. In this Master Thesis was demonstrated that with the correct selection of couplers and minimizing the difference between two optical ways of MZI is possible to maximize ER. In the other hand the problem of Polarization it is more difficult to solve because we don't have tools to control this random process passively, however the geometry designed in MZI was used like passive compensator to improve ER and using an external polarizer was possible maximize the ER under the limitation. The important conclusion of the study demonstrate that using more precise techniques is possible to obtain better result for all fiber MZI.

Another important conclusion is related with FSR of MZI. In MZI the FSR present high flexibility to be designed. This property is very important because it presents a powerful tool to change the channel bandwidth of each MZI, this is possible changing relative difference between its two optical ways. This flexibility of all fiber MZI is making a cost effective solution in access network. It is very interesting to note that for relatively low FSR, for example 10 GHz, the necessary precision in the difference between two optical ways is smaller than in the case of a 60 GHz.

Other parameter, like Return Loss has been compared for the devices: RL in the MZI (47.85 dB) is smaller than in Interleaver (49.9 dB). Thereby obtaining very similar features the MZI and Interleaver it is showing that MZI is like a low cost solution.

Another one of the important parameter in this project is IL. Implemented result shows that all fiber interferometer has the same IL like a commercial Interleaver. So it is possible to improve it if we will work in better conditions. It is showing that it is possible to reduce cost of network access devices using alternative devices like MZI against of Interleaver maintaining the same losses, because constructor of all fiber MZI it is simple as it was not the process of built with complicated devices inside.

CHAPTER 5

GENERAL CONCLUSION

The goal of this project was to study, to simulate and to test in the laboratory a complex structure based on MZI working as an Interleaver allocated into the access network. The MZI is introduced as a cost-effective device for PON with less loss and with the possibility of maximize the number of users by cascade-stages.

We studied basic parameters of a system composed, mainly, of two devices that are the MZI and the commercial Interleaver. We described these devices, with their possible configurations and their transfer functions. The MZI, in particular, was our Device under Test. This device has been created in our laboratory and all parameters like Extinction Ratio, Return Loss, Insertion Loss, Free Spectrum Range and Polarization Dependent Loss of the MZI and the commercial Interleaver have been measured and analyzed in order to assess and compare the quality of these devices.

To begin, in the second chapter was demonstrated simple method of designing double-stage unbalanced MZI with fiber coupled structure, which could work like an Interleaver. This simple double-stage MZI was simulated in the third chapter.

We have started using the analytical expression of the MZI transfer function simulated in Matlab to evaluate the Ideal and Non-ideal MZI as an Optical filter. Having a double-stage MZI the two desired FSRs (FSR1 and FSR2) were obtained by using the expression (3.3). After simulating and proving that the system would split the odd harmonics of the even harmonics with the first (sin) and the second (cos) response respectively.

In the simulation part, Insertion Loss and Maximum ER has been obtained for total system of all-fiber MZI and commercial Interleaver as filters. The study compares behavior of these two optical devices and results showed that it is possible to build a MZI and consider this device as one of the cost-effective option in the FTTH with technology DWDM. However, to bring it to market and to use it in the Passive Optical Access Network it still needs to be developed with better strategy to control and to use it in the Access part.

Once we got the good simulation results we built the system in the laboratory, which is explained in the chapter 4. According to the section () it has been achieved one of the goal of our thesis, which was to use the cost-effective MZI as an Interleaver to filter the channels. Moreover we have tested the device, and compared with the other possible devices (Interleaver and coupler), under what it could be a real DWDM PON including a complete OLT simulating one carrier and ONU connected after the Device under Test.

Several problems have been appeared during our practical work in the laboratory:

The first one was produced by the internal structure of the MZI: the fusion protectors do not have enough flexibility to maintain the circular geometry, and this complicates the attachment of the fiber to the metal surface causing a rupture in the fiber winding geometry.

The second problem was found with the stabilization of the frequency response of the interferometer. Finally the solution was to minimize the loop size. This means that MZI area is smaller and then the local conditions can be considered more stable.

But even so, the non-stabilities of the Mach-Zehnder were too large and that caused many troubles in our laboratory experience. As a conclusion we would say that although it has been proved that

the MZI could replace the Interleaver in the Access part, our homemade MZI had poor features and not enough stability for the real DWDM network. That means if we could control, somehow, the stability of MZI we would be able achieve that performance.

Future Work

At this point we can see how new research areas born in order to improve our goal. These possible research topics are commented and briefly introduced below but not deeply covered since they are already beyond this thesis and its main purpose.

As a recommendation for further research we propose the following new techniques to improve the multi-stage system:

Challenge 1:

- a. Problem:** low flexibility of the connectors used
- b. Possible solution:** to change the connectors type or even using fusions.
- c. Suggestions for the future work:**

To improve the MZI could be an interesting option to change the internal structure in order to achieve the circular geometry.

Challenge 2:

- a. Problem:** non-stabilities of the frequency response.
- b. Possible solution:** to include some kind of circuit to control it.
- c. Suggestions for the future work:**

MZI as a filter requires a great stability in the frequency response, therefore the best frequency stabilization required a feedback loop to provide active compensation and it will be necessary work with the piezoelectric transducer. A feedback circuit deployment needs to be created to convert deviations in phase (in output) into a signal to control piezoelectric transducer and stabilize the MZI. We need to insert the feedback circuit in the first output of MZI and piezoelectric transducer inside of MZI in first length of fiber.

The implementation of this control system present high difficulty and to build it in non-professional condition does not guarantee to integrate piezoelectric and fiber successfully, for this reason the MZI with passive compensation has been constructed. This integrates winding and temperature isolation provides a cost effective solution that guarantee functionality of complete system.

Challenge 3:

- a. Suggestions for the future work:**

This third challenge is not a solution to any problem experimented in the laboratory but to encourage the ones who really believe in the idea of this thesis. After improving the MZI device and providing stabilization to it the next step could be to implement the double-stage MZI totally.

APPENDIX 1

MATLAB IDEAL MZI SIMULATION

This appendix attach the complete Matlab code to performance the ideal case of the MZI simulation described and discussed in Section 3.4.1 of the Chapter 3.

```
function[] =sim_mzi(FSR1,FSR2,f1,f2,f3,f4)
%%
%CLS
close all
%

% Change default axes fonts.
set(0,'DefaultAxesFontName','Times')
set(0,'DefaultAxesFontSize',25)
%

% Change default text fonts.
set(0,'DefaultTextFontname','Times')
set(0,'DefaultTextFontSize',35)
%

%Rescaling FSR1 & FSR2
FSR1 = FSR1*1e3;
FSR2 = FSR2*1e3;
%

%Constants
c = 3e8;
neff = 1.4682;
n = 2.387;
%

%Setting the 4 users
fmuest4 = (1/(25*f4));

t = 0:fmuest4:10;

u1 = sin(2*pi*f1*t);
u2 = sin(2*pi*f2*t);
u3 = sin(2*pi*f3*t);
u4 = sin(2*pi*f4*t);
%

%Plotting the 4 users
figure(1);

subplot(3,2,1)
plot(t,u1,'b');
xlabel('Time');
ylabel('Amplitude');
title('User1');

subplot(3,2,2)
plot(t,u2,'r');
xlabel('Time');
```

```

    ylabel('Amplitude');
    title('User2');

subplot(3,2,3)
    plot(t,u3,'g');
    xlabel('Time');
    ylabel('Amplitude');
    title('User3');

subplot(3,2,4)
    plot(t,u4,'k');
    xlabel('Time(s)');
    ylabel('Amplitude');
    title('User4');
%

%Plotting all 4 users together
subplot(3,2,5:6)
    plot(t,u1,'b');
    hold on
    plot(t,u2,'r');
    hold on
    plot(t,u3,'g');
    hold on
    plot(t,u4,'k');
    xlabel('Time');
    ylabel('Amplitude');
    title('Users');
%

%Creating the Frequency signal of U1+U2+U3+U4
S = u1+u2+u3+u4;

N = length(S);
X = abs(fft(S,N));
X = fftshift(X);
F = [-N/2:N/2-1]/N;
%

%Plotting the time and Frequency of the S signal
figure(2);

subplot(2,1,1)
    plot(t,S,'b');
    xlabel('Time');
    ylabel('Amplitude');
    title('U1+U2+U3+U4 (TIME DOMAIN)');

subplot(2,1,2)
    plot(F.*1e11,X,'b');
    xlim([0 5e9]);
    xlabel('Frequency (THz)');
    ylabel('Amplitude');
    title('U1+U2+U3+U4 (Frequency DOMAIN)');
%

%%
%FIRST MZI

    %Setting f, and length_dif

```

```

f = (1:(1/(0.0025*f4)):50e3);
length_dif = c/(neff*FSR1);
length_dif2 = c/(neff*FSR2);
%

%MZI 1 T1
T111=((sin((2.*pi.*neff.*f.*length_dif)./(c*2))).^2));
%

%MZI 1 T2
T112=((cos((2.*pi.*neff.*f.*length_dif)./(c*2))).^2));
%

%Plotting the two arms of the MZI1 and the output
figure(3);

%SIGNAL + MZI1 T1
subplot(2,2,1)
    semilogy(f*1e6,T111,'r');
    hold on;
    semilogy((F.*1e11),X./500);
    xlim([0 15e9]);
    xlabel('Frequency');
    ylabel('Amplitude');
    title('S Signal and MZI1 T1');
%

%Cutout of vector of spectrum
auxSignal=X((length(X)+2)/2:length(S));
A1=T111.*auxSignal./500;
A2=T112.*auxSignal./500;
%

%MZI1 OUT1
subplot(2,2,2)
    out11= T111.*auxSignal;
    plot(f*1e6,out11./500);
    xlim([0 5e9]);
    xlabel('Frequency');
    ylabel('Amplitude');
    title('MZI1 OUT1');
%

%SIGNAL + MZI1 T2
subplot(2,2,3)
    semilogy(f*1e6,T112,'g');
    hold on;
    semilogy((F.*1e11),X./500);
    xlim([0 15e9]);
    xlabel('Frequency');
    ylabel('Amplitude');
    title('S Signal and MZI1 T2');
%

%MZI1 OUT2
subplot(2,2,4)
    out12 = T112.*auxSignal;
    plot(f*1e6,out12./500);
    xlim([0 5e9]);

```

```

        xlabel('Frequency');
        ylabel('Amplitude');
        title('MZI1 OUT2');
    %
%
%%
%Second MZI

%Setting f, and length_dif
f = (1:(1/(0.0025*f4)):50e3);
length_dif = c/(neff*FSR1);
length_dif2 = c/(neff*FSR2);
%

%MZI 2 T1
T211=((cos(((pi.*neff.*f.*length_dif)./(c*2))-pi/4).^2));
%

%MZI 2 T2
T212=((sin(((pi.*neff.*f.*length_dif)./(c*2))-pi/4).^2));
%

%Plotting the two arms of the MZI1 and the output
figure(4);

%SIGNAL + MZI2 T1
subplot(2,2,1)
    semilogy(f*1e6,T211,'r');
    hold on;
    semilogy(f*1e6,out11./500);
    xlim([0 15e9]);
    xlabel('Frequency');
    ylabel('Amplitude');
    title('OUT1 Signal and MZI2 T1');
%

%MZI2 OUT1
subplot(2,2,2)
    plot(f*1e6,T211.*A1);
    xlim([0 5e9]);
    xlabel('Frequency');
    ylabel('Amplitude');
    title('MZI2 OUT1');
%

%SIGNAL + MZI2 T2
subplot(2,2,3)
    semilogy(f*1e6,T212,'g');
    hold on;
    semilogy(f*1e6,out11./500);
    xlim([0 15e9]);
    xlabel('Frequency');
    ylabel('Amplitude');
    title('OUT1 Signal and MZI2 T2');
%

%MZI2 OUT2

```



```

subplot(2,2,4)
    plot(f*1e6,T212.*A1);
    xlim([0 5e9]);
    xlabel('Frequency');
    ylabel('Amplitude');
    title('MZI2 OUT2');
%
%
%%
%Third MZI
    %MZI 3 T1
    T311=((sin((pi.*neff.*f.*length_dif)./(c*2))).^2));
%
    %MZI 3 T2
    T312=((cos((pi.*neff.*f.*length_dif)./(c*2))).^2));
%
%
%%
%Final System Simulation

figure(5);

subplot(7,3,10);
    plot(f*1e6,T211.*A1,'b');
    hold on
    plot(f*1e6,T212.*A1,'r');
    hold on
    out31= T311.*A2;
    plot(f*1e6,out31,'g');
    hold on
    out32= T312.*A2;
    plot(f*1e6,out32,'k');
    xlim([0 5e9]);
    xlabel('Frequency');
    ylabel('Amplitude');
    title('U1+U2+U3+U4 (Frequency DOMAIN)');

subplot(7,3,5);
    plot(f*1e6,T211.*A1,'b');
    hold on
    plot(f*1e6,T212.*A1,'r');
    xlim([0 5e9]);
    xlabel('Frequency');
    ylabel('Amplitude');
    title('MZI1 OUT1');

subplot(7,3,17);
    plot(f*1e6,out31,'g');
    hold on
    plot(f*1e6,out32,'k');
    xlim([0 5e9]);
    xlabel('Frequency');
    ylabel('Amplitude');
    title('MZI1 OUT2');

subplot(7,3,3);

```

```
plot(f*1e6,T211.*A1,'b');
xlim([0 5e9]);
xlabel('Frequency');
ylabel('Amplitude');
title('MZI2 OUT1');

subplot(7,3,9);
plot(f*1e6,T212.*A1,'r');
xlim([0 5e9]);
xlabel('Frequency');
ylabel('Amplitude');
title('MZI2 OUT2');

subplot(7,3,15);
out31= T311.*A2;
plot(f*1e6,out31,'g');
xlim([0 5e9]);
xlabel('Frequency');
ylabel('Amplitude');
title('MZI3 OUT1');

subplot(7,3,21);
out32= T312.*A2;
plot(f*1e6,out32,'k');
xlim([0 5e9]);
xlabel('Frequency');
ylabel('Amplitude');
title('MZI3 OUT2');

%

end
```

APPENDIX 2

MATLAB NON-IDEAL MZI SIMULATION

This appendix attach the complete Matlab code to performance the non-ideal case of the MZI simulation described and discussed in Section 3.4.2 of the Chapter 3.

```
function[B1,B2,C1,C2]=sim_nmzi(FSR1,FSR2,f1,f2,f3,f4)
%%
%CLS
close all
%

% Change default axes fonts.
set(0,'DefaultAxesFontName','Times')
set(0,'DefaultAxesFontSize',25)
%

% Change default text fonts.
set(0,'DefaultTextFontname','Times')
set(0,'DefaultTextFontSize',35)
%

%Rescaling FSR1 & FSR2
FSR1 = FSR1*1e3;
FSR2 = FSR2*1e3;
%

%Constants
c = 3e8;
neff = 1.4682;
n = 2.387;

%Coupler
a1 = 0.51;
a2 = 0.49;
b1 = 0.55;
b2 = 0.45;

alpha=1;
%
%

%Setting the 4 users
fmuest4 = (1/(25*f4));

t = 0:fmuest4:10;

u1 = sin(2*pi*f1*t);
u2 = sin(2*pi*f2*t);
u3 = sin(2*pi*f3*t);
u4 = sin(2*pi*f4*t);
%

%Plotting the 4 users
figure(1);

subplot(3,2,1)
plot(t,u1,'b');
```

```

    xlabel('Time');
    ylabel('Amplitude');
    title('User1');

subplot(3,2,2)
    plot(t,u2,'r');
    xlabel('Time');
    ylabel('Amplitude');
    title('User2');

subplot(3,2,3)
    plot(t,u3,'g');
    xlabel('Time');
    ylabel('Amplitude');
    title('User3');

subplot(3,2,4)
    plot(t,u4,'k');
    xlabel('Time');
    ylabel('Amplitude');
    title('User4');
%

%Plotting all 4 users together
subplot(3,2,5:6)
    plot(t,u1,'b');
    hold on
    plot(t,u2,'r');
    hold on
    plot(t,u3,'g');
    hold on
    plot(t,u4,'k');
    xlabel('Time');
    ylabel('Amplitude');
    title('Users');
%

%Creating the frequency signal of U1+U2+U3+U4
S = u1+u2+u3+u4;

N = length(S);
X = abs(fft(S,N));
X = fftshift(X);
F = [-N/2:N/2-1]/N;
%

%Plotting the time and frequency of the S signal
figure(2);

subplot(2,1,1)
    plot(t,S,'k');
    xlabel('Time');
    ylabel('Amplitude');
    title('U1+U2+U3+U4 (TIME DOMAIN)');

subplot(2,1,2)
    plot(F.*1e11,X,'k');
    xlim([0 5e9]);
    xlabel('Frequency');
```

```

ylabel('Amplitude');
title('U1+U2+U3+U4 (FREQUENCY DOMAIN)');
%

%%
%FIRST MZI

%Setting f, and length_dif
f = (1:(1/(0.0025*f4)):50e3);
length_dif = c/(neff*FSR1);
length_dif2 = c/(neff*FSR2);
%

%MZI 1 T1
T111=a1*a1*a2*a2 + b1*b1*b2*b2*alpha*alpha -
2*a1*a2*b1*b2*alpha*cos((2.*pi.*neff.*f.*length_dif)./(c));
%

%MZI 1 T2
T112=a1*a1*b2*b2 + b1*b1*a2*a2*alpha*alpha +
2*a1*a2*b1*b2*alpha*cos((2.*pi.*neff.*f.*length_dif)./(c));
%

%Plotting the two arms of the MZI1 and the output
figure(3);

%SIGNAL + MZI1 T1
subplot(2,2,1)
plot(f*1e6,10*log10(T111),'--','color',[0 0 0]);
hold on;
plot((F.*1e11),10*log10(X./500),'k');
xlim([0 15e9]);
ylim([-100 0]);
xlabel('Frequency');
ylabel('Amplitude');
title('S Signal and MZI1 T1');
%

%Cutout of vector of spectrum
auxSignal=X((length(X)+2)/2:length(S));
A1=T111.*auxSignal./500;
A2=T112.*auxSignal./500;
%

%MZI1 OUT1
subplot(2,2,2)
out11= T111.*auxSignal;
plot(f*1e6,out11./500,'k');
xlim([0 5e9]);
xlabel('Frequency');
ylabel('Amplitude');
title('MZI1 OUT1');
%

%SIGNAL + MZI1 T2
subplot(2,2,3)
plot(f*1e6,10*log10(T112),'--','color',[0 0 0]);
hold on;
plot((F.*1e11),10*log10(X./500),'k');
xlim([0 15e9]);

```

```

        ylim([-100 0]);
        xlabel('Frequency');
        ylabel('Amplitude');
        title('S Signal and MZI1 T2');
    %

    %MZI1 OUT2
    subplot(2,2,4)
        out12 = T112.*auxSignal;
        plot(f*1e6,out12./500,'k');
        xlim([0 5e9]);
        xlabel('Frequency');
        ylabel('Amplitude');
        title('MZI1 OUT2');
    %
%
%%
%Second MZI

    %Setting f, and length_dif
    f = (1:(1/(0.0025*f4)):50e3);
    length_dif = c/(neff*FSR1);
    length_dif2 = c/(neff*FSR2);
    %

    %MZI 2 T1
    T211=a1*a1*a2*a2 + b1*b1*b2*b2*alpha*alpha -
    2*a1*a2*b1*b2*alpha*cos(((2.*pi.*neff.*f.*length_dif2)./(c))-pi/2);
    %

    %MZI 2 T2
    T212=a1*a1*b2*b2 + b1*b1*a2*a2*alpha*alpha +
    2*a1*a2*b1*b2*alpha*cos(((2.*pi.*neff.*f.*length_dif2)./(c))-pi/2);
    %

    %Plotting the two arms of the MZI1 and the output
    figure(4);

    %SIGNAL + MZI2 T1
    subplot(2,2,1)
        plot(f*1e6,10*log10(T211),'--','color',[0 0 0]);
        hold on;
        plot(f*1e6,10*log10(out11./500),'k');
        xlim([0 15e9]);
        xlabel('Frequency');
        ylabel('Amplitude');
        title('OUT1 Signal and MZI2 T1');
    %

    %MZI2 OUT1
    subplot(2,2,2)
        plot(f*1e6,T211.*A1,'k');
        xlim([0 5e9]);
        xlabel('Frequency');
        ylabel('Amplitude');
        title('MZI2 OUT1');
    %

```

```

%SINGAL + MZI2 T2
subplot(2,2,3)
    plot(f*1e6,10*log10(T212),'--','color',[0 0 0]);
    hold on;
    plot(f*1e6,10*log10(out11./500),'k');
    xlim([0 15e9]);
    xlabel('Frequency');
    ylabel('Amplitude');
    title('OUT1 Signal and MZI2 T2');
%

%MZI2 OUT2
subplot(2,2,4)
    plot(f*1e6,T212.*A1,'k');
    xlim([0 5e9]);
    xlabel('Frequency');
    ylabel('Amplitude');
    title('MZI2 OUT2');
%

%%

%%
%Third MZI
    %MZI 3 T1
    T311=a1*a1*a2*a2 + b1*b1*b2*b2*alpha*alpha -
2*a1*a2*b1*b2*alpha*cos(((2.*pi.*neff.*f.*length_dif2)./(c)));
    %

    %MZI 3 T2
    T312=a1*a1*b2*b2 + b1*b1*a2*a2*alpha*alpha +
2*a1*a2*b1*b2*alpha*cos(((2.*pi.*neff.*f.*length_dif2)./(c)));
    %

%

%%

%Final System Simulation

figure(5);

subplot(7,3,10);
    plot(f*1e6,T211.*A1.*50/3,'b');
    hold on
    plot(f*1e6,T212.*A1.*50/3,'r');
    hold on
    out31= T311.*A2;
    plot(f*1e6,out31.*50/3,'g');
    hold on
    out32= T312.*A2;
    plot(f*1e6,out32.*50/3,'k');
    xlim([0 5e9]);
    xlabel('Frequency');
    ylabel('Amplitude');
    title('U1+U2+U3+U4 (FREQUENCY DOMAIN)');

subplot(7,3,5);
    plot(f*1e6,T211.*A1.*4,'b');
    hold on
    plot(f*1e6,T212.*A1.*4,'r');

```

```

    xlim([0 5e9]);
    xlabel('Frequency');
    ylabel('Amplitude');
    title('MZI1 OUT1');

subplot(7,3,17);
    plot(f*1e6,out31.*4,'g');
    hold on
    plot(f*1e6,out32.*4,'k');
    xlim([0 5e9]);
    xlabel('Frequency');
    ylabel('Amplitude');
    title('MZI1 OUT2');

subplot(7,3,3);
    plot(f*1e6,T211.*A1,'b');
    xlim([0 5e9]);
    xlabel('Frequency');
    ylabel('Amplitude');
    title('MZI2 OUT1');

subplot(7,3,9);
    plot(f*1e6,T212.*A1,'r');
    xlim([0 5e9]);
    xlabel('Frequency');
    ylabel('Amplitude');
    title('MZI2 OUT2');

subplot(7,3,15);
    out31= T311.*A2;
    plot(f*1e6,out31,'g');
    xlim([0 5e9]);
    xlabel('Frequency');
    ylabel('Amplitude');
    title('MZI3 OUT1');

subplot(7,3,21);
    out32= T312.*A2;
    plot(f*1e6,out32,'k');
    xlim([0 5e9]);
    xlabel('Frequency');
    ylabel('Amplitude');
    title('MZI3 OUT2');

%

end

```


APPENDIX 3

INTERLEAVER DATASHEET

In this appendix is attached the Datasheet of the commercial Interleaver used in the experiments of the Chapter 4.

GREEN 50GHz COMPACT FIBER OPTICAL INTERLEAVER

CFOI050GHz

Oplink's compact, low-dispersion interleavers greatly expand wavelength channel counts in DWDM systems. It is the best solution to upgrade existing 100GHz spacing transport system. Oplink's DWDM interleavers feature excellent wide, flat passband and high isolation. Both Mux and Demux functions are supported. These interleavers are athermal and therefore require no temperature control. Its stable center wavelength accuracy over C or L band 80 channels is suitable for higher bit rate application. The Green CFOI is compliant with industry green initiatives such as RoHS and WEEE.



Performance Specifications

Parameter	Min.	Typical	Max.	Unit
Central Wavelength Range	1529.55		1561.42	nm
Central Frequency Range	192000		196000	GHz
Channel Center Wavelength		ITU Grid		
Input Channel Spacing		50		GHz
Output Channel Spacing		100		GHz
Clear Bandwidth		+/-8		GHz
Insertion Loss ¹		1.0	1.8	dB
Ripple		0.2	0.3	dB
Insertion Loss Uniformity		0.2	0.4	dB
Adjacent Channel Isolation	22			dB
Polarization Dependent Loss (PDL)		0.2	0.3	dB
Polarization Mode Dispersion (PMD)		0.2	0.3	ps
Chromatic Dispersion	-30		+30	ps/nm
Return Loss	45	50		dB
Directivity	50	55		dB
Operating Power Handling			24	dBm
Operating Temperature	0		65	°C
Storage Temperature	-40		+85	°C
Fiber Type	Corning SMF-28			
Packaging Dimensions ³	100.5 (L) x 60 (W) x 10.3 (H)			mm

Note:

1. The maximum IL is under all states of polarization and within the full operating temperature and wavelength ranges specified.

2. All the parameters are excluding connectors.

3. The mechanical tolerance should be +/-0.2mm on all package dimensions unless otherwise custom specified.

Features

- ◆ Compact Size
- ◆ Low Dispersion
- ◆ Completely Passive
- ◆ Ultra-low Insertion Loss
- ◆ Highly Stable & Reliable
- ◆ Epoxy-Free Optical Path
- ◆ Environmental Green Plan Compliance

Applications

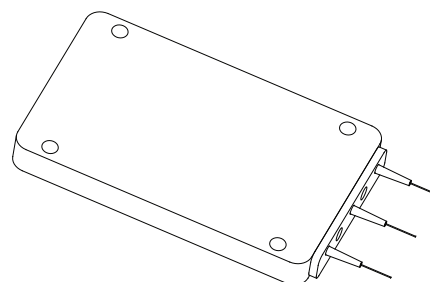
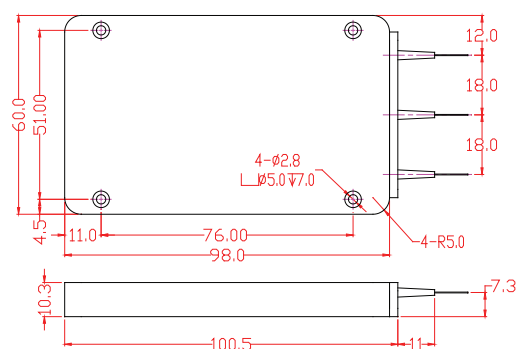
- ◆ Metro and Long Haul DWDM Systems
- ◆ Network Capacity Expansion
- ◆ Signal Comb Filtering



GREEN 50 GHz COMPACT FIBER OPTICAL INTERLEAVER

CFOI050 SERIES

Mechanical Drawing / Package Dimensions (dimension in mm)

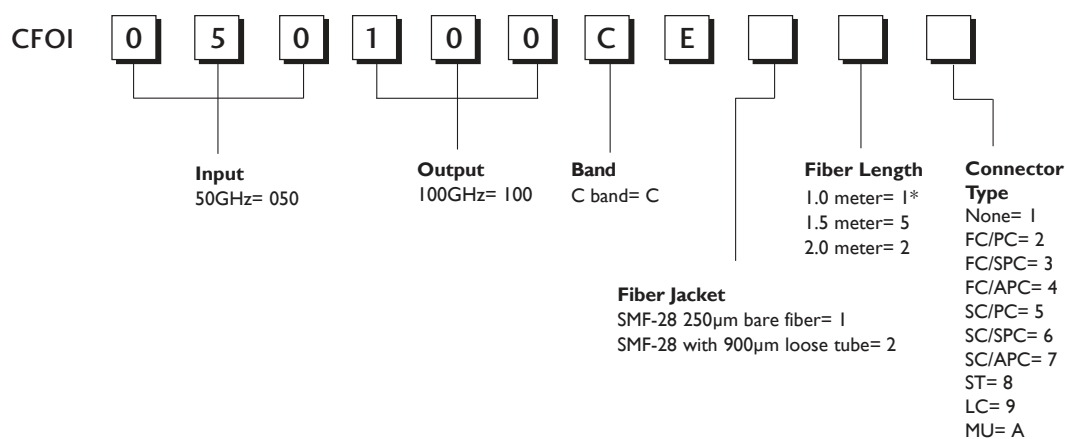


NOTE:

1. MAT'L OF HSG & CVR: ALUM 6061-T6.
2. FINISH: COLOR INHERENT QUALITIES.
3. UNITS: MM.
4. TOL'S: .X=±0.2
.XX=±0.1
5. PROJECTION:

Ordering Information

Oplink can provide a remarkable range of customized optical solutions. For detail, please contact Oplink's OEM design team or account manager for your requirements and ordering information (510) 933-7200.



* The tolerance of fiber length is +/-0.1m. 1 meter is standard. The lead-time for special fiber length will be longer.

R5.20080410

Product Lines ✦ Mux/Demux ✦ Switching/Router ✦ Coupling/Splitting ✦ Monitoring/Conditioning ✦ Amplification ✦ Transceivers ✦ Interconnect ✦ RGB Laser Modules

APPENDIX 4

BER TABLES

INTERLEAVER

REFERENCE

Power Monitor (dBm)	Input (dBm)	Output (dBm)	OSA (dBm)	IL (dB)	Sensitivity (dBm)		
					BER = 10^{-3}	BER = 10^{-6}	BER = 10^{-9}
-25.7	-15.7	-17.6	-29	1.9			

Wavelength: 1549.98nm

Power Monitor (dBm)	Input (dBm)	Output (dBm)	OSA (dBm)	IL (dB)	Sensitivity (dBm)		
					BER = 10^{-3}	BER = 10^{-6}	BER = 10^{-9}
-25.4	-15.4	-16.2	-27.6	0.8		-18.7	
-34.6	-24.6	-25.3	-36.7	0.7	-28.5		

Wavelength: 1550.02nm

Power Monitor (dBm)	Input (dBm)	Output (dBm)	OSA (dBm)	IL (dB)	Sensitivity (dBm)		
					BER = 10^{-3}	BER = 10^{-6}	BER = 10^{-9}
-24.8	-14.8	-15.5	-26.9	0.7			-18.2
-31.1	-21.1	-21.8	-33.2	0.7		-24.4	
-36.8	-26.8	-27.6	-39	0.8	-31.1		

Wavelength: 1550.06nm

Power Monitor (dBm)	Input (dBm)	Output (dBm)	OSA (dBm)	IL (dB)	Sensitivity (dBm)		
					BER = 10^{-3}	BER = 10^{-6}	BER = 10^{-9}
-24.4	-14.4	-15.1	-26.5	0.7			-17.6
-27.3	-17.3	-18.1	-29.5	0.8		-20.5	
-35.3	-25.3	-26	-37.4	0.7	-28.8		

Wavelength: 1550.1nm

Power Monitor (dBm)	Input (dBm)	Output (dBm)	OSA (dBm)	IL (dB)	Sensitivity (dBm)		
					BER = 10^{-3}	BER = 10^{-6}	BER = 10^{-9}
-23.7	-13.7	-14.5	-35.9	0.8		-17.1	
-36	-26	-26.6	-38	0.6	-30		

Wavelength: 1550.14nm

Power Monitor (dBm)	Input (dBm)	Output (dBm)	OSA (dBm)	IL (dB)	Sensitivity (dBm)		
					BER = 10^{-3}	BER = 10^{-6}	BER = 10^{-9}
-21.9	-11.9	-12.6	-24	0.7			-15
-26.3	-16.3	-17.1	-28.5	0.8		-19.5	
-34.5	-25.5	-26.2	-37.6	0.7	-29.8		

Wavelength: 1550.14nm

Power Monitor (dBm)	Input (dBm)	Output (dBm)	OSA (dBm)	IL (dB)	Sensitivity (dBm)		
					BER = 10^{-3}	BER = 10^{-6}	BER = 10^{-9}
-26	-16	-17.6	-29	1.6			-19.5
-30.4	-20.4	-22.2	-33.6	1.8		-23.5	
-38.2	-28.2	-29.9	-41.3	1.7	-32.8		

Wavelength: 1550.18nm

Power Monitor (dBm)	Input (dBm)	Output (dBm)	OSA (dBm)	IL (dB)	Sensitivity (dBm)		
					BER = 10^{-3}	BER = 10^{-6}	BER = 10^{-9}
-27.6	-17.6	-18.9	-30.3	1.3			-20.6
-32.4	-22.4	-24.1	-35.5	1.7		-25.8	
-36.5	-26.5	-28.2	-39.6	1.7	-30		

Wavelength: 1550.22nm

Power Monitor (dBm)	Input (dBm)	Output (dBm)	OSA (dBm)	IL (dB)	Sensitivity (dBm)		
					BER = 10^{-3}	BER = 10^{-6}	BER = 10^{-9}
-24.6	-14.6	-16.3	-27.7	1.7			-18
-29.7	-19.7	-21.4	-32.8	1.7		-23.5	
-37.7	-27.7	-29.3	-40.7	1.6	-31.8		

Wavelength: 1550.26nm

Power Monitor (dBm)	Input (dBm)	Output (dBm)	OSA (dBm)	IL (dB)	Sensitivity (dBm)		
					BER = 10^{-3}	BER = 10^{-6}	BER = 10^{-9}
-22	-12	-13.6	-25	1.6			-16
-29.8	-19.8	-21.5	-32.9	1.7		-24	
-35.1	-25.1	-26.8	-38.2	1.7	-29.8		

Wavelength: 1550.3nm

Power Monitor (dBm)	Input (dBm)	Output (dBm)	OSA (dBm)	IL (dB)	Sensitivity (dBm)		
					BER = 10^{-3}	BER = 10^{-6}	BER = 10^{-9}
-24.2	-14.2	-18.1	-29.5	3.9			
-27.3	-17.3	-21.2	-32.6	3.9		-23.8	
-33.5	-23.5	-27.4	-38.8	3.9	-30.5		

MZI

REFERENCE

Power Monitor (dBm)	Input (dBm)	Output (dBm)	OSA (dBm)	IL (dB)	Sensitivity (dBm)		
					BER = 10^{-3}	BER = 10^{-6}	BER = 10^{-9}
-21.1	-11.6	-12.5	-22.7	0.9			

Wavelength: 1549.98nm

Power Monitor (dBm)	Input (dBm)	Output (dBm)	OSA (dBm)	IL (dB)	Sensitivity (dBm)		
					BER = 10^{-3}	BER = 10^{-6}	BER = 10^{-9}
-20.9	-11.4	-13	-23.2	1.6			-14.9
-27.2	-17.7	-19.9	-30.1	2.2		-22	
-35.7	-26.2	-27.6	-37.8	1.4	-30		

Wavelength: 1550.02nm

Power Monitor (dBm)	Input (dBm)	Output (dBm)	OSA (dBm)	IL (dB)	Sensitivity (dBm)		
					BER = 10^{-3}	BER = 10^{-6}	BER = 10^{-9}
-27.2	-17.7	-20.1	-30.3	2.4		-22	
-35.2	-25.7	-29.1	-39.3	3.4	-31.1		

Wavelength: 1550.06nm

Power Monitor (dBm)	Input (dBm)	Output (dBm)	OSA (dBm)	IL (dB)	Sensitivity (dBm)		
					BER = 10^{-3}	BER = 10^{-6}	BER = 10^{-9}
-20.9	-11.5	-15.2	-25.4	3.7			-16
-28.2	-18.7	-22.7	-32.9	4		-24.4	
-34.25	-24.75	-28.4	-38.6	3.65	-31.1		

Wavelength: 1550.1nm

Power Monitor (dBm)	Input (dBm)	Output (dBm)	OSA (dBm)	IL (dB)	Sensitivity (dBm)		
					BER = 10^{-3}	BER = 10^{-6}	BER = 10^{-9}
-20.9	-11.5	-17.2	-27.4	5.7			-18
-28.2	-18.7	-20.3	-30.5	1.6		-21.5	
-34.2	-24.7	-29.8	-40	5.1	-32		

Wavelength: 1550.14nm

Power Monitor (dBm)	Input (dBm)	Output (dBm)	OSA (dBm)	IL (dB)	Sensitivity (dBm)		
					BER = 10^{-3}	BER = 10^{-6}	BER = 10^{-9}
-23.04	-13.54	-16.4	-26.6	2.86			-18.7
-28.18	-18.68	-20.4	-30.6	1.72		-22.4	
-35.2	-25.7	-28.5	-38.7	2.8	-31		

Wavelength: 1550.18nm

Power Monitor (dBm)	Input (dBm)	Output (dBm)	OSA (dBm)	IL (dB)	Sensitivity (dBm)		
					BER = 10^{-3}	BER = 10^{-6}	BER = 10^{-9}
-24.1	-15.2	-18.5	-28.7	3.3			-20
-27.7	-18.2	-20.8	-31	2.6		-23	
-33.7	-24.2	-26.2	-36.4	2	-28.5		

Wavelength: 1550.22nm

Power Monitor (dBm)	Input (dBm)	Output (dBm)	OSA (dBm)	IL (dB)	Sensitivity (dBm)		
					BER = 10^{-3}	BER = 10^{-6}	BER = 10^{-9}
-23.5	-14	-16.3	-26.5	2.3			-18
-28.7	-19.2	-23.5	-33.7	4.3		-25.4	
-33.2	-23.7	-27.8	-38	4.1	-31.1		

Wavelength: 1550.26nm

Power Monitor (dBm)	Input (dBm)	Output (dBm)	OSA (dBm)	IL (dB)	Sensitivity (dBm)		
					BER = 10^{-3}	BER = 10^{-6}	BER = 10^{-9}
-23	-13.5	-16.4	-26.6	2.9			-18.5
-28.1	-18.6	-22.9	-33.1	4.3		-25	
-33.2	-23.7	-28.1	-38.3	4.4	-31		

Wavelength: 1550.3nm

Power Monitor (dBm)	Input (dBm)	Output (dBm)	OSA (dBm)	IL (dB)	Sensitivity (dBm)		
					BER = 10^{-3}	BER = 10^{-6}	BER = 10^{-9}
-26.1	-16.6	-22	-32.2	5.4		-24.1	
-31.2	-21.7	-27.4	-37.6	5.7	-29.8		

Wavelength: 1550.34nm

Power Monitor (dBm)	Input (dBm)	Output (dBm)	OSA (dBm)	IL (dB)	Sensitivity (dBm)		
					BER = 10^{-3}	BER = 10^{-6}	BER = 10^{-9}
-22	-12.5	-21.9	-32.1	9.4		-23.5	
-26.1	-16.6	-26.5	-36.7	9.9	-28.1		

REFERENCES

- [1] Cheng, N., Effenberger, F., Wei, G., Liao, Z., Ye, F., Zhou, L., & Gao, J. (2011). Dynamic Spectrum Management in Passive Optical Networks. 37th European Conference and Exposition on Optical Communications, We.9.C.2. doi:10.1364/ECOC.2011.We.9.C.2
- [2] López, Eduardo T. WDM/TDM PON Bidirectional Networks Single-Fiber/Wavelength RSOA-based ONUs Layer 1/2 Optimization, ppg=28-37. UPC. Sept, 2013.
- [3] Lam, Cedric F. "Passive Optical Networks: Principles and practices". Academic Press, ppg=19-31, Oct 2010.
- [4] López, Eduardo T. WDM/TDM PON Bidirectional Networks Single-Fiber/Wavelength RSOA-based ONUs Layer 1/2 Optimization, ppg=28-37. UPC. Sept, 2013.
- [5] Rigby, P. (2011). FTTH Handbook. FTTH Council Europe, 1–100. Retrieved from <http://scholar.google.com/scholar?hl=en&btnG=Search&q=intitle:FTTH+Handbook#0>
- [6] Paper, W. (2013). White Paper GPON - EPON Comparison, (October).
- [7] Prat, Josep J. Next Generation FTTH Passive Optical Networks. Springer, 2008
- [8] Ducournau, G., Lamy, O., & Ketata, M. (n.d.). The All-fiber MZI Structure for Optical DPSK Demodulation and Optical PSBT Encoding, 4(4), 78–89.
- [9] Benefits, K., Waveready, T., & Frequency, O. (n.d.). WaveReady 50 / 100 GHz Dual Optical Frequency Interleaver (OFI) Module.
- [10] Cao, S., Chen, J., Damask, J. N., Doerr, C. R., Guiziou, L., Harvey, G., Hibino, Y., et al. (2004). Interleaver Technology: Comparisons and Applications Requirements. Journal of Lightwave Technology, 22(1), 281–289. doi:10.1109/JLT.2003.822832
- [11] Chiba, T., Arai, H., Nounen, H., & Ohira, K. (2003). Waveguide interleaving filters, 5246, 532–538.
- [12] Sultan, D. M. S., & Arefin, T. (n.d.). GPON , the Ultimate Pertinent of Next Generation Triple-play Bandwidth Resolution, 53–60.
- [13] Betoule, C., Telecom, F., & Tid, A. T. (2011). D23: NG-PON massive deployment techno-economic assessment.
- [14] Fttth, G., & Architecture, N. (n.d.). Genexis FTTH Network Architecture.
- [15] In, O. (2008). T OPICS IN O PTICAL C OMMUNICATIONS PON in Adolescence: From TDMA to WDM-PON, (January), 26–34.
- [16] Effenberger, F. J., & Member, S. (2011). The XG-PON System: Cost Effective 10 Gb / s Access, 29(4), 403–409.

- [17] Effenberger, F. (2012). XG-PON1 versus NG-PON2: Which One Will Win? European Conference and Exhibition on Optical Communication, Tu.4.B.1. doi:10.1364/ECEOC.2012.Tu.4.B.1
- [18] Brenot, R., Harstead, E., Heron, R., Pfeiffer, T., Poehlmann, W., Smith, J., & Veen, D. Van. (2012). TDM-PON TWDM-PON WDM-PON OFDM-PON TDM: Time Division Multiplexing.